UNIVERSIDADE DE BRASÍLIA – UnB
INSTITUTO DE GEOCIÊNCIAS – IG

Christie Helouise Engelmann de Oliveira

EVOLUÇÃO TECTONO-ESTRATIGRÁFICA DAS BACIAS SANTA BÁRBARA E GUARITAS, RIO GRANDE DO SUL.

DISSERTAÇÃO DE MESTRADO N° 306

Brasília

2012

Christie Helouise Engelmann de Oliveira

EVOLUÇÃO TECTONO-ESTRATIGRÁFICA DAS BACIAS SANTA BÁRBARA E GUARITAS, RIO GRANDE DO SUL.

Trabalho de Diplomação a ser apresentado ao Instituto de Geociências da Universidade de Brasília, como parte dos requisitos para obtenção do título de Mestre em Geociências.

Orientador:

Prof. Dr. Farid Chemale Júnior

Banca examinadora:

Prof. Dr. Elton Luiz Dantas

Prof. Dr. Leo Afraneo Hartmann

Brasília

2012

AGRADECIMENTOS

RESUMO

As bacias Santa Bárbara e Guaritas, localizadas no extremo sul do Brasil, representam o último episódio deposicional da Bacia do Camaquã. Compreendem arenitos, siltitos e conglomerados depositados no final do Neoproterozoico e início do Paleozoico em resposta ao período pós-colisional do Ciclo Brasiliano/Pan-Africano. Análises combinadas de U-Pb e Lu-Hf em zircões detríticos foram realizadas no Laboratório de Geocronologia da Universidade de Brasília, e integradas com dados de paleocorrentes a fim de determinar as idades deposicionais, a proveniência sedimentar e a evolução tectônica destas bacias. Foram coletadas duas amostras representativas de cada bacia e amostras dos furos de sondagem, CQP-01 e CQP-02, realizados pelo Serviço Geológico do Brasil. Os dados geocronológicos U-Pb apresentaram idades concordantes dominantemente Paleoproterozoicas e Neoproterozoicas para as duas bacias, com um aumento de zircões Mesoproterozoicos e Neoproterozoicos para a bacia Guaritas. A idade máxima de deposição obtida para a bacia Santa Bárbara é de 553 ± 16 Ma. Para a bacia Guaritas, os dados bibliográficos, reunidos com os dados obtidos, permitem concluir que a idade máxima de deposição é de 540-535 Ma. As idades modelo Lu-Hf (TDM) mostram que os zircões contêm uma herança dominantemente Arqueana e Paleoproterozoica para as duas bacias, com valores de εHf dominantemente negativos, indicando uma origem crustal a partir de uma litosfera subcontinental para as rochas fonte que preencheram as bacias estudadas.

PALAVRAS-CHAVE: Bacia do Camaquã; Proveniência; U-Pb; Lu-Hf; Idade de deposição; Cinturão Dom Feliciano.

Abstract

The Santa Bárbara and Guaritas basins, located in southern Brazil, represent the last episode of the depositional Camaquã Basin, including sandstone, siltstone and conglomerates deposited during the late Neoproterozoic and early Paleozoic as part of the response made to the collisional period of the Brasiliano/Pan-African Cycle. Combined U-Pb and Lu-Hf analyses of detrital zircons from outcrops and drill holes of both basins, together with an analysis of paleocurrent data, provide information on the sedimentary provenance and tectonic evolution of the basins. The U-Pb geochronological data present concordant ages that are dominantly Paleoproterozoic and Neoproterozoic for both basins, with an increasing contribution of Neoproterozoic and Mesoproterozoic zircons for the Guaritas basin. The maximum depositional age obtained for the Santa Bárbara basin is 553 ± 16 Ma. For the Guaritas basin, previous data and these current data show that the maximum depositional age is 540-535 Ma. The Lu-Hf model ages (TDM) show that the zircons contain an inheritance dominantly Archean and Paleoproterozoic for both basins, with dominantly negative εHf values, which indicates a crustal origin from a subcontinental lithosphere for the source rocks of these basins.

KEYWORDS: Camaquã Basin; Provenance; U-Pb; Lu-Hf; Depositional age; Dom Feliciano Belt.

LISTA DE FIGURAS

SUMÁRIO

1 INTRODUÇÃO

A evolução de cinturões orogênicos é marcada pela geração de diferentes tipos de bacias, sendo que a maioria delas está parcialmente preservada no registro geológico. O Neoproterozoico ao Eopaleozoico, no sudeste da América do Sul, foi marcado pelo desenvolvimento do Cinturão Dom Feliciano, como resultado da colisão dos crátons Rio de La Plata e Kalahari (Fernandes et al, 1992;. Basei et al, 2000;. Chemale Jr., 2000; Hartmann et al, 2000; Chemale Jr. et al, 2012). As últimas fases deste evento foram marcadas por eventos tectônicos extensionais com geração de espaço de acumulação para sedimentos e desenvolvimento de bacias. Essas bacias apresentam o registro de estabilização do Gondwana, e dentre elas a maior e mais completa é a Bacia do Camaquã (Paim et al., 2000; Chemale Jr., 2000), localizada na região centro-sul do Rio Grande do Sul.

A Bacia do Camaquã pode ser definida como um *locus* deposicional, constituída pela superposição de diferentes bacias individualizáveis tectonicamente, geocronologicamente e termodinamicamente (Chemale Jr., 1993; Paim et al., 2000; Borba, 2006), formada pelos grupos Maricá, Bom Jardim, Santa Bárbara e Guaritas. Os grupos Santa Bárbara e Guaritas representam as últimas unidades da Bacia do Camaquã, formadas em um ambiente tectônico dominantemente transtracional, sendo seus intervalos de idade de deposição ainda controversos.

Este estudo tem como objetivo determinar a idade máxima de deposição e as principais áreas fontes dos grupos Santa Bárbara e Guaritas, através de análises isotópicas U-Pb e Lu-Hf em zircões detríticos. Além disso, buscamos um melhor entendimento sobre os estágios tectônicos finais do Cinturão Dom Feliciano e a aglutinação e estabilização inicial da Plataforma Sul Americana.

Os resultados da pesquisa realizada constam nesta dissertação em cinco capítulos. No capítulo dois é apresentado um texto integrador, com o objetivo de introduzir o contexto geológico da região de estudo. Na sequência, no capítulo três, são apresentados os materias e métodos utilizados para a realização do trabalho. A

amostragem, os resultados, assim como uma discussão detalhada, estão contidos no capítulo quatro dispostos em formato de artigo, cujo título é "U-Pb AND Lu-Hf ISOTOPES APPLIED TO THE LATE TO POST-OROGENIC TRANSTENSIONAL BASINS OF THE DOM FELICIANO BELT, BRAZIL.", que encontra-se submetido à revista Precambrian Research. Por fim, o capítulo cinco apresenta as conclusões finais e as recomendações para trabalhos futuros.

1.1 LOCALIZAÇÃO

Os grupos Santa Bárbara e Guaritas estão inseridos na Bacia do Camaquã, localizada na região central do estado do Rio Grande do Sul sobre o Escudo Sul-Rio-Grandense, entre os paralelos -54°00'00" e -53°00'00" de latitude e os meridianos -30°00'00" e -31°00'00" de longitude, mais precisamente ao sul do município de Caçapava do Sul e a oeste-noroeste do município de Santana da Boa Vista, estendendo-se para norte até a região de Encruzilhada do Sul e distando cerca de 250 km de Porto Alegre via BR-290 (Fig. 1). A Bacia do Camaquã é recortada por uma densa rede de estradas municipais e vicinais, bem como por rodovias pavimentadas federais e estaduais (BR-392, BR-153 e RS-11).
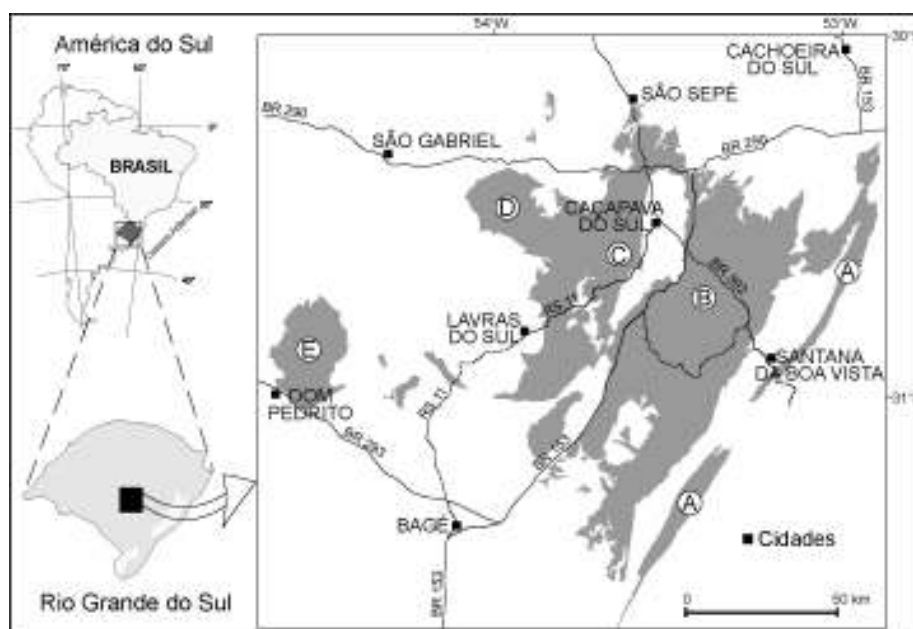
Fig. 1 - Mapa com a localização da Bacia do Camaquã e suas sub-bacias: (A) Boici-Piquiri, (B) Guaritas, (C) Santa Bárbara, (D) Ramada, (E) Taquarembó.

2 CONTEXTO GEOLÓGICO REGIONAL

A Bacia do Camaquã é uma das últimas unidades geradas do Cinturão Dom Feliciano e sua formação ocorreu no intervalo temporal entre 601 ± 13 e 473,7 ± 9,4 Ma (Almeida et al., 2012; Maraschin et al., 2010). Está delimitada geograficamente ao norte pelas rochas sedimentares da Bacia do Paraná e pelas unidades metamórficas do Terreno São Gabriel, que também a delimita ao oeste. Ao leste faz limite tectônico com os granitóides do Batólito Pelotas e ao sul recobrem as unidades do Complexo Granulítico Santa Maria Chico, no Terreno Taquarembó e dos Complexos Porongos e Encantadas no Terreno Tijucas, sendo ainda em parte recoberta pelas coberturas Fanerozoicas (Fig. 2).
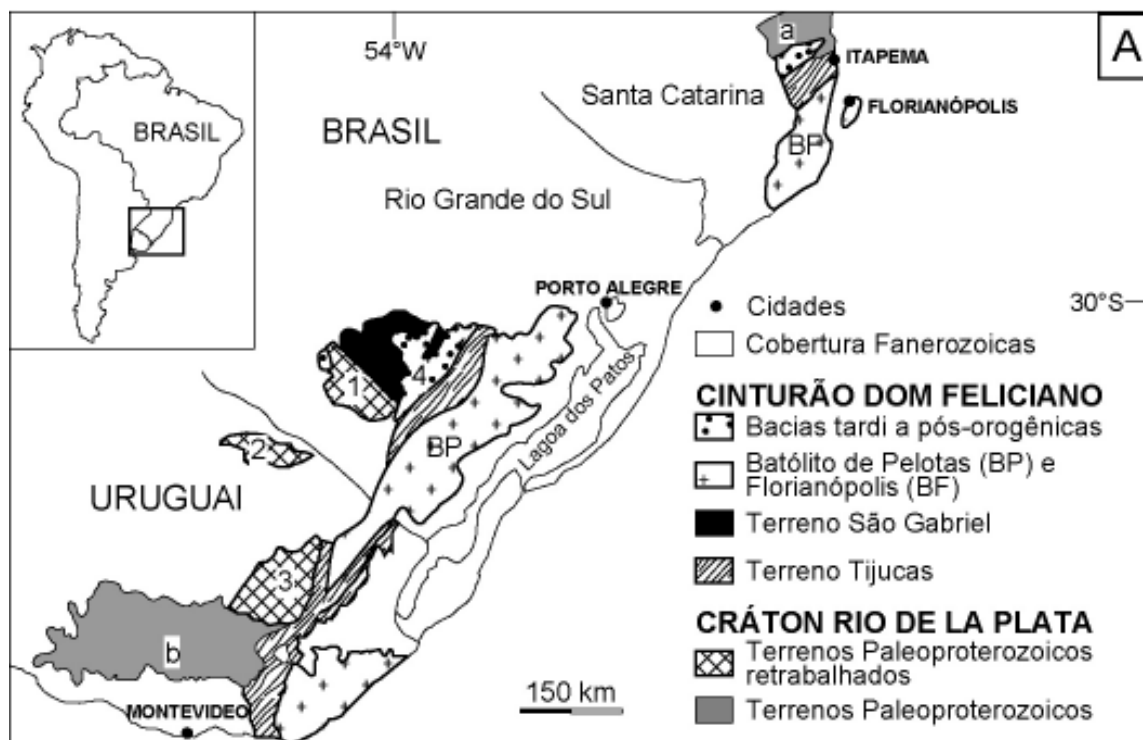
Fig. 2 - Mapa esquemático geotectônico do sul do Brasil e Uruguai. a= Terreno Luis Alves, b= Terreno Pedras Altas, 1= Terreno Taquarembó, 2= Terreno Rivera, 3= Terreno Valentines, 4= Bacia do Camaquã (modificado de Chemale Jr., 2000).

2.1 PRINCIPAIS UNIDADES DO ESCUDO SUL-RIO-GRANDENSE

As rochas da Bacia do Camaquã repousam em contato de não-conformidade sobre as rochas ígneas e metamórficas do Escudo Sul-Rio-Grandense (Leinz & Almeida, 1941; Robertson, 1966; Paim et al., 2000). O Escudo Sul-Rio-Grandense é composto por terrenos metamórficos de médio a alto grau, que constituem as áreas de embasamento Paleoproterozoico, representadas pelos Terrenos Taquarembó e parte do Terreno Tijucas, intercalados com as unidades do Cinturão Dom Feliciano, representadas pelos Terrenos São Gabriel, Tijucas e o Batólito Pelotas. O embasamento do Cinturão Dom Feliciano representa fragmentos do Cráton Rio de La Plata, sendo que suas unidades têm uma evolução relacionada à convergência de placas litosféricas durante o Ciclo Brasiliano (950-550 Ma). O limite entre estas unidades é definido por zonas de cisalhamento regionais, gerando um fragmentado conjunto de faixas alongadas segundo a direção NE-SW (Fig. 2).

O **Terreno Taquarembó** está localizado na porção sudoeste do Escudo Sul-Rio-Grandense, é limitado ao norte pelo Lineamento de Ibaré, ao leste pela anomalia magnética e Sutura de Caçapava do Sul e, ao oeste e ao sul, é recoberto pelos sedimentos da Bacia do Paraná. A principal unidade litoestratigráfica deste terreno é o Complexo Granulítico Santa Maria Chico, que é composto por rochas infra-crustais, com predomínio de granulitos félsicos (gnaisses trondhjemíticos) e máficos (gt-cpx-plag gnaisses), além de metapiroxenitos, lentes de metaultramafitos (harzburgito), com ocorrência subordinada de metassedimentos (gt-bt-silimanita gnaisses, mármores e gnaisses calci-silicáticos), com idades protólitas em torno de 2,45 Ga (Hartmann et al., 2000). Foram afetadas intensamente por retrometamorfismo de contato devido à intrusão de grande volume de magmas graníticos Neoproterozoicos de 0,65 a 0,55 Ga (Gastal et al., 2005). O evento colisional gerador dos granulitos é datado em 2,1 to 2,0 Ga (Hartmann et al., 2008a).

O **Terreno São Gabriel** é limitado ao sul pelo Lineamento de Ibaré e a leste pela Zona de Sutura Caçapava do Sul. É constituído por associações pré-colisionais relacionadas a subducção de litosfera oceânica durante o Neoproterozoico e interpretadas como um prisma acrecionario. Estas associações são caracterizadas por sequências meta-vulcano-plutono-sedimentares de composição cálcico-alcalina

baixo a médio-K, intercaladas com complexos máfico-ultramáficos (ofiolitos), formadas entre 1,0 a 0,69 Ga (Babinski et al., 1996; Chemale Jr., 2000; Saalmann et al., 2005; Hartmann et al., 2011). As associações sin e pós-colisionais ocorrem dominantemente na porção centro-leste do escudo e estão representadas por granitóides com composição cálcico-alcalina alto-K, metaluminosos a peraluminosos, alcalinos e peralcalinos, cuja geração ocorreu entre 650 e 550 Ma (Soliani Jr., 1986; Leite et al., 1998; Silva et al., 1999; Philipp et al., 2002, 2003; Philipp & Campos, 2010).

O **Terreno Tijucas** apresenta forma alongada N30E, e ocorre ao leste do Terreno São Gabriel. Este terreno pode ser dividido em porções leste e oeste, separados por estreitos grabens, delimitados por falhas rúpteis, e preenchidos por sedimentos siliciclásticos da Bacia do Camaquã ou truncados por rochas gnáissicas pré-Brasilianas (Hartmann et al., 2007). O limite leste do Terreno Tijucas ocorre ao longo da Zona de Cisalhamento Dorsal de Canguçu. Esta zona de cisalhamento tem movimentação transcorrente e grande escala, apresentando disposição alongada segundo a direção N30-60E, e movimentação sinistral (Fernandes et al., 1992; Philipp et al., 1993; Philipp & Machado, 2005), colocando em contato o Terreno Tijucas e o Batólito Pelotas, a leste. O Terreno Tijucas é composto pelo Complexo Porongos, uma associação de rochas metasedimentares e metavulcânicas de fácies xisto verde a anfibolito, com idade de 783 ± 8 Ma (Chemale Jr., 2000), que está sobreposto ao Complexo Encantadas, uma unidade definida por ortognaisses, metagranitos, anfibolitos e hornblenditos de idade 2,2-2,3 Ga (Hartmann et al., 2003; Philipp et al., 2008), sendo ainda formado por intrusões graníticas e rochas sedimentares de 0,65 a 0,55 Ga. O embasamento deste terreno está exposto no núcleo de antiformes de grande escala (Jost & Bitencourt, 1980).

O **Batólito Pelotas** constitui a porção leste do escudo, sendo composto por um expressivo complexo plutônico multi-intrusivo ocupando cerca de 400 km de extensão por 80 a 120 km de largura. A maior área deste batólito está ocupada por suítes graníticas de caráter pós-colisional com idades entre 650-550 Ma (Babinski et al., 1997; Hartmann et al., 2000; Philipp et al., 2003; Philipp & Machado, 2005). As unidades mais antigas, representadas pelo Granito Quitéria e pelos granitóides da Suíte Cordilheira são posicionadas na fase final do processo de colisão entre os

Crátons do Rio de La Plata e Kalahari. Posteriormente, posicionam-se os granitóides do Complexo Pinheiro Machado e as suítes Erval, Viamão, Piquiri, Encruzilhada do Sul, Dom Feliciano e Itapuã (Philipp et al., 2000, 2002, 2007; Oliveira et al., 2001). Apesar da ocorrência de rochas básicas a intermediárias, os dados isotópicos indicam que os granitóides foram gerados essencialmente pelo retrabalhamento de uma crosta Paleoproterozoica (2,3-2,0 Ga) e mais raramente Arqueana (Leite et al. 2000; Philipp et al, 2003).

2.2 GEOLOGIA DA BACIA DO CAMAQUÃ

As associações de rocha da Bacia do Camaquã já foram alvo de diversos estudos, apresentando ao longo do tempo diferentes propostas de interpretação litoestratigráfica (Fig. 3) muitas vezes relacionadas à evolução do conhecimento da geotectônica global, da evolução estrutural e tectônica de bacias, sendo primeiramente estudada por Carvalho (1932) e Leinz & Almeida (1941), que sugeriram uma idade deposicional Eopaleozoica. Paim et al. (2000) interpretam a Bacia do Camaquã como um *locus* deposicional no qual se sucederam diferentes bacias, com características próprias e processos tectônicos distintos, divididas em diferentes sub-bacias geográficas: Taquarembó, Ramada, Santa Bárbara, Guaritas, e Boici-Piquiri (Fig. 1). Estas sub-bacias correspondem a ciclos bacinais tardi a pós-orogênico do Ciclo Brasiliano no Cinturão Dom Feliciano (Chemale Jr. et al., 1995; Paim et al., 2000).

Com base nas informações sedimentológicas, estratigráficas e estruturais, e utilizando os dados geocronológicos disponíveis apresentados por Paim et al. (2000), Borba & Misuzaki (2003), Sommer et al. (2005), Janikian et al. (2012) e Almeida et al. (2012), dividimos a Bacia do Camaquã em três ciclos bacinais principais, formados em diferentes ambientes tectônicos, e separados entre si por discordâncias: a) Grupo Maricá – formado em um ambiente de antepaís de retroarco; b) Grupo Bom Jardim – formado em um ambiente transcorrente; e c) Grupo Santa Bárbara e Guaritas – formados em um ambiente transtracional.

Figura 3 - Principais propostas estratigráficas para as unidades da Bacia do Camaquã.

a) 601 ± 13 a 593 Ma – Grupo Maricá. A porção inferior da Bacia do Camaquã é composta pelas rochas do Grupo Maricá, que repousam em contato de não-conformidade sobre as rochas ígneas e metamórficas do Escudo Sul-Rio-Grandense (Paim et al., 2000), recobrindo as unidades metamórficas do Terreno São Gabriel. As exposições de rocha do Grupo Maricá limitam-se à parte oeste da Bacia do Camaquã, destacando-se as regiões do Passo do Salsinho e Vila Nova, localizadas a leste e norte da sub-bacia Ramada, e as de Lavras do Sul, Cordilheiras e Serra do Maricá, a sul do platô, abrangendo os municípios de Caçapava do Sul, Lavras do Sul, São Sepé, Bagé e Vila Nova do Sul.

O Grupo Maricá consiste de arenitos arcoseanos, localmente conglomeráticos, e, de forma subordinada, pelitos. Estas rochas ocorrem em camadas de geometrias e dimensões variadas conforme o processo gerador; apresentam colorações ora amarela, bege, marrom claro ou esverdeada, com presença comum de níveis de minerais pesados que dão às rochas um aspecto que lembra uma mistura "sal e pimenta", conforme apontado como aspecto marcante por Leinz & Almeida (1941) e Ribeiro et al. (1966). Seus depósitos possuem cerca de 4000 m de espessura (Paim et al., 2000) com rochas vulcânicas ácidas associadas (Borba et al., 2008; Almeida et al., 2012). Borba et al. (2007) separou as rochas sedimentares do Grupo Maricá em três sucessões deposicionais: inferior, intermediária e superior. A sucessão inferior, de origem flúvio-aluvial, compreende arenitos subarcóseos e quartzarenitos com lentes conglomeráticas. A sucessão intermediária é composta por siltitos e argilitos, maciços ou estratificados, com laminação plano-paralela, ondulada e lenticular, ocorrendo ainda arenitos com estratificação do tipo hummocky, interpretados por Paim et al. (2000) e Borba et al. (2006) como uma sucessão marinha transgressiva. A sucessão superior é similar à sucessão inferior, sendo composta por arenitos grossos a conglomeráticos, com estratificação cruzada acanalada, planar e horizontal de origem fluvial. Estas sucessões foram intrudidas por rochas vulcânicas intermediárias a ácidas do Grupo Bom Jardim e pelos granitos Lavras do Sul, São Sepé, Ramada e Cerro da Cria, considerados como comagmáticos ao vulcanismo desta formação (Nardi & Lima, 1985; Soliani Jr., 1986).

Estudos de proveniência, paleocorrentes, petrográficos e geocronológicos desenvolvidos por Pelosi & Fragoso-Cesar (2003), revelaram que as principais

áreas-fonte do Grupo Maricá compunham-se de granitos, tonalitos e milonitos graníticos de idade Arqueana e Paleoproterozoica, além de contribuição pouco significativa de quartzo, quartzitos e rochas vulcânicas ácidas e intermediárias. Borba et al. (2006) integrou dados petrográficos de contagem estatística pelo método Gazzi-Dickinson e de geologia isotópica Sm-Nd e também identificou fonte Paleoproterozoica. Para os arenitos da sucessão inferior, Borba et al. (2006) obteve εNd de -19,6 e -21,8 e idades TDM de 1,76 e 1,81 Ga, o que sugere proveniência de bloco crustal. Para a sucessão intermediária, os estudos de proveniência indicaram arco dissecado, com εNd de -18,1 a -23,6 e idades TDM de 2,16 a 2,37 Ga. A sucessão fluvial superior, que também possui fragmentos vulcânicos (até 22%) tem proveniência de arco dissecado e de reciclagem orogênica com εNd de -21,0 a -22,4 e idade TDM de 2,07 Ga.

As rochas do Grupo Maricá foram depositadas entre 630 e 593 Ma em uma bacia de antepaís de retroarco (Gresse et al., 1996; Paim et al., 2000), com idade máxima de deposição de 601 ± 13 Ma, baseada em análises U-Pb em zircões detríticos de arenitos arcoseanos (Almeida et al., 2012).

b) 593 ± 6 a 580 ± 3,6 Ma – Grupo Bom Jardim. O Grupo Bom Jardim compreende uma sequência vulcano-sedimentar, com 2000 m de espessura, depositado sobre as rochas do Grupo Maricá em discordância angular que localmente se assemelha à uma desconformidade. Este grupo é caracterizado por uma sucessão granocrescente e estratocrescente, relacionada à progradação de deltas de planície entrelaçada longitudinais, representada na base por ritmitos pelíticos e areno-pelíticos (turbiditos distais) que gradam verticalmente para ritmitos arenosos (turbiditos proximais), esparsos corpos arenosos sigmoidais (frente deltaica) e níveis pelíticos com gretas de contração (Paim, 1994). Seus contatos são limitados por falhas, a leste com unidades do Grupo Santa Bárbara e, a oeste com rochas do embasamento metamórfico. Unidades paleozoicas da Bacia do Paraná são também encontradas nesta região em discordância erosiva ou, localmente, justapostas ao Grupo Bom Jardim por falhas.

Na região da Ramada/Taquarembó e Santa Bárbara/Caçapava do Sul, o Grupo Bom Jardim está dominado por derrames de lava, magmatismo hipabissal, piroclastos e

_____

Christie Helouise Engelmann de Oliveira. Brasília: IG/UnB, 2012

epiclastos, que constituem a Formação Hilário (Robertson, 1966). O magmatismo é representado por rochas básicas a intermediárias, calcio-alcalinas com alto-K e afinidade shoshonítica (e.g., Nardi & Lima 1985; Almeida et al., 2012), e idade SHRIMP U-Pb em zircão de 593 ± 6 Ma (Remus et al., 1999) a 580 ± 3,6 Ma (Janikian et al., 2012). Almeida et al. (2012) dataram em 591,8 ± 3 Ma as várias intrusões de lamprófiros shoshoníticos. Com base em análise estrutural, Gresse et al. (1996) sugerem que as unidades vulcano-sedimentares desse grupo foram depositadas em uma bacia do tipo *strike-slip*.

c) 574 ± 7 a 544,2 ± 5,5 Ma – Formação Acampamento Velho e Grupo Santa Bárbara. No presente trabalho incluímos no mesmo ciclo bacinal a Formação Acampamento Velho (Ribeiro & Fantinel, 1978) e o Grupo Santa Bárbara (como descrito por Paim et al., 2000 e Borba & Mizusaki, 2003). O Grupo Santa Bárbara apresenta dobras abertas e encontra-se basculado, apresentando mergulhos que variam de poucos graus até subverticais junto ao contato com algumas falhas regionais, refletindo a movimentação dos sistemas de falhas, que são dominantemente normais e direcionais (Paim et al. 2000).

A Formação Acampamento Velho, com cerca de 500 m de espessura (Paim et al., 2000), recobre em discordância angular os depósitos flúvio-deltaicos do Grupo Bom Jardim no flanco oeste da Serra do Espinilho, e os depósitos do Grupo Maricá, na parte oeste da sub-bacia Ramada, e é recoberta em desconformidade pelos depósitos do Grupo Santa Bárbara, sendo localmente relatada discordância angular entre estas unidades (Paim, 1995). É composta por rochas vulcânicas ácidas de afinidade alcalina (fluxos de lava, ignimbritos e vulcanoclastos), relacionado com um ambiente tectônico extensional pós-orogênico (Wildner et al., 1999; Sommer et al., 1999), e localmente basaltos andesíticos. Esta unidade apresenta idades U-Pb em zircão de 549,3 ± 5 Ma (Sommer et al., 2005) para a porção riolítica e 553 ± 5,4 Ma (Almeida et al., 2012) para os basaltos andesíticos da sub-bacia Ramada. Janikian et al. (2012) obteve idade de 574 ± 7 Ma para os riolitos da sub-bacia Ramada e 544,2 ± 5,5 Ma para os lápili tufos da sub-bacia Taquarembó.

O Grupo Santa Bárbara é composto por três ciclos sedimentares (sub-unidades), que foram definidos por Borba & Mizusaki (2003) como Sequência I, II e III,

representados por associações de fácies de leques aluviais, frente deltaica e lacustrina, canais fluviais entrelaçados arenosos e cascalhosos. A Sequência I, com uma espessura estimada de 800-100 m, está depositada em paraconformidade sobre as rochas vulcânicas da Fm. Acampamento Velho. É composta por associações de fácies aluviais com grande contribuição de fragmentos vulcânicos (principalmente riolitos basais da Fm. Acampamento Velho e andesitos shoshoníticos da Fm. Hilário), sendo recoberta por um sistema deposicional transgressivo representado por depósitos de frente deltaica e lacustre. A Sequência II possui aproximadamente 1100 m de espessura e é paraconcordante à Sequência I. É formada na base por sedimentos de canais fluviais entrelaçados seguidos de depósitos de leques aluviais e lacustrinos, formando uma sequência progradacional. As Sequências I e II possuem paleocorrentes com transporte de sul para norte, com contribuição lateral de leques aluviais e pequenos lagos (periodicamente ressecados) junto à borda leste da bacia, o "alto de Caçapava". A Sequência III ocorre em discordância de baixo ângulo sobre a Sequência II, sugerindo um rearranjo da bacia; possui cerca de 200-300 m de espessura e é formada por depósitos de canais fluviais entrelaçados cascalhosos com transporte para o sul e sudoeste, reforçando a idéia de inversão do sentido de preenchimento da bacia. Alguns autores também reconhecem estruturas sedimentares que denotam sedimentação marinha nestes depósitos (Fambrini et al., 2005).

De acordo com Bicca et al. (2010) a idade máxima de deposição da bacia Santa Bárbara é de 558 ± 13 Ma, obtida em conglomerados da Janela Bom Jardim pelo método U-Pb.

547 ± 6,3 to 473,7 ± 9,4 Ma – Grupo Guaritas. O Grupo Guaritas, originalmente descrito por Goñi et al. (1962), tem aproximadamente 800 m de espessura e representa o último episódio deposicional preservado da Bacia do Camaquã. Suas rochas sedimentares foram depositadas em uma bacia tipo rifte transtracional com *trend* N40E (Chemale Jr., 1993; Borba, 2006), com sua borda leste limitada pelo Domo de Santana (Complexo Encantadas). Segundo Paim et al. (2000), este grupo apresenta-se dominantemente horizontal e é afetado por uma deformação rúptil de caráter direcional e gravitacional compreendendo duas unidades limitadas entre si

por discordância erosiva que ocorre ao longo de toda a bacia: a Formação Pedra Pintada, na base, e a Formação Varzinha, no topo.

As rochas da Formação Pedra Pintada, com cerca de 400 m de espessura, recobrem as rochas sedimentares do Grupo Santa Bárbara em discordância angular, e é composta por arenitos finos a médios, bem selecionados, com estratificação cruzada acanalada de grande porte, interpretados como associações de fácies de dunas. Em menor proporção ocorrem arenitos grossos, pelitos e arenitos finos a médios, com laminação cruzada por corrente e por onda, interpretados como depósitos de interdunas e flúvio-lacustres. As paleocorrentes desta formação indicam campos de dunas migratórias paralelo à tendência NE da bacia, em um clima semi-árido (Paim, 1994; Paim & Scherer, 2007). Lateralmente, próximo à borda leste da bacia Guaritas, conglomerados e arenitos substituem as acumulações eólicas e representam leques aluviais contemporâneos que se desenvolveram ao longo da margem ativa da bacia (Almeida et al, 2009; Marconato et al, 2009). Intercalados à base das fácies fluviais e eólicas desta formação encontram-se derrames de rochas vulcânicas denominadas "Andesito Rodeio Velho".

As unidades da Formação Varzinha, com espessura em torno de 400 m, são depositadas concordantemente sobre as unidades da Fm. Pedra Pintada, e é composta dominantemente por arenitos finos a muito grossos de origem aluvial seguidos por acumulações eólicas, na base, recobertos por uma sucessão lacustre e deltas associados. A seção superior da Formação Varzinha corresponde a vários conjuntos de parasequências progradacionais de origem deltaica, desenvolvidos no interior de uma bacia lacustre rasa, com abundância de feições de dissecação de lama e precipitação de silcretes e calcretes (De Ros et al., 1994). Tanto as fácies aluviais (base) quanto as deltaicas (topo) foram associadas a sistemas transversais de leques deltaicos provenientes da borda leste da bacia Guaritas (Paim, 1995; Paim et al. 2000). As paleocorrentes provenientes das fácies eólicas desta formação indicam um padrão de ventos para SSW, com uma direção oposta à circulação de ventos da Formação Pedra Pintada (Paim & Sherrer, 2007).

O zircão mais jovem do Andesito Rodeio Velho foi datado em 547 ± 6,3 Ma (método U-Pb, Almeida et al., 2012), enquanto que ilitas autigênicas de arenito eólico (topo

da Fm. Pedra Pintada) foram datadas em 473,7 ± 9,4 Ma (método K-Ar, Maraschin et al., 2010). De acordo com a Hartmann et al. (2008b), a idade U-Pb em zircões detríticos obtida a partir da seção superior do Grupo Guaritas (Formação Varzinha) corresponde ao início da deposição Guaritas em 535 ± 10 Ma. Os dados sugerem que a deposição da bacia Guaritas ocorreu entre 547 ± 6,3 Ma e 473,7 ± 9,4 Ma.

A grupos Santa Bárbara e Guaritas foram formados em um ambiente continental sob a influência final de uma tectônica transcorrente sinistral (Chemale Jr., 2000) ou nos estágios finais de formação do Cinturão Dom Feliciano (Tommasi et al., 1994), durante a aglutinação final do Gondwana Ocidental. Neste contexto, a grupos Santa Bárbara e Guaritas podem ser interpretados como bacias individualizáveis tipo rifte, que se desenvolveram em um ambiente transtracional (Chemale Jr., 1993; Borba, 2006) separados pelo Alto de Caçapava e, de acordo com Borba (2006), possuem modelos evolutivos semelhantes.

3 GEOCRONOLOGIA E MÉTODOS ANALÍTICOS

Os sedimentos presentes nas bacias sedimentares são dependentes do conjunto de rochas fonte expostas à ação intempérica durante os processos de formação e deposição da bacia. Os processos responsáveis pelo soerguimento e exposição de rochas do embasamento, bem como pela subsidência e geração de bacias deposicionais, dependem do ambiente tectônico dominante. Dickinson (1974) relacionou aspectos da relação entre tectônica, sedimentação e magmatismo de bacias, e propôs que a composição dos sedimentos ou rochas sedimentares que preenchem as bacias são diagnósticas do ambiente tectônico de evolução da bacia.

As características de clima e relevo dominantes na área fonte, assim como os processos de transporte e deposição dos sedimentos, constituem outro fator decisivo para a composição dos fragmentos detríticos presentes nas bacias. Após a deposição, a composição do arcabouço dos sedimentos ainda pode sofrer profundas alterações devido à dissolução de fragmentos detríticos e à precipitação de novas fases minerais por efeito da diagênese.

Considerando o fato de que a composição dos sedimentos e rochas sedimentares depende dos fatores citados acima, os estudos de proveniência começam por uma identificação correta e segura dos minerais e fragmentos de rochas presentes em seu arcabouço. Para isso, é recomendável a utilização de diferentes escalas e técnicas de observação e análise. Os dados geocronológicos em minerais detríticos constituintes das bacias, têm sido utilizados como indicadores da idade de deposição da bacia e das rochas fonte, e portanto, como traçadores de proveniência

Nesse capítulo serão abordadas inicialmente as metodologias adotadas para a coleta e preparação das amostras e, em seguida, os aspectos teóricos referentes aos sistemas isotópicos U-Pb e Lu-Hf utilizados para o desenvolvimento dessa pesquisa.

3.1 COLETA DE AMOSTRAS

Foram coletadas duas amostras de cada bacia, Santa Bárbara e Guaritas, e amostras dos furos de sondagem realizados pelo Serviço Geológico do Brasil (CPRM) CQP-01 e CQP-02, localizados a sudeste da cidade de Caçapava do Sul e na região de Minas do Camaquã (Janela Bom Jardim), respectivamente. Para o furo CQP-01 foram coletadas 3 amostras de diferentes profundidades: T01-11 a 41 m, T01-144 a 569 m e T01-176 a 729 m. Para o furo CQP-02 foram analizadas 2 amostras: T02-07 a 27 m e T02-202 a 926 m.

Para cada bacia foi coletado em média 5 kg de cada amostra a fim de que fosse possível obter um número ideal de zircões a serem analisados. Nos furos foi coletado um metro de cada amostra, sendo que foi retirado apenas metade do testemunho.

3.2 PREPARAÇÃO DAS AMOSTRAS PARA ANÁLISE U-Pb E Lu-Hf

Os concentrados minerais foram obtidos a partir de britagem e moagem da amostra, resultando em fração de granulação inferior a 500 mesh. Em seguida a amostra foi bateada, onde foi feita a separação mineral por densidade. Após concentração hidrodinâmica dos minerais pesados, utilizou-se o separador isodinâmico Frantz com amperagens variando entre 0,2 a 0,6, a fim de separar os minerais ferro-magnesianos.

Os grãos de zircão foram separados manualmente e aleatoriamente sob uma lupa binocular, dispostos de maneira organizada em uma pastilha de resina epóxi, lixados e polidos. Em cada pastilha foi realizado o imageamento (tipo *back scatered*) no microscópio eletrônico de varredura (MEV), a fim de definir os melhores cristais a serem analisados.

3.3 MÉTODOD U-Pb EM ZIRCÕES

O sistema isotópico U-Th-Pb é um dos mais utilizados pela geocronologia moderna uma vez que se baseia em três geocronômetros independentes, com meias-vidas distintas e muito longas (Faure, 1986). Este método se baseia principalmente no decaimento do U e Th em isótopos estáveis de Pb. Isso não se deve apenas a transformação do U e Th em Pb, mas também derivado da evolução do Pb comum, do decaimento de isótopos-filhos intermediários de U, e da composição isotópica resultante do He, como pela acumulação de danos radioativos nos cristais.

O Urânio tem três isótopos de ocorrência natural, ^{238}U, ^{235}U e ^{234}U. O Tório existe inicialmente como ^{232}Th. Cinco isótopos radioativos adicionais de Th ocorrem na natureza devido à curta vida dos seus isótopos-filhos, intermediários do decaimento do ^{238}U, ^{235}U e ^{232}Th.

As seguintes equações resumem as séries de decaimento do U e Th em função da emissão de partículas α e β:

^{238}U → ^{206}Pb + 8α + 6β- + Q (T1/2= 4468 Ma)

^{235}U → ^{207}Pb + 7α + 4β- + Q (T1/2= 704 Ma)

^{232}Th → ^{208}Pb + 6α + 4β- + Q (T1/2= 14010 Ma)
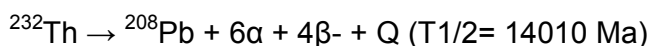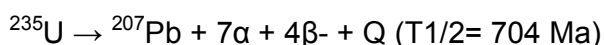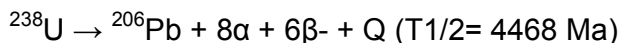
Onde temos que: α é a partícula-alfa emitida e β- é a partícula-beta negativa, além de T1/2 ser a representação da meia-vida dos elementos U e Th e Q ser a energia liberada na reação.

Projetando-se as razões de ^{206}Pb/^{238}U versus ^{207}Pb/^{235}U para diferentes valores de t, que é o tempo passado desde o fechamento do mineral para os isótopos de U e Pb, obtém-se uma curva chamada concórdia (Fig. 4), que é calibrada em intervalos de 500 Ma, sendo definida como o local onde são plotados todos os pontos cujas idades ^{238}U/^{206}Pb e ^{235}U/^{207}Pb são iguais. Se o sistema isotópico permaneceu fechado para U e Pb desde sua formação, as idades ^{238}U-^{206}Pb e ^{235}U-^{207}Pb devem ser as mesmas e, portanto, cair sobre esta curva concórdia. Estas idades são chamadas de concordantes.

Idades discordantes normalmente resultam da perda de Pb durante eventos metamórficos. Neste caso, zircões (ou outros minerais apropriados) derivados de uma mesma amostra caem sobre uma linha, chamada discórdia, cujos interceptos superior e inferior com a concórdia podem ser interpretados em alguns casos como as idades de cristalização e do evento metamórfico, respectivamente. Discórdias também podem resultar da presença de zircões herdados da fonte ou da perda contínua de Pb. No primeiro caso, o intercepto inferior fornece a idade da rocha e o superior dá uma indicação da idade de seu protólito. No segundo caso, o intercepto superior corresponde à idade da rocha e o inferior é forçado para zero.
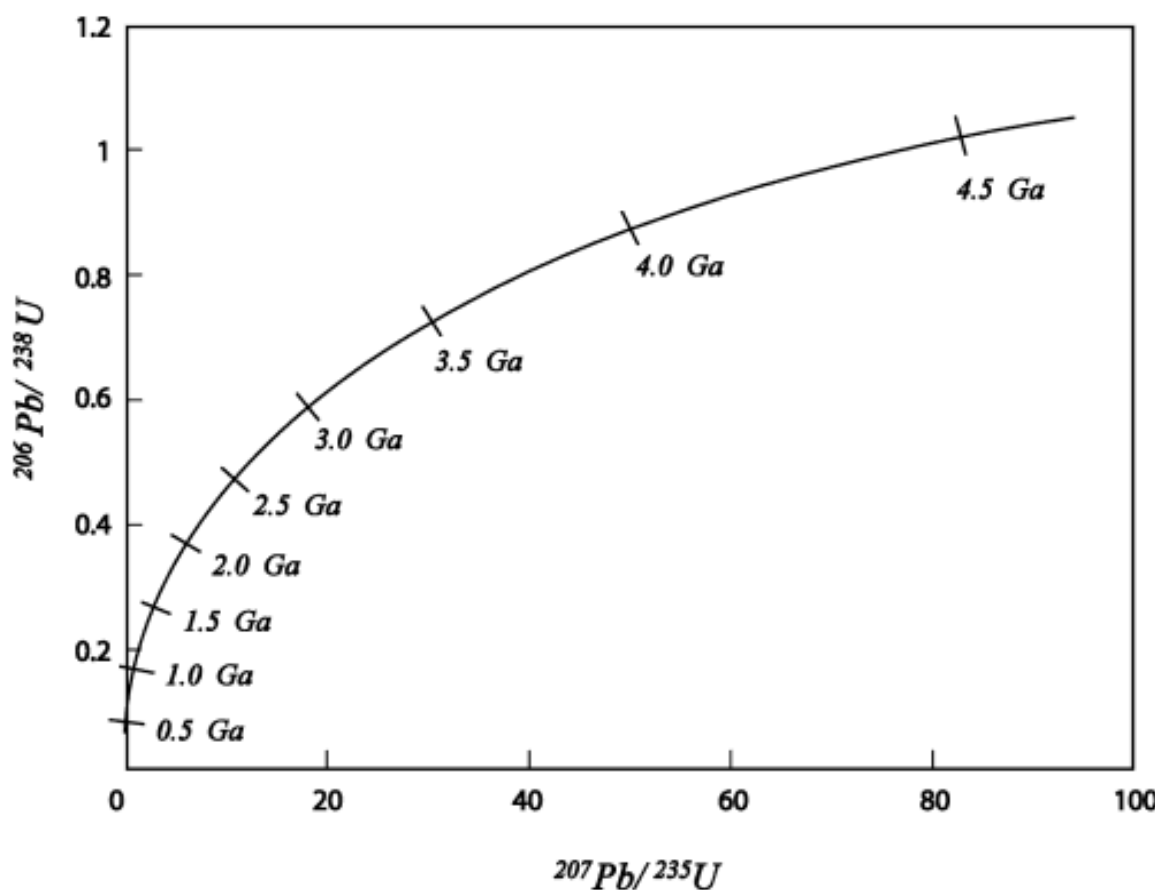
Fig. 4 - Diagrama concórdia (retirado de Faure & Mensing 2005).

3.4 MÉTODOD Lu-Hf

Os zircões podem conter de 0,5% a >2% de Hf, e o alto conteúdo deste elemento e a baixa razão Lu/Hf podem prover importante informação complementar para o sistema U-Pb (Patchett et al., 1981) assim, quando combinado com o método U-Pb, o método Lu-Hf possibilita caracterizar isotopicamente o magma a partir do qual estes cristais foram gerados.

O Lu faz parte da série final dos lantanídeos e apresenta dois isótopos (^{175}Lu e ^{176}Lu) com respectivas abundâncias de 97,4% e 2,6%. ^{175}Lu é um radionuclídeo instável que sofre decaimento espontâneo β- para ^{176}Hf, com uma meia-vida de aproximadamente 35 Ga. O decaimento de Lu para Hf segue o modelo a seguir, de acordo com Patchett e Tatsumoto (1980), onde o λ representa o decaimento constante do ^{176}Lu:

$(^{176}Hf/^{177}Hf)_t = (^{176}Hf/^{177}Hf)_{inicial} + (^{176}Hf/^{177}Hf)_t$; λ=1,94x10-11

Háfnio é membro do grupo IV-B, da tabela periódica e tem camada de valência +4, que mostra uma composição química mais enriquecida de Zr (Zr/Hf ~ 35 em rochas crustais). O Háfnio ocorre em 6 tipos de isótopos naturais: ^{176}Hf, ^{177}Hf, ^{178}Hf, ^{179}Hf e ^{180}Hf.

A razão inicial Lu/Hf condrítica da Terra (CHUR) tem sido progressivamente modificada ao longo do tempo por fusão parcial do manto superior que, na geração de magmas basálticos, tem depletado o manto residual em Hf (o mais incompatível dos dois elementos) e enriquecido a crosta basáltica gerada. De acordo com Tatsumoto et al. (1981), para o CHUR (*Chondritic Uniform Reservoir*), o valor da relação de massas ^{176}Lu/^{176}Hf é igual a 0,0332 ± 0,002. A razão isotópica inicial de ^{176}Hf/^{177}Hf em 4,56 Ga é igual a 0,279742 ± 29, enquanto a atual é de 0,282772 ± 29. Para o manto empobrecido (DM) o valor obtido é de 0,0390. Estes parâmetros definem a curva de crescimento Hf, sendo que o fracionamento de Lu para Hf ocorre durante a geração do magma (Fig. 5).
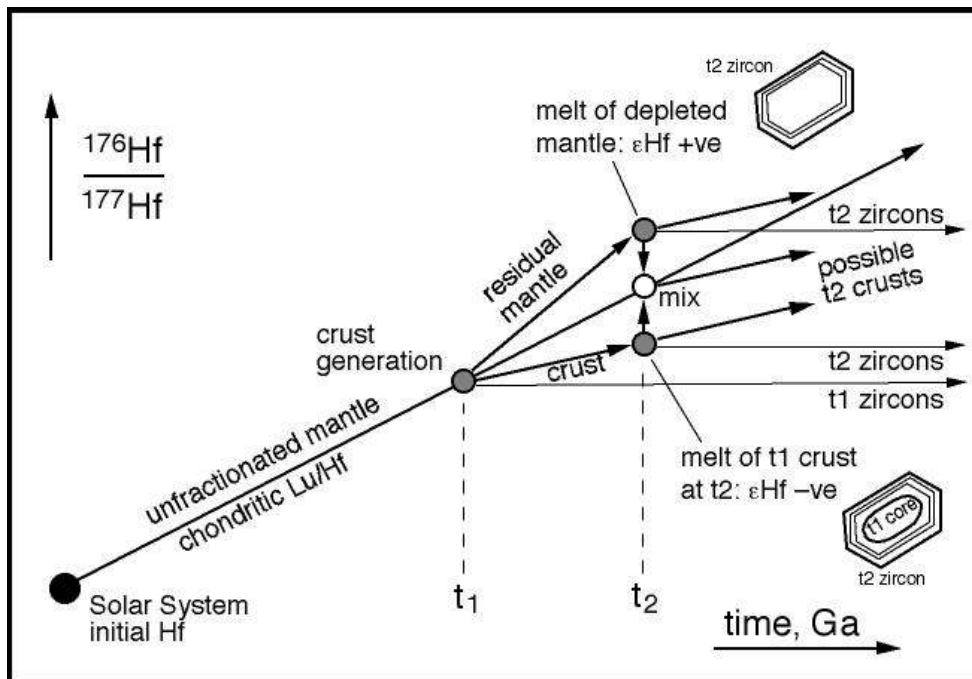
Fig. 5 - Diagrama de evolução isotópica Hf, modificada de Patchett et al. (1981), mostrando como um episódio de fusão parcial no manto da Terra em tempo t1 resulta em divergentes caminhos de evolução dos isótopos Hf para a crosta recém-gerada (baixo Lu/Hf) e do manto residual (alto Lu/Hf).

Durante a fase de cristalização do zircão são incorporados ao cristal quantidade relativamente pequena de Lu e quantidade de isótopos de Hf em torno de 1%. Devido a grande quantidade de Hf inicialmente incorporado, cuja concentração é da ordem de 100 ppm, a quantidade de ^{176}Hf transmutado do ^{176}Lu após cristalização torna-se muito pequena. Para comparar os isótopos de Hf com do CHUR em qualquer tempo, t, foi criado o parâmetro εHf (partes por 10.000 de Hf), dado pela seguinte fórmula:

$$\varepsilon Hf = [(^{176}Hf/^{177}Hf)_t / (^{176}Hf/^{177}Hf)_{CHUR} - 1] \times 10^4$$

As composições iniciais de Hf no zircão podem apresentar a história da magmatogênese (petrogênese) de sua fonte. A concentração de Hf em zircão varia entre 5000 e 10000 ppm, ^{176}Lu/^{177}Hf ~ <0.0005 e εHf do manto depletado atual tem valor de 16 (Chu et al., 2002). O parâmetro εHf inicial em zircão representa uma importante ferramenta no estudo relativo à evolução da crosta continental: a) se εHf for maior que zero, o material fonte do zircão tem uma origem mantélica; b) se o εHf for menor que zero, o material fonte é de origem crustal.

A partir da década de 90, o método LA-MC-ICPMS, que permite excelente ionização em amostras de soluções impuras, se tornou o método ideal para análises de isótopos de Hf. A precisão e acurácia obtida pelo LA-MC-ICPMS é comparável àquela obtida pelo TIMS, sendo a preparação das amostras muito mais fácil e a eficiência das análises muito mais alta pelo LA-MC-ICPMS.

3.5 LA-MC-ICPMS

As análises deste trabalho foram realizadas utilizando o LA-MC-ICPMS (*laser ablation inductively coupled plamsa mass espectrometer*) do Laboratório de Geocronologia e Geologia de Isótopos da Universidade de Brasília. O equipamento é do modelo Neptune da Thermo Finnigan equipado com 9 copos Faraday, uma multiplicadora de elétrons, e 6 contadoras de íon do tipo MIC (*multi íon channel*), com Microssonda à Laser acoplada.

O LA-MC-ICPMS consiste de um equipamento de ablação a laser acoplado a um espectrômetro de massa e permite a obtenção de razões isotópicas in situ com alta resolução espacial. Tal característica torna essa sistemática importante para estudos de proveniência sedimentar. As análises são rápidas e, portanto, os custos são menos elevados quando comparados aos das microssondas iônicas. A principal desvantagem dessa sistemática é o efeito matriz, o que demanda a análise de padrões intercalados às amostras para a correção de desvios instrumentais.

4 ARTIGO SUBMETIDO À REVISTA PRECAMBRIAN RESEARCH

U-Pb AND Lu-Hf ISOTOPES APPLIED TO THE LATE TO POST-OROGENIC TRANSTENSIONAL BASINS OF THE DOM FELICIANO BELT, BRAZIL.

Christie Helouise Engelmann de Oliveira[1]; Farid Chemale Junior[1]; Andréa Ritter Jelinek[2]; Ruy Paulo Philipp[2]; Marcos Müller Bicca[2].

[1]Programa de Pós-graduação em Geologia, Instituto de Geociências, Universidade de Brasília, 70.904-970, Brasília – DF, Brazil

[2]Instituto de Geociências, Universidade Federal do Rio Grande do Sul, 91.501-970, Porto Alegre – RS, Brazil

Abstract

The Santa Bárbara and Guaritas basins, located in southern Brazil, represent the last episode of the depositional Camaquã Basin, including sandstone, siltstone and conglomerates deposited during the late Neoproterozoic and early Paleozoic as part of the response made to the collisional period of the Brasiliano/Pan-African Cycle. Combined U-Pb and Lu-Hf analyses of detrital zircons from outcrops and drill holes of both basins, together with an analysis of paleocurrent data, provide information on the sedimentary provenance and tectonic evolution of the basins. The U-Pb geochronological data present concordant ages that are dominantly Paleoproterozoic and Neoproterozoic for both basins, with an increasing contribution of Neoproterozoic and Mesoproterozoic zircons for the Guaritas basin. The maximum depositional age obtained for the Santa Bárbara basin is 553 ± 16 Ma. For the Guaritas basin, previous data and these current data show that the maximum depositional age is 540-535 Ma. The Lu-Hf model ages (TDM) show that the zircons contain an inheritance dominantly Archean and Paleoproterozoic for both basins, with

dominantly negative εHf values, which indicates a crustal origin from a subcontinental lithosphere for the source rocks.

1. Introduction

The evolution of orogenic belts is marked by the presence of different types of basins, including passive margin, active margin, syn- and post-collisional (e.g., Dickinson, 1974; DeCelles and Giles, 1996; Ingersoll, 2008; Oliveira et al., 2010). Most of the basins that occurred after the continental collision are partially preserved in the geological cycle. The Neoproterozoic to Early Paleozoic Dom Feliciano Belt formed as a result of the collision of the Kalahari and Rio de la Plata cratons, evolving from the rifting, drifting and amalgamation from ca. 1.0 Ga to 0.5 Ga (e.g., Fernandes et al., 1992; Basei et al., 2000; Chemale Jr., 2000; Hartmann et al., 2000; Chemale Jr. et al., 2012) with well-defined tectonic terranes of juvenile and crustal recycled signature. The latest phases of these orogenic processes were marked by lateral escape tectonic events (Tommasi et al., 1994) with important extensional components that generated space for sediment accumulation and basin development. These basins have a record of stabilization of Gondwana, and the largest and most complete of these in the Dom Feliciano Belt is the Camaquã Basin (Paim et al., 2000; Chemale Jr., 2000) located in the central-south region of Rio Grande do Sul. Structurally, the Camaquã Basin may be defined as a depositional locus with a superposition of different basinal cycles distinguished by age and tectonic setting (Chemale Jr., 1993; Paim et al., 2000; Borba, 2006); these units are composed of the Maricá, Bom Jardim, Santa Bárbara and Guaritas groups, each with distinct structural and lithological characteristics. The Santa Bárbara and Guaritas groups represent the latest units of the Camaquã Basin, formed in a dominant transtensional tectonic setting and deposited on juvenile and crustal-derived orogenic terranes of the Dom Feliciano Belt (e.g., Chemale Jr. et al., 2012). These basins

have provided important information about the tectonic terrane contribution, the crustal continental growth and the tectonic history of the orogenic belt (Paim, 1994; De Ros et al., 1994; Chemale et al., 1995; Gresse et al., 1996; Paim et al 2000; Hartmann et al. 2007; Philipp et al. 2007). The in situ U-Pb and Lu-Hf isotope analyses of zircons allow us to distinguish the different source areas, providing us with a better understanding regarding the crustal growth of the Neoproterozoic to Eopaleozoic belts. This methodology has been applied to recent sediments formed in rivers in studies in which Bodet and Shaerer (2000), Condie et al. (2005) and Iizuka et al. (2005) obtained important information about the source rocks of sedimentation, gaining an understanding of crustal reworking and continental growth rates. Similar studies have been conducted in older rocks to ascertain the geological evolution of sedimentary basins and magmatic rocks; such studies have also determined the amount of crustal recycling and juvenile mantle contribution (Amelin et al., 2000; Davis et al., 2005; Gerdes and Zeh, 2006; Howard et al., 2011).

This study applies the U-Pb and Lu-Hf detrital zircon methodology to establish the main source areas and the maximum depositional age of the Santa Bárbara and Guaritas Group units. In addition, we also seek to understand the final tectonic stages of the Dom Feliciano Belt and the agglutination and initial stabilization of the South America Platform.

2. Geological Setting

The Santa Bárbara (Santa Bárbara Group) and Guaritas (Guaritas Group) basins are members of Camaquã Basin, located in the region of Caçapava do Sul in the central portion of Rio Grande do Sul State, southern Brazil (Fig. 1); this region is part of the Sul-Rio-Grandense Shield formed by Archean to Eopaleozoic crystalline rocks (Fernandes et al., 1992; Chemale Jr., 2000; Hartmann et al., 2007).

The Sul-Rio-Grandense Shield is composed of the following four units (Fig. 1) bounded by regional shear zones oriented NE-SW and NW-SE: (1) the Taquarembó Terrane, limited by the NW-SE trending Ibaré Shear Zone, is composed mainly of Paleoproterozoic granulites with protolithic ages of 2.45 Ga and metamorphisms from

2.1 to 2.0 Ga (Hartmann et al., 2008a), several granitic intrusions from 0.65 to 0.55 Ga (Gastal et al., 2005) and Neproterozoic to Eopaleozoic volcano-sedimentary rocks (Wildner et al., 2002); (2) the São Gabriel Terrane, bounded in the south by the Ibaré Shear Zone and in the east by the Caçapava do Sul Shear Zone (suture), consists of an association of ophiolite slabs, arc-related plutonic and volcano-sedimentary rocks formed from 1.0 to 0.69 Ga (Babinski et al., 1996; Chemale Jr., 2000; Saalmann et al., 2005; Hartmann et al., 2011) that have been interpreted as an accretionary prism and as having a juvenile signature and late to post-orogenic granitic intrusions and volcano-sedimentary cover (as part of the Camaquã Basin), formed from 0.63 to 0.47 Ga; (3) the Tijucas Terrane, composed of metasedimentary and metavolcanic rocks of the Porongos Complex with an age of 783 ± 8 Ma, (Chemale Jr., 2000), older basement portions of granitic-gneissic rocks of the Encantadas Complex from 2.2-2.3 Ga (Hartmann et al., 2003; Philipp et al., 2008) and granitic intrusions and sedimentary rocks formed from 0.65 to 0.55 Ga; and (4) the Pelotas Batholith, represented predominantly by granitic rocks with ages between 650-550 Ma (Babinski et al., 1997; Hartmann et al., 2000; Philipp et al., 2003; Philipp and Machado, 2005), Paleoproterozoic reworking crust and, more rarely, Archean rocks (Leite et al., 2000; Philipp et al, 2003). The Neoproterozoic granitic-gneissics and metamorphosed volcano-sedimentary rocks of the Tijucas Terrane and the Pelotas Batholith contain a crustal signature with TDM Nd Model ages from 1.2 Ga to 2.4 Ga (Babinski et al., 1997; Saalmann et al., 2005) and are interpreted as part of the continental magmatic arc formed by the melting of the Paleoproterozoic crust with different proportions of juvenile Neoproterozoic crust.

According to Chemale Jr. (2000), the tectonic evolution of the Sul-Rio-Grandense Shield during the Brasiliano/Pan-African Cycle involved phases of subduction eastward in an island arc (900-800 Ma) and a continental arc (800-700 Ma), then a westward subduction (650-595 Ma) and the final collision (595-540 Ma) of the Rio de la Plata (west) and the Kalahari (east) plates. In response to the late and postcollisional continental stresses, foreland basins in retroarc positions and rift or pull-apart basins developed, and sedimentary deposits were made in what became the Camaquã Basin.
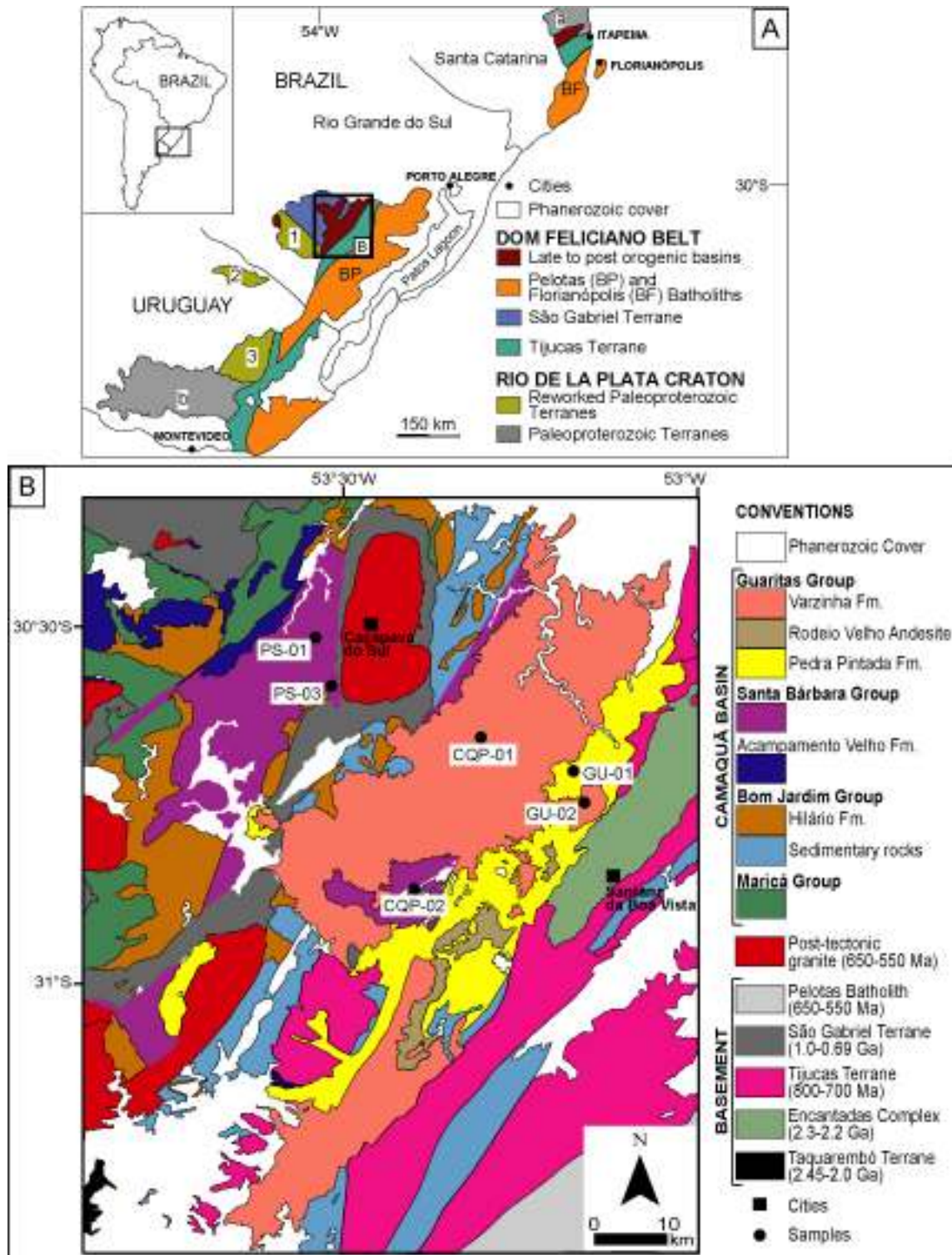
Fig. 6 - (A) Schematic geotectonic map of southern Brazil and Uruguay, including the location of the study area. a = Luis Alves Terrane, b = Piedras Altas Terrane, 1 = Taquarembó Terrane, 2 = Rivera Terrane, 3 =Valentines Terrane (modified after Chemale Jr., 2000). (B) Detail of area outlined in Fig. 1 (A). Geological map of the stratigraphic units exposed in the Camaquã Basin in the region of the Caçapava do Sul with the location of samples.

3. Camaquã depositional locus ("Camaquã Basin")

The Camaquã Basin comprises different geographic sub-basins, including the Ramada, Santa Bárbara, Guaritas, Boici-Piquiri and Taquarembó sub-basins from west to east (Fig. 2); it also corresponds to late to post-orogenic basinal cycles of the Brasiliano Cycle in the Dom Feliciano Belt (e.g., Chemale Jr. et al., 1995; Paim et al., 2000). The Camaquã Basin is part of the main volcano-plutonic-sedimentary association of the Dom Feliciano Belt, as described by Chemale Jr. (2000). It comprises three main basinal cycles formed in different tectonic settings: the basal cycle is in a retroarc foreland, the intermediate cycle is in a strike-slip, and the upper cycle formed in a transtensional environment (Fig. 3). The Camaquã Basin strata were first investigated by Carvalho (1932) and Leinz and Almeida (1941), who suggested an Eopaleozoic age for its deposition. In the late 1960s, Robertson (1966) defined the main stratigraphic units of the Camaquã Basin in the Camaquã Series; this definition has been modified over recent decades. Based on sedimentological, stratigraphic and structural information, and utilizing the available geochronological data presented by Paim et al. (2000), Borba and Misuzaki (2003), Sommer et al. (2005), Janikian et al. (2012) and Almeida et al. (2012), we divided the Camaquã Basin into three primary basinal cycles separated by the following main unconformities:

a.   **601 ± 13 to 593 Ma – The Maricá Group.** This group is the basal basinal cycle of the late to post-orogenic basins of the Dom Feliciano Belt. It comprises a 4000 m thick sedimentary package (Paim et al., 2000) with some acid volcanism activity (Borba et al., 2008; Almeida et al., 2012) overlying in unconformity the juvenile São Gabriel Terrane (with an age of 0.9 to 0.7 Ga) (Chemale Jr. et al., 1995; Babinski et al., 1997; Hartmann et al., 2011). It comprises three primary sequences: lower, intermediate and upper. The lower sequence consists of a basal fluvial-alluvial with braided channels including conglomeratic and subarkose and quartzarenitic sandstones. The intermediate succession, which is transgressive on the lower sequence, is composed of interlayered siltstone and shales with plane-parallel laminae, wave and climbing ripples, and lenticular lamination; it is hummocky and has been interpreted by Paim et al. (2000) and Borba et al. (2006) as a marine succession. The upper succession is similar to the lower one, composed of fluvial

conglomerates and sandstones with large-scale troughcross and low-angle stratifications. These fluvial deposits contain important contributions of granite-gneiss pebble and rare rhyolitic rocks; importantly, a significant proportion of volcanic rocks (14% to 24%) occur in the conglomeratic layers of the upper sequence (Borba et al., 2006). These sequences were deposited 630 to 593 Ma in a retro-arc foreland setting (Gresse et al., 1996; Paim et al., 2000) with sedimentary provenance from continental to arc-related material (Borba et al., 2006). The maximum depositional age is 601 ± 13 Ma based on detrital zircon determinations from arkosean sandstone of the Maricá Group (Almeida et al., 2012).
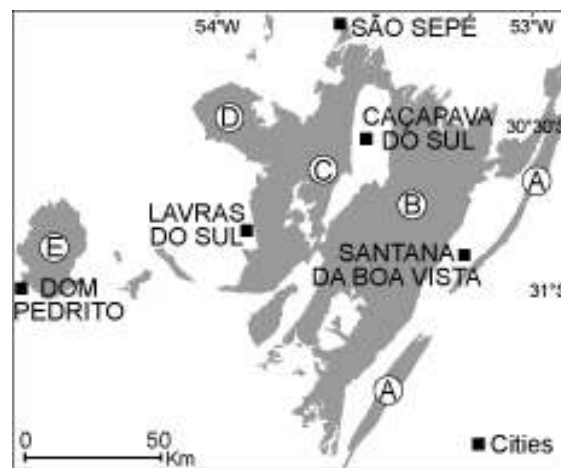
Fig. 7 - Geographic sub-basins of the Camaquã Basin: A) Boici-Piquiri; B) Guaritas; C) Santa Bárbara; D) Ramada; E) Taquarembó.

b.   593 ± 6 to 580 ± 3.6 Ma – The Bom Jardim Group. This group is a volcano-sedimentary sequence overlying the Maricá group units in angular unconformity. It corresponds to a 2000 m thick volcano-sedimentary sequence dominated by lava flows, hypabissal magmatism, pyroclastic and epiclastic deposits and siliclastic sediments deposited in an alluvial-deltaic depositional system. Magmatism is represented by high-K calk-alkaline intermediate to basic rocks with a shoshonistic signature (e.g., Nardi and Lima 1985; Almeida et al., 2012) as member of the Hilário Andesite (Roberson, 1966). The U-Pb SHRIMP zircon ages of the andesites range from 593 ± 6 Ma (Remus et al., 1999) to 580 ± 3.6 Ma (Janikian et al., 2012). In addition, there are several intrusions of shoshonitic lamprophyres dated to 591.8 ± 3 Ma (Almeida et al., 2012). Based on detailed structural features, these units were

strongly controlled by strike-slip deformation during the volcano-sedimentary deposition (Gresse et al., 1996).
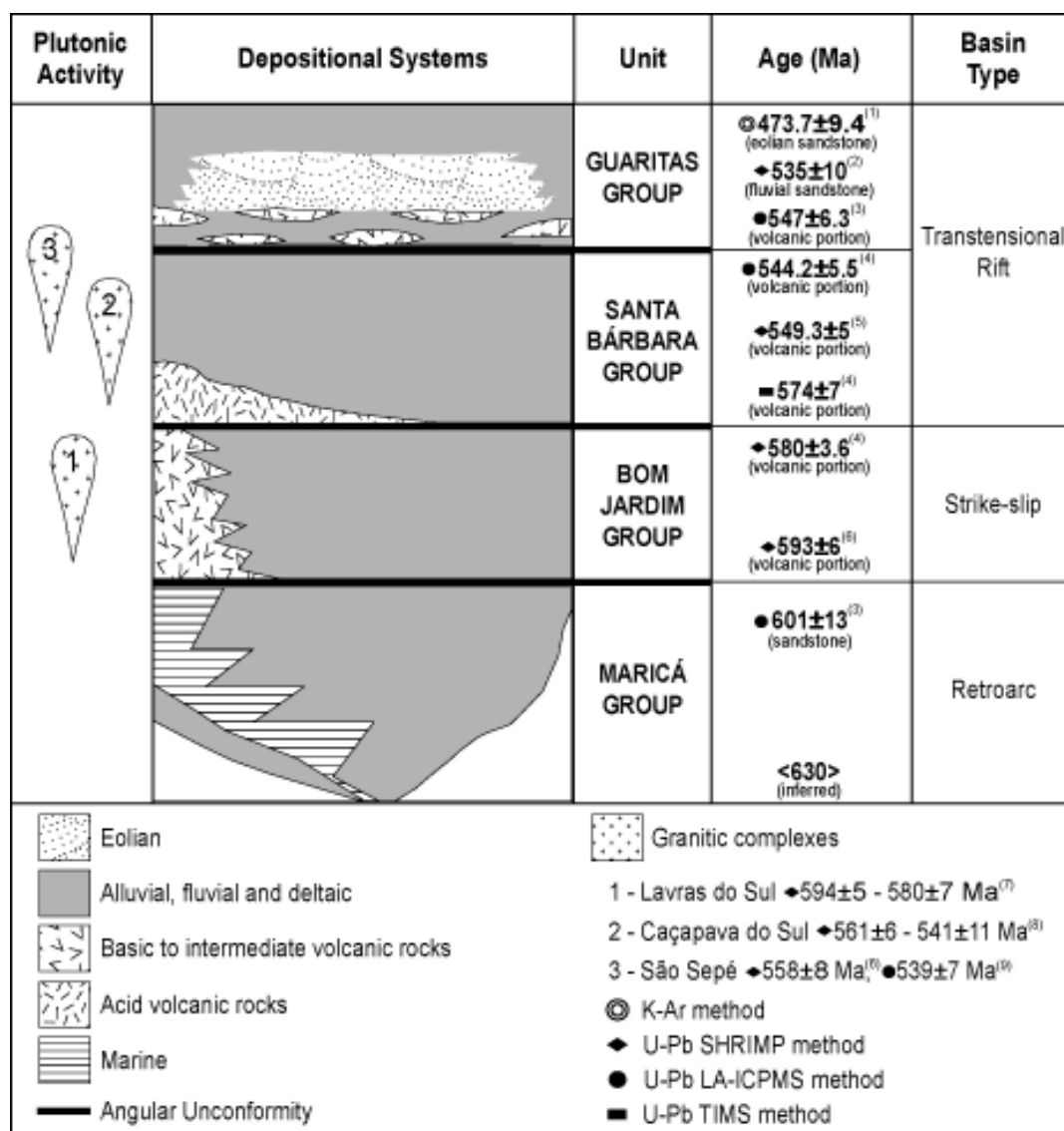
Fig. 8 - Summary of main basinal cycles of the Camaquã Basin units with contemporary igneous events. Reference ages: (1) Maraschin et al., 2010; (2) Hartmann et al., 2008b; (3) Almeida et al., 2012; (4) Janikian et al., 2012; (5) Sommer et al., 2005; (6) Remus et al., 1999; (7) Remus et al., 2000a; (8) Leite et al., 1998; (9) Gastal et al., 2010.

c.   **574 ± 7 to 544.2 ± 5.5 Ma – The Acampamento Velho Formation and the Santa Bárbara Group.** In this work we include in the same basinal cycle the Acampamento Velho Formation (Ribeiro and Fantinel, 1978) and the Santa Bárbara Group (as described by Paim et al., 2000 and Borba and Mizusaki, 2003). The

Acampamento Velho Formation is composed of basal volcanic acid rocks of alkaline affinity (lava flows, ignimbrites and related volcanoclastic rocks) and a local occurrence of andesitic basalts. The thickness of the Acampamento Velho Formation is estimated to be 500 m (Paim et al., 2000). These units have been dated by U-Pb zircon and present ages of 549.3 ± 5 Ma on rhyolites (Sommer et al., 2005) and 553 ± 5.4 Ma on the andesitic basalt portion (Almeida et al., 2012) of the Acampamento Velho Formation in the Ramada sub-basin (Fig. 2). Janikian et al. (2012) obtained ages of 574 ± 7 Ma for rhyolitic rocks from the Ramada sub-basin and 544.2 ± 5.5 Ma for lapilli tuffs from the Taquarembó sub-basin (Fig. 2). The Santa Bárbara Group is composed of three sedimentary cycles (sub-units), which were defined by Borba and Mizusaki (2003) as Sequences I, II and III (Fig. 4) and which are represented by alluvial fans and fan-delta fronts, and lacustrine, sandy braided and gravel-bed braided facies associations. Sequence I paraconformably deposited volcanic and volcanic-clastic rocks with an estimated thickness of 800-100 m on the Acampamento Velho Fm. It is composed of alluvial facies associations with a large contribution of volcanic fragments (mainly of basal rhyolites from the Acampamento Velho Formation and shoshonitic andesites of the Hilário Formation). A transgressive depositional system represented by fan-delta fronts and lacustrine deposits occurs on the alluvial facies sedimentary rocks. Sequence II is approximately 1100 m thick and is paraconcordant on Sequence I, represented by basal braided fluvial sediments, intermediated fan-deltas, lacustrine deposits and upper progradational sediments. Sequence III occurs in low angle unconformity on Sequence II, suggesting a rearrangement of the basin; it is ca. 200-300 m thick and formed by gravel braided fluvial. According to Bicca et al. (2010), the maximum depositional age of the Santa Bárbara Group is 558 ± 13 Ma based on a detrital zircon determination using sandstone from the Bom Jardim Window (Fig. 5).

547 ± 6.3 to 473.7 ± 9.4 Ma – The Guaritas Group. Originally described by Goñi et al. (1962), the Guaritas Group is approximately 800 m thick and comprises sediments; it represents the last depositional episode preserved in the Camaquã Basin. The sedimentary rocks were deposited trending N40E in a transtensional rift basin (Chemale Jr., 1993; Borba, 2006) with the eastern border delimited by the Santana Dome (Encantadas Complex). The Guaritas Group is composed of two formations from the base to the top, the Pedra Pintada and the Varzinha, which are

bounded by an erosive unconformity (Fig. 4). De Ros et al. (1994) believed that the Guaritas Group sedimentation was deposited in an arid to semi-arid climate based on eodiagenetic features.
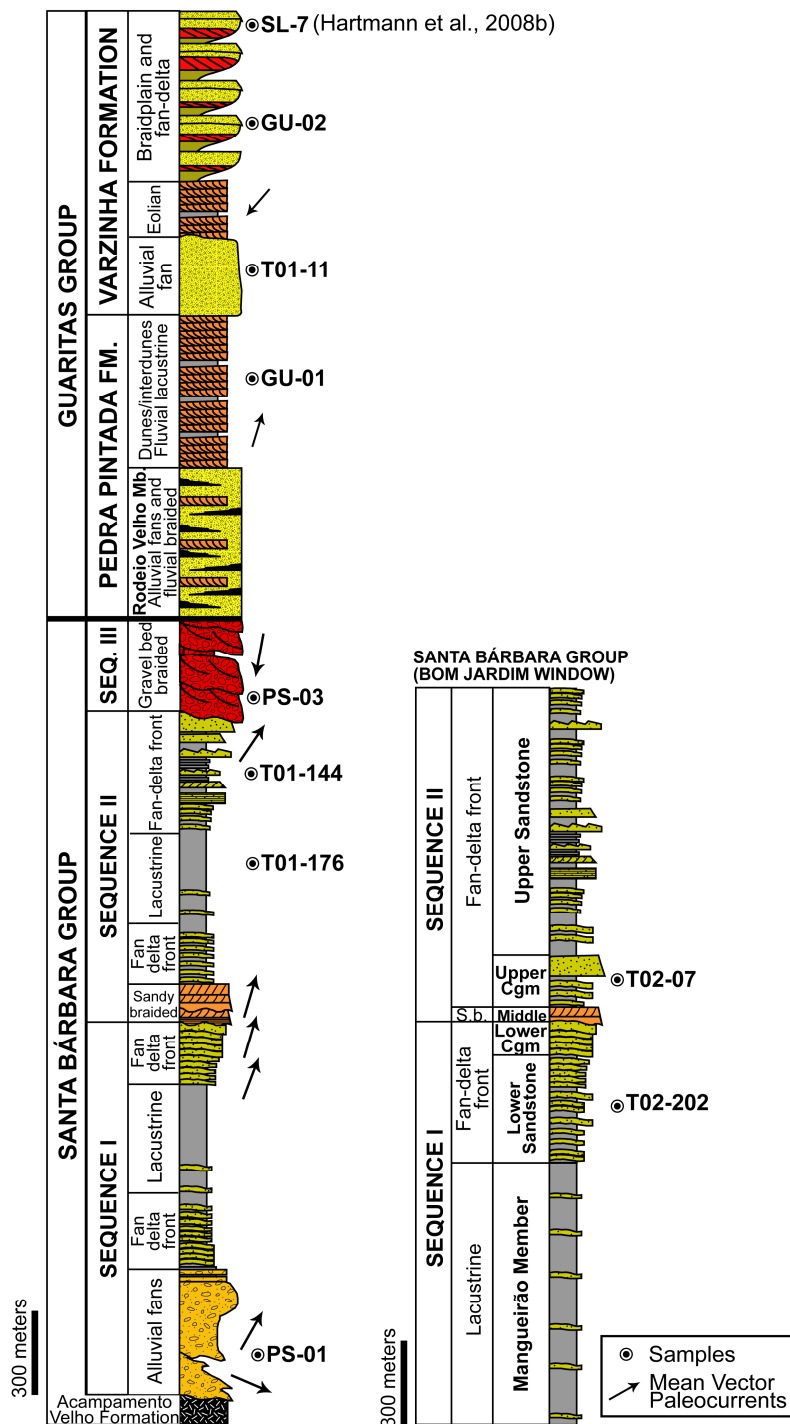
Fig. 9 - Simplified stratigraphic column of the Santa Bárbara and Guaritas groups and the sample location (modif. from Paim and Scherer, 2007; Borba and Misuzaki, 2003).

The Pedra Pintada Formation overlies the Santa Bárbara sedimentary rock in an angular unconformity in which the Guaritas Group units dip ca. 5 degrees and the top of the Santa Bárbara units dips 15-30 degrees NW (Fig. 5). The Pedra Pintada Formation, which is 400 m thick, comprises dunes, interdunes and fluvial-lacustrine facies associations. The paleocurrents of this formation indicate dune fields migrating parallel to the NE trend of the basin in a semi-arid climate (Paim, 1994; Paim and Scherer, 2007). Laterally, near the eastern edge of the Guaritas basin, conglomerates and sandstones replace the eolian accumulations and represent contemporary alluvial fans that developed along the active margin of the basin (Almeida et al., 2009; Marconato et al., 2009). Intercalated at the base of fluvial and eolian facies of this formation are volcanic rocks known as "Rodeio Velho Andesite".

The Varzinha Formation units are deposited concordantly on the Pedra Pintada units. The formation is ca. 400 m thick, and its sedimentation is composed predominantly of sediments of alluvial and eolian facies associations at the base and is covered with lacustrine associations and associated deltas. The upper section of the Varzinha Formation corresponds to a set of paragradational parasequences of deltaic origin with desiccation features and precipitation of calcretes and silcretes (De Ros et al., 1994). The deltaic systems present westward paleocurrents (Paim, 1995; Paim et al., 2000); the paleocurrent data from the eolian facies of this formation indicate a pattern of SSW winds, which entails a paleowind inversion relative to the eolian strata of the Pedra Pintada Formation (Paim and Sherrer, 2007).

The youngest zircon from the basal "Rodeio Velho Andesite" has been dated to 547 ± 6.3 Ma (U-Pb method, Almeida et al., 2012), whereas an authigenic illite from an eolian sandstone (top of Pedra Pintada Fm.) was dated to 473.7 ± 9.4 Ma (K-Ar method, Maraschin et al., 2010). According to Hartman et al. (2008b), the obtained U-Pb age from a detrital zircon from the upper section of the Guaritas Group (Varzinha Formation) should correspond to the onset of the Guaritas deposition at 535 ± 10 Ma. The present data suggest that the deposition of the Guaritas basin occurred between 547 ± 6.3 Ma and 473.7 ± 9.4 Ma.
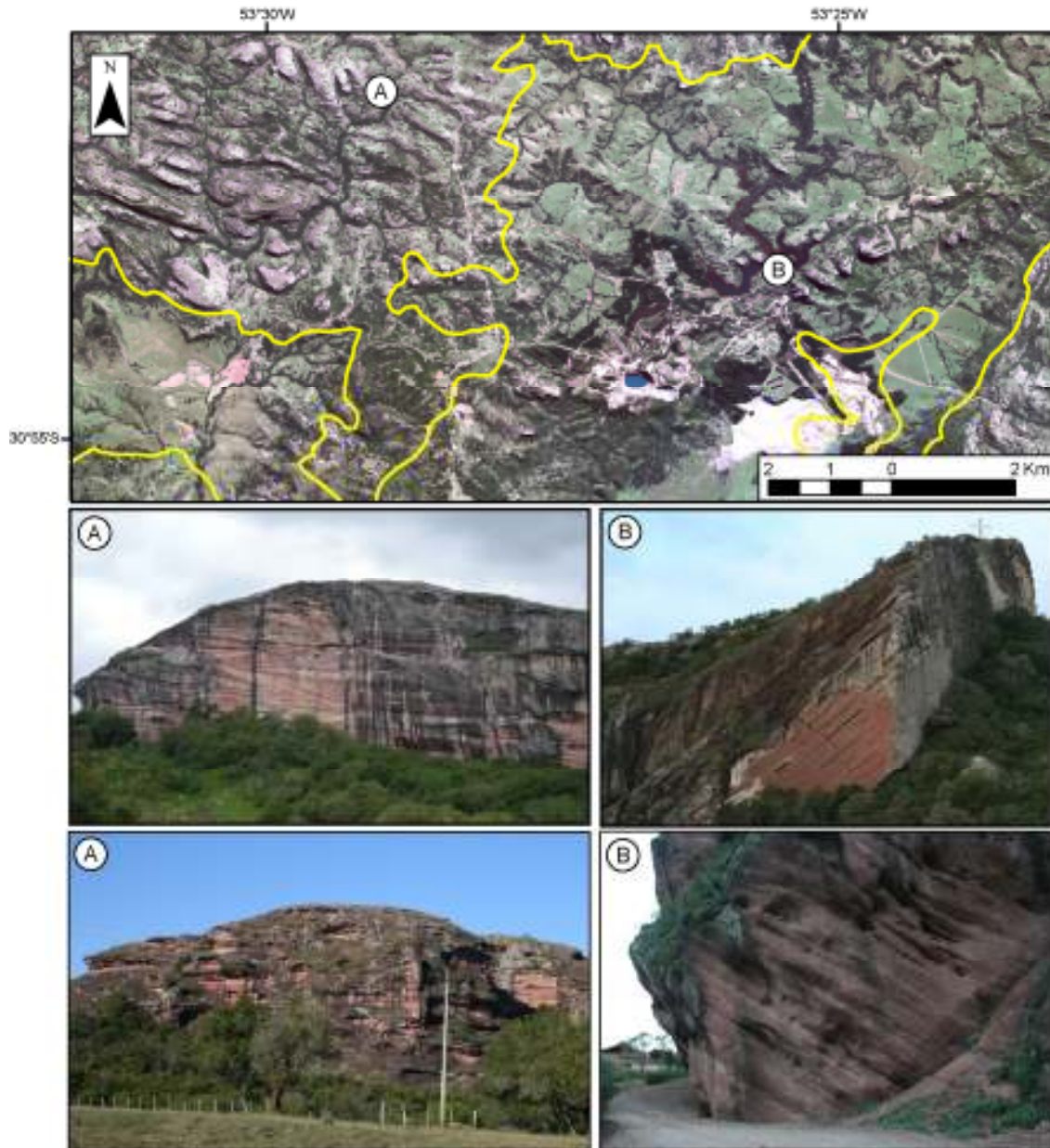
Fig. 10 - Close limits of Santa Bárbara and Guaritas Group rocks in angular unconformity at the Bom Jardim Window. A) Guaritas Group units dip ca. 5 degrees. B) Santa Bárbara Group units dip 15-30 degrees to NW.

The Santa Bárbara and Guaritas groups were both formed in a continental environment under the influence of the late left-handed strike-slip tectonics (Chemale Jr., 2000) or late stages of the lateral escape tectonics of the Dom Feliciano Belt (Tommasi et al., 1994) during the final agglutination of the Western Gondwana. In this context, the Santa Bárbara and Guaritas groups may be interpreted as individualized rift basins that developed in a transtensional environment (Chemale

Jr., 1993; Borba, 2006) separated by Caçapava High and, according to Borba (2006), have similar evolutionary models (Fig. 6).
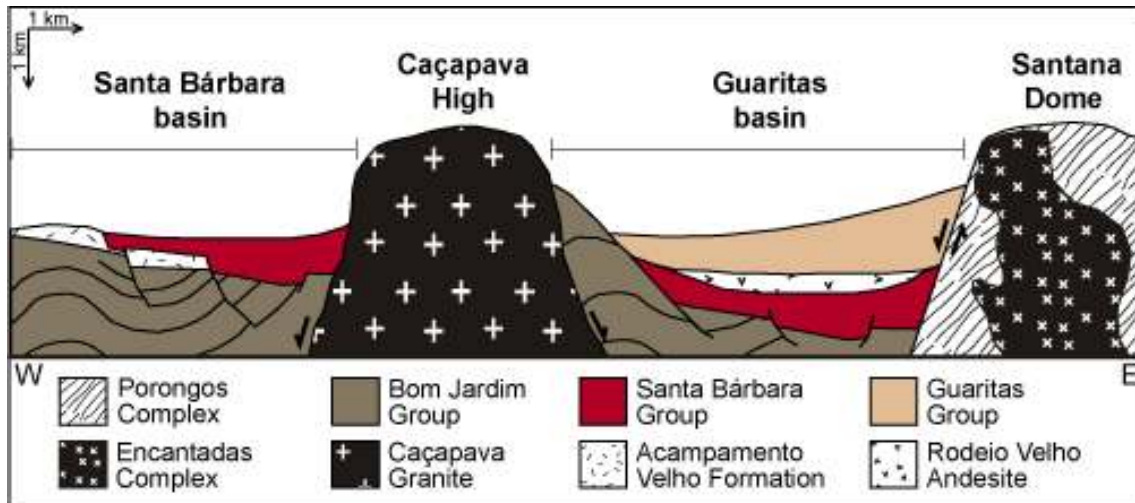
Fig. 11 - Schematic evolution of the Santa Bárbara and Guaritas basins.

3. Sampling and Analytical Methods

Four outcrop samples and five hole samples were collected from the Guaritas and Santa Bárbara basins for U-Pb and Lu-Hf analysis. The stratigraphic position and sample location are shown in Figs. 4 and 1, respectively. The conglomerate samples from the Santa Bárbara basin were collected in two regions (Fig. 1), the Pedra do Segredo region (PS-01) and the region east of the Pedra do Segredo Fault (PS-03), near the edge of the Caçapava High. The PS-01 sample comprises conglomerates with normal grading, cross bedding and subrounded clasts, representing the facies association (Borba and Mizusaki, 2003) of the gravel-bed braided river deposits of Sequence III. The PS-03 sample is a matrix-supported disorganized conglomerate with a red sandy matrix and angular clasts composed predominantly of quartzite and metavolcanic greenschists, representing the alluvial fans deposited on the eastern edge of the basin of Sequence I. One sample was collected near the eastern edge of the Guaritas basin for each representative formation of the group (Figs. 1 and 4). GU-01 is a sandstone eolian of the Pedra Pintada Formation, and GU-02 is a conglomerate of the deltaic facies association of the Varzinha Formation. The borehole CQP-01, made by Geological Survey of Brazil (CPRM), is located southeast of Caçapava do Sul city and has a depth of 1200 meters. We collected three samples

from CQP-01: T01-11, T01-144 and T01-176. Sample T01-11, obtained from a depth of 41 m, is a medium micaceous sandstone color board with granules and pebbles of quartzite and granite rocks that belong to the Varzinha Formation (alluvial-fan facies) of the Guaritas basin. Sample T01-144, obtained from a depth of 569 m, is a medium to fine micaceous sandstone color board with ripple marks that belongs to the fan-delta front facies of Sequence II of the Santa Bárbara basin. Sample T01-176, obtained from a depth of 729 m, is a medium to fine micaceous sandstone color board with ripple marks that is intercalated with medium sandstone pink, representing the lacustrine facies of Sequence II of the Santa Bárbara basin. Borehole CQP-02 is located in the Uruguai Mine (Minas do Camaquã) in a region known as the Bom Jardim Window and has a depth of 1200 meters. As reported by CPRM, the CPQ-02 hole has copper mineralization in the form of chalcopyrite, bornite and calcosina. We collected two samples from different depths, T02-07 and T02-202. The sample T02-07, obtained from a depth of 27 m, is a pink conglomerate with chloritic pebbles and beads of granite, quartz and gneiss, representing the fan-delta front facies of Sequence II of the Santa Bárbara basin. Sample T02-202, obtained from a depth of 926 m, is a greenish-gray micaceous siltstone and represents the fan-delta front facies of Sequence I of the Santa Bárbara basin.

The samples, each weighing approximately 5 kg, were crushed, pulverized and sieved for zircon separation at the Rio Grande do Sul Federal University (UFRGS) in Brazil. The zircon grains were concentrated by conventional magnetic heavy-liquid and then approximately 200 zircon grains were handpicked and mounted in epoxy resin. The mounts were polished using different granulometric diamond pastes to expose internal surfaces. The grains used for zircon dating were imaged with backscattered electrons to determine their internal structure and crystallization phases (Fig. 7). Only zircon grains free of imperfections, fractures and mineral inclusions were selected for analysis. Analyses using the isotopes U-Pb and Lu-Hf were conducted at the Geochronology Laboratory of the University of Brasília (UnB - Brazil) by LA-MC-ICPMS. The U-Pb isotopic data were acquired using the static mode with a diameter of 30 μm. The Lu-Hf isotope data were acquired in the same site or phase of zircon grain previously analyzed by the U-Pb method. Details of analytical procedures U-Pb and Lu-Hf in zircon are described by Chemale et al. (2011, 2012).

The U-Pb and Lu-Hf analytical data of the analyzed samples are in the supplementary material as Table 1 and 2. The results were integrated with the geological, isotopic, and geochronological data available in the literature.
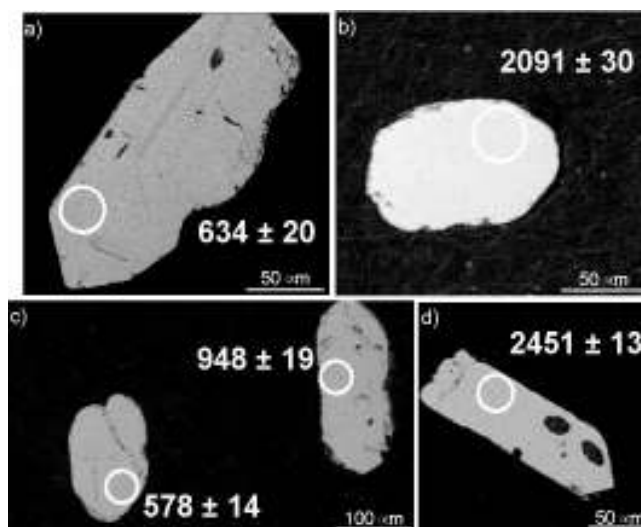
Fig. 12 - Backscattered electron images of zircon grains that are representative of the analyzis with LA-MC-ICP-MS. The spots (white circles) and the measured U-Pb concordia ages are indicated. The samples are (a) GU-01, (b) GU-02, (c) PS-01, and (d) PS-03.

4. Results

4.1. The PS-01 and PS-03 Samples

A total of 60 zircon grains for each sample were dated by the U-Pb method, totaling 120 zircon grains (Table 1). Twelve of these grains were highly discordant for the PS-01 sample, and 12 grains of the PS-03 sample were also discordant. Based on the results of the concordant ages, a concordant diagram was generated for each sample (Fig. 8).

The results obtained for the 48 concordant grains show that the ages of the PS-01 sample range from 567 Ma to 2760 Ma, with two dominant populations. In the first, 47% of the zircons derived from Neoproterozoic rocks (aged from 567 and 947 Ma) and, in the second, 41.7% of the zircons derived from Paleoproterozoic rocks (aged from 1664 and 2436 Ma). Additionally, 8.3% are Mesoproterozoic grains, and the only zircon grain is Archean (2.76 Ga).
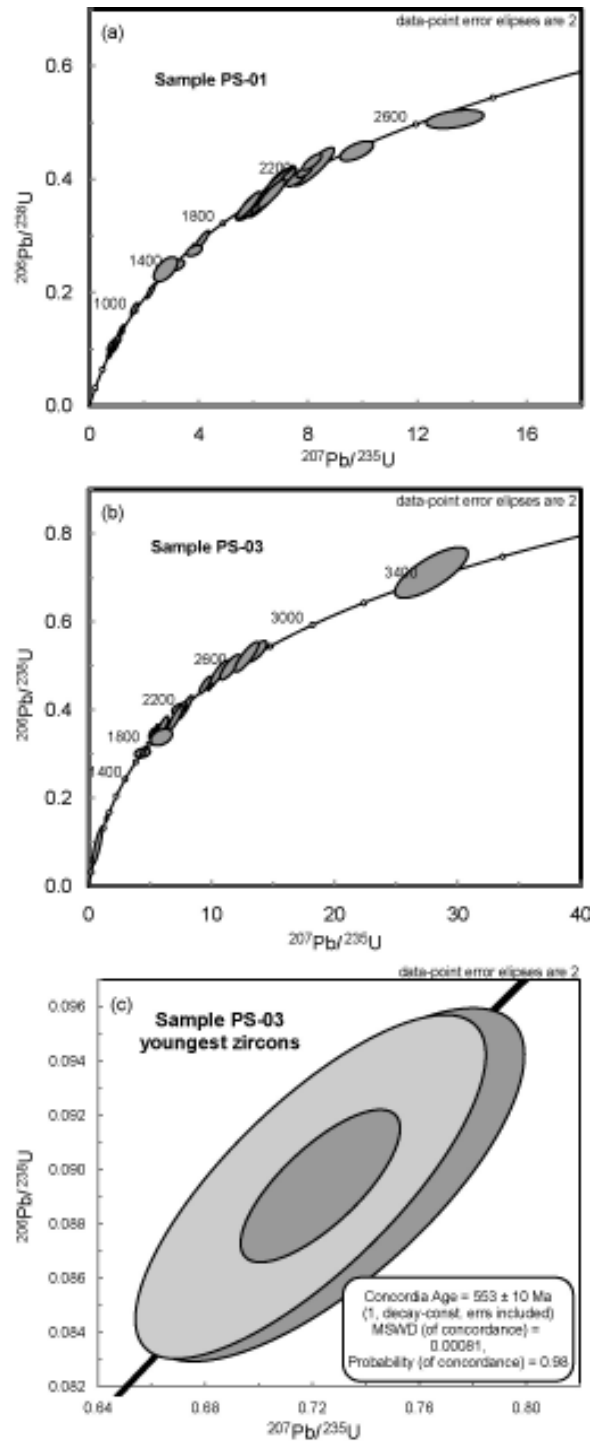
Fig. 13 - U-Pb concordia data diagram for the Santa Bárbara basin. (a) U-Pb concordia data diagram for the PS-01 sample; (b) U-Pb concordia data diagram for the PS-03 sample; (c) U-Pb concordia data diagram with tracing considering only the youngest zircon ages for the PS-03 sample.

The PS-03 sample has ages ranging from 553 to 3389 Ma range, with two dominant populations. In the first population, 58.3% of the zircons derived from Neoproterozoic

rocks (aged between 553 and 947 Ma), and in the second, 33.3% of the zircons derived from Paleoproterozoic rocks (aged between 1728 and 2451Ma). The 2 youngest zircon grains from the sample give a concordia age dating to 553 ± 10 Ma (Fig. 8). Additionally, there are 4 Archean grains (dated to 2542-3389 Ma; constituting 8.3%).

Ten zircons from the PS-01 sample and 12 zircons from the PS-03, previously analyzed using the U-Pb method, were selected for Lu-Hf dating. As discussed above, the initial Hf composition of each zircon was calculated using the U-Pb age previously obtained on the same grain (Table 2). The zircon of Neoproterozoic U-Pb age presented negative εHf values, and only the zircon aged to 604 Ma presented positive εHf values. For these zircons, the TDM Hf model ages are predominantly Paleoproterozoic (0.77-2.61 Ga). The Paleoproterozoic zircons have negative and positive εHf values, with TDM ages between 1.96 and 2.98 Ga. The Archean zircons have TDM ages that are also Archean and have negative εHf values.

4.2. The GU-01 and GU-02 Samples

A total of 60 zircon grains were analyzed for each sample, totaling 120 zircon grains for all samples (Table 1). Eighteen zircon grains from the GU-01 sample and 20 zircon grains from the GU-02 sample were highly discordant. Based on the results of concordant ages, a concordant diagram for each sample was generated (Fig. 9).

The ages in the GU-01 sample range from 575 Ma to 2213 Ma. Of the 42 concordant zircon grains, 85.7% are Neoproterozoic (dated between 575 and 873 Ma), 9.5% are Mesoproterozoic (from between 1050-1530 Ma) and only one zircon was Paleoproterozoic (dated to 2213 Ma, Rhyacian age).

The ages in the GU-02 sample range from 565 Ma to 2812 Ma, with three dominant populations. In the first, 72.5% of zircons derived from Neoproterozoic rocks (dated from 565 to 828 Ma), 12.5% were from Mesoproterozoic zircons (dated from 1022 to 1496 Ma) and 22.5% zircons derived from Paleoproterozoic rocks (dated from 1986 to 2489 Ma). Archean zircons were also found with ages from 2.71 to 2.81 Ga.
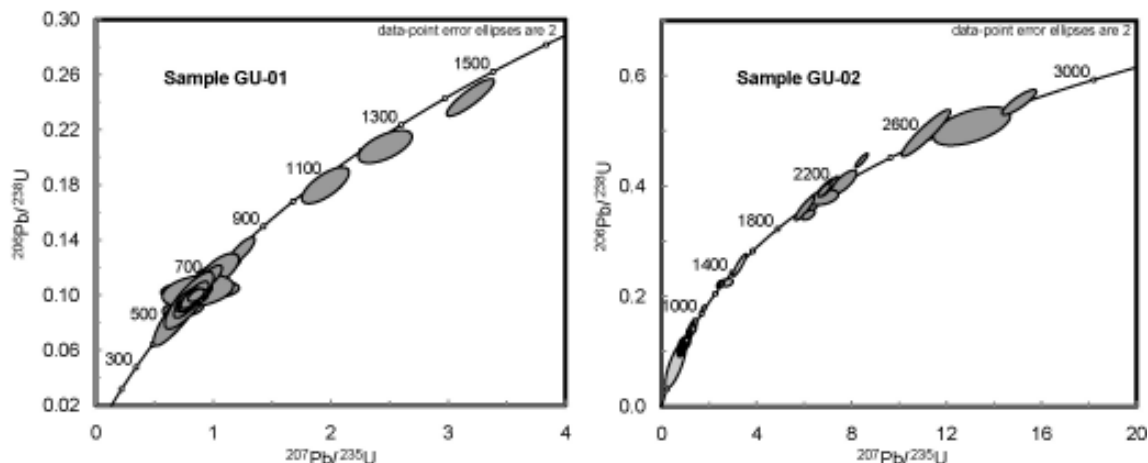
Fig. 14 - U-Pb concordia data diagram of zircon U-Pb ages for the GU-01
and GU-02 samples.

4.3. The T01-011 Sample

We determined the ages of 124 zircon grains, of which 32 were discordant (Table 1). The ages for this sample range from 556 to 3273 Ma. Of the 92 concordant crystals, 37% of the zircons derived from the Neoproterozoic (dated from 556 to 862 Ma), 51% were from the Paleoproterozoic (dated from 1673 to 2476 Ma), 9.8% are from Archean rocks (dated from 2551 to 3273 Ma) and 2 zircons are Mesoproterozoic (1121 and 1212 Ma).

Thirty zircons from the T01-11 sample, previously analyzed using the U-Pb method, were selected for Lu-Hf dating. The initial Hf composition of each zircon was calculated using the U-Pb age previously obtained on the same grain (Table 2). The Neoproterozoic zircons have dominantly negative εHf values, and only the zircon from 749 Ma is εHf positive. The TDM ages for these zircons are predominantly Paleoproterozoic (1673-2476 Ma). The two Mesoproterozoic zircons analyzed present positive εHf values and TDM ages from 1.57 Ga to 1.66 Ga. The Paleoproterozoic zircons have dominantly negative εHf values, with only two zircons showing mildly positive values and with Archean TDM ages. The Archean zircons have Archean TDM ages with negative εHf values.

4.4 The T01-144 Sample

A total of 115 zircon grains were dated by the U-Pb method, and 31 grains are discordant (Table 1). The ages for this sample are limited from 535 to 2824 Ma, with two dominant populations. In the first, 66.6% of the zircons derived from Neoproterozoic rocks (dated from 535 to 910 Ma) and 27.4% of the zircons derived from Paleoproterozoic rocks (dated from 1657 to 2367 Ma). Additionally, there were three Mesoproterozoic grains and two Archean zircons.

4.5 The T01-176 Sample

Of the 103 zircon grains analyzed by the U-Pb method, 34 are highly discordant (Table 1). The ages for this sample are limited from 564 to 2867 Ma, with 82.6% zircons derived from Neoproterozoic rocks (dated from 564 to 963 Ma). Additionally, 14.5% zircons derived from Paleoproterozoic rocks (dated from 1722 to 2346 Ma), one derived from Mesoproterozoic rocks (1116 Ma), and one derived from Archean rocks (2867 Ma).

4.6 The T02-07 Sample

Of the 125 zircon grains analyzed by the U-Pb method, 36 are discordant (Table 1). The ages for this sample are limited from 555 Ma to 2687 Ma, with two dominant populations. In the first, 59.6% of the zircons derived from the Neoproterozoic (dated from 555 to 837 Ma) and 33.7% were derived from Paleoproterozoic rocks (dated from 1748 to 2212 Ma). Additionally, 4.5% of the zircons are derived from Archean rocks and two grains derived from Mesoproterozoic rocks.

Twenty-four zircons that were previously analyzed by the U-Pb method were selected for Lu-Hf dating (Table 2). The U-Pb age of the zircons from the Neoproterozoic have high negative εHf values (with a mean of -20 to -30), with Paleoproterozoic TDM ages from 1.82 to 2.62 Ga. The Paleoproterozoic zircons have negative εHf values and TDM ages that are predominantly Archean. Only one Archean zircon was

analyzed with the Lu-Hf method, presenting a negative εHf value and an Archean TDM age.

4.7 The T02-202 Sample

A total of 113 zircon grains were dated by the U-Pb method from this sample, and only 45 grains are concordant because of the large amount of common lead (Table 1). The ages for this sample are limited from 542 to 2439 Ma, with only one dominant population, represented by 93% of the zircons and deriving from Neoproterozoic rocks (dated from 542 to 825 Ma). Additionally, there is one Mesoproterozoic grain (1213 Ma) and two Paleoproterozoic grains (from 2413 to 2439 Ma, Syderian ages).

5. Discussion

The integration of the geological data, U–Pb zircon dating (Fig. 10), and Sm–Nd and Lu–Hf radiogenic isotope geochemistry provides insight into the depositional age, provenance, and tectonic setting of the Santa Bárbara and Guaritas basins. Some implications of the results presented in this paper are discussed below.
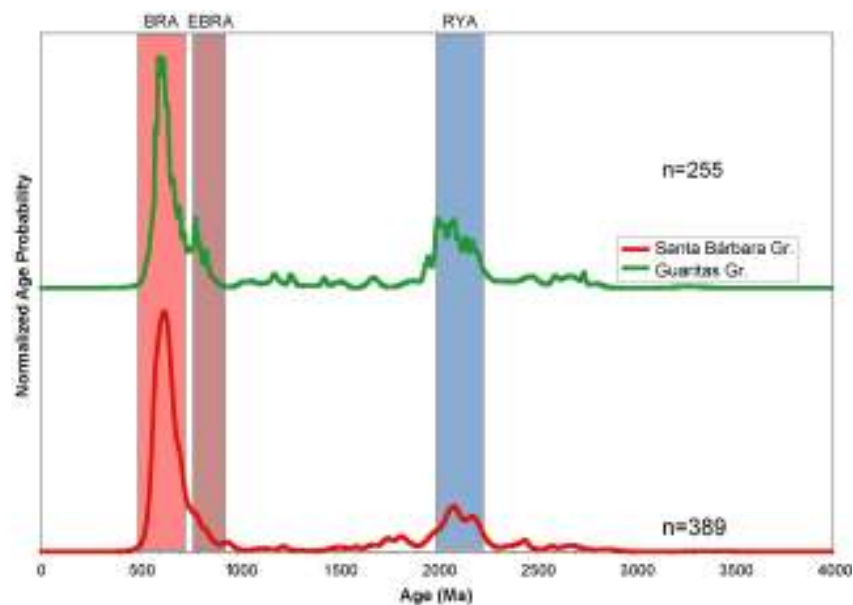
Fig. 15 - Frequency histograms of zircon U-Pb ages, Santa Bárbara and Guaritas groups.

Depositional age of the Santa Bárbara and Guaritas groups

In our study, we determined consistent zircon ages for the Santa Bárbara Group that define the maximum depositional age of this group. Until now, the rocks of the Bom Jardim Window were described as belonging to either the Bom Jardim Group (593-580 Ma, Paim et al., 2000) or to the Santa Bárbara Group (570-540 Ma, Janikian et al., 2012). In the CQP-02 hole, the presence of one concordant zircon dated to 542 ± 36 Ma. Despite this error, rocks from the Bom Jardim Window are definitely included in the Santa Bárbara Group; in the PS-03 sample there are zircons with a concordant age of 553 ± 10 Ma, which are similar to those zircon ages found by Bicca et al. (2010) in the Bom Jardim Window. However, we should use the results of two or more of the youngest zircons of the dated samples to define the following maximum depositional age for each sample of the Santa Bárbara Group: T01-144 = 550 ± 59 Ma, T01-202 = 552 ± 44 Ma, and PS-03 = 553 ± 10 Ma. The Pb-Zn- and Cu-hosted sedimentary rocks of the Bom Jardim Window, in which the main Pb-Zn and Cu (Au) mineralization of the Dom Feliciano Belt are located, are cronocorrelate to the Santa Bárbara Group rocks situated in the Santa Bárbara valley west of the Caçapava High.

The samples from the Guaritas Group (from this study and from Hartmann et al., 2008b) present the youngest zircons, dated to 536 ± 98 Ma and 535 ± 10 Ma, from the upper section of the Guaritas Group. The K-Ar results presented by Maraschin et al. (2010) suggested ages as young as 473.7 ± 9.4 Ma. The present data indicate that the minimum depositional age for the Varzinha Formation is 473.7 ± 9.4 Ma and the maximum depositional age is 535 ± 10 Ma. The basal section of the Pedra Pintada Formation has only the U-Pb zircon age of andesite Rodeio Velho (547 ± 6 Ma), thus, this age is defined as the maximum depositional age for the base of the Guaritas Group.

Sedimentary provenance of the Santa Bárbara and Guaritas groups

The Sm-Nd data (Borba et al., 2003) of the Santa Bárbara Group show εNd (for t=550 Ma) and TDM ranging from -1.3 to -7.7 and 0.99 Ga to 1.75 Ga, respectively.

The εNd values (for t=540) and Nd Model ages (TDM) of Guaritas Group sample (Borba et al., 2003) vary from -5.8 to -7.5 and 1.38 Ga to 1.47 Ga, respectively. This result suggests that the Nd isotope signature for the sedimentary rocks of both groups formed with a contribution of Paleoproterozoic and Neoproterozoic rocks, as previously suggested by Borba et al. (2003).

However, the U-Pb detrital zircon ages of the Santa Bárbara and Guaritas Group indicate that there are two main age groups, the Trans-Amazonian (Rhyacian) and Brasiliano (Neoproterozoic to Eopaleozoic), as previously suggested by Hartmann et al. (2008b), who analyzed a single sample of the upper section of the Guaritas Group. These authors previously identified the presence of these two main orogenic crustal growth cycles in the crystalline rocks of southernmost Brazil. However, the main differences between these two stratigraphic units are the following: (i) there is a larger contribution of Brasiliano zircons in the Santa Bárbara Group samples; (ii) there is a larger contribution of Paleoproterozoic zircons and some Mesoproterozoic zircons in the Guaritas Group units; and (iii) some zircons formed between 800-700 Ma (Early Brasiliano) and the local Archean are present in the Guaritas Group. The larger contribution of the Paleoproterozoic zircons and the early Neoproterozoic and Mesoproterozoic zircons characterized in the Guaritas Group compared to lower the lower contributions in the Santa Bárbara Group samples indicates a stratigraphic inversion during sedimentation, therefore suggesting that older Paleoproterozoic rocks were exposed and denudated during the Guaritas deposition.

By analyzing the paleocurrent measurements of the sedimentary rocks of both groups (data of Borba and Mizusaki, 2003; Paim et al., 2000; Fambrini et al., 2007), we observe that there are two different patterns during the deposition of the Santa Bárbara units (Fig. 11). In the first pattern, located to the west of the Caçapava High, the paleocurrent flowed eastward during the deposition of Sequences I and II and to the west during Sequence III. On other side of the Caçapava High, the Santa Bárbara units only outcrop in the Bom Jardim Window, in which the paleocurrent flowed to the north during Sequence I and eastward during Sequence II. The integration of this information with the U-Pb zircon data suggests that the most probable sources for the Santa Bárbara units are the Paleoproterozoic gneissic and

Neoproterozoic granitic rocks of the Taquarembó Block. Thus, the Brasiliano granitic bodies were the main source for the sediments of the Santa Bárbara Group.
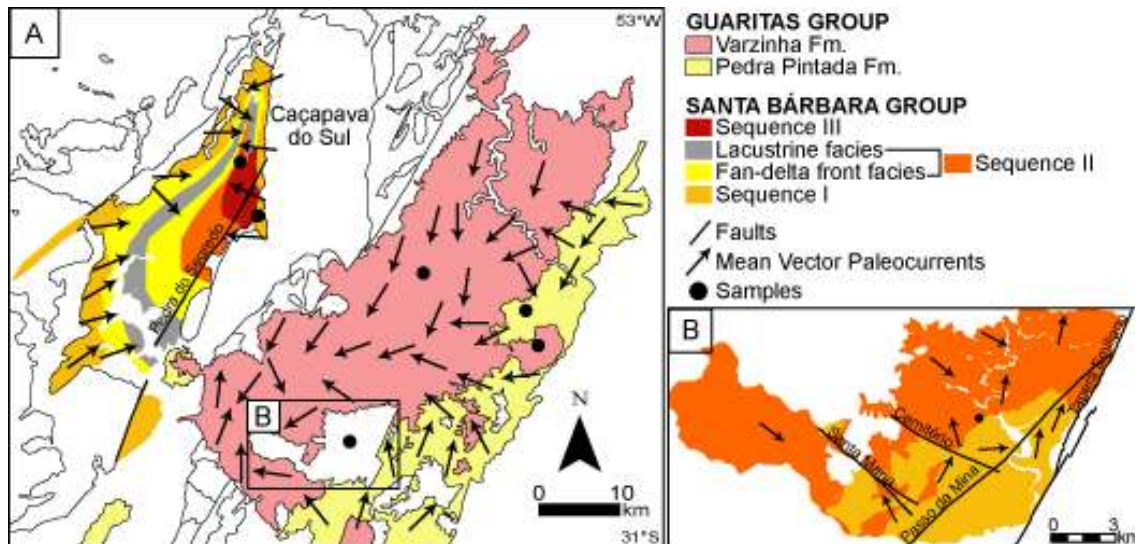
Fig. 16 - A) Paleocurrent map of the Santa Bárbara and Guaritas basins (modif. from Borba and Mizusaki, 2003; Paim et al., 2000). B) Paleocurrent map of Bom Jardim Window with (modif. from Fambrini et al., 2007).

The Guaritas units present distinct paleocurrent patterns in which the major sedimentary influx in the basin occurred to the south and west and was controlled by the master fault situated at the eastern margin of the Guaritas sub-basin. The increase in the Paleoproterozoic zircon contribution and the presence of Mesoproterozoic (1.5-1.7 Ga) and Early Neoproterozoic (0.7-0.8 Ga) zircons are thus related to the source area of the Tijucas Terrane, comprising Neoproterozoic to Early Paleozoic units of the Metamorphic Porongos Complex and the Paleoproterozoic Santana Dome rocks, and rocks from the Pelotas Batholith, both of which are situated east of the Guaritas sub-basin (Fig. 1).

Brasiliano ages are attributed to the rocks from the pre- to post-collisional granites (650-550 Ma) of the Dom Feliciano Belt exposed in the Taquarembó Terrane, Tijucas Terrane and Pelotas Batholith as well as to the volcanic rocks of the Hilário Formation (593 ± 6 Ma) and the Acampamento Velho Formation (570 to 550 Ma) and to the reworked sediments of the basal groups of the Camaquã Basin. The contribution of early Brasiliano zircons in the samples is likely due to volcanism from 0.8 to 0.7 Ga of the Porongos Complex, as described by Chemale Jr. (2000) and

Saalmann et al. (2011). Another important detail is that the Mesoproterozoic to Paleoproterozoic Hf model ages for the zircons date between 0.7 to 1.0 Ga (see below), confirming that most of the rocks come from the east. Thus, the rocks of the São Gabriel Terrane, in which there are juvenile Neoproterozoic zircons (Babisnki et al., 1997; Hartmann et al., 2011), must have been exposed only at the end of the Guaritas or even during the Paleozoic.

Mesoproterozoic U-Pb zircon ages are correlated to the Tijucas Terrane rocks, in which Gruber et al. (2008) described detrital zircon aging from metasediments between 1000-1550 Ma. The contribution of zircon Mesoproterozoic ages dating to approximately 780 Ma in the PS-01 sample suggests a contribution of rocks from the eastern Caçapava Granite that are correlated to the Porongos Complex and the Tijucas Terrane. This result indicates that the Caçapava Granite (the Caçapava High) was formed early in the process of uplift, not even setting a structural high to the formation of the Santa Bárbara sub-basin. In the PS-03 sample, the concentration of Archean zircon (8.3%) can be correlated to the Caçapava Granite and rocks of the Passo Feio Formation, where Archean zircon was found by Remus et al. (2000b).

Hf and Nd signature of the Santa Bárbara and Guaritas groups

The Lu-Hf model ages (TDM) show that the detrital zircons contain a dominantly Archean and Paleoproterozoic inheritance for both basins (Fig. 12), with dominantly negative εHf values, indicating a strong crustal origin for the zircons. The Brasiliano zircons have little radiogenic Hf and Mesoproterozoic and Paleoproterozoic model ages. Chemale Jr. (2000) and Saalmann et al. (2011) characterize the units of the São Gabriel Terrane, situated west of the Santa Bárbara and Guaritas sub-basins, as a typical juvenile Neoproterozoic Terrane. On the eastern side, the rocks of the Tijucas Terrane present an age similar to those of the São Gabriel Terrane but with a strong crustal component (Paleoproterozic). The Lu-Hf isotope data of the detrital zircon combined with the U-Pb age thus provided substantial proof for the eastern provenance of the Guaritas Group units, with source areas from the Porongos Complex and the Pelotas Batholith. In the Guaritas basin, the two Mesoproterozoic zircons have positive εHf values and Mesoproterozoic TDM ages, indicating juvenile

material correlated to Capivarita Anorthosite (Chemale Jr. et al., 2011). The juvenile zircons occur more frequently in the Paleoproterozoic material, occurring only locally in Brasiliano zircons.
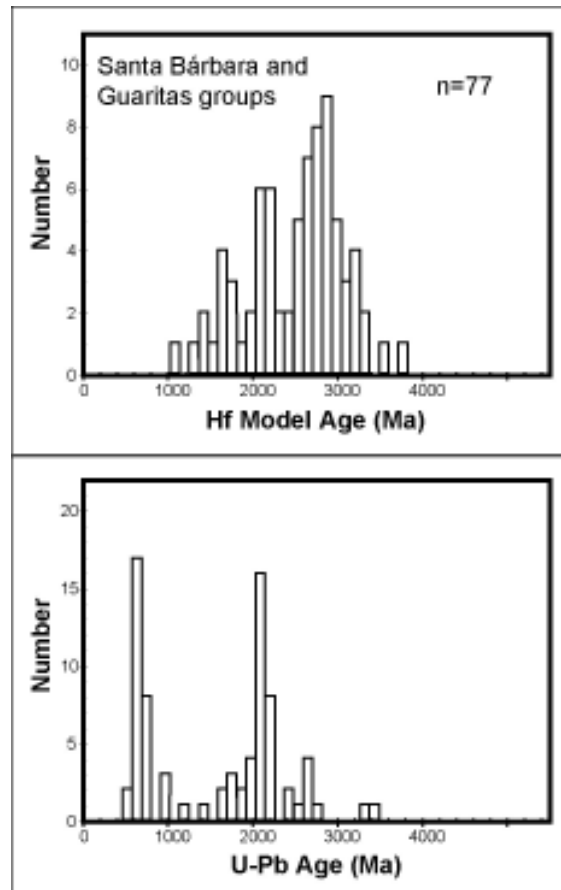
Fig. 17 - Frequency histograms of Hf model ages and zircon U-Pb ages, Santa Bárbara and Guaritas groups.

The diagram "U-Pb x Crustal Residential Time" (Fig. 13) indicates that Brasiliano and Paleoproterozoic sources fed the transtensional rifts of Santa Bárbara and Guaritas in greater proportion. In general, the Brasiliano zircons have little radiogenic Hf, as described above, and high crustal residence time (dated to 500 to 1500 Ma), suggesting that the source was formed from a Neoproterozoic subcontinental lithosphere, as described by Almeida et al. (2005) and Chemale Jr. et al. (2012) for rocks of the Dom Feliciano Belt. The few zircons from the Early Brasiliano Cycle have a Hf signature of crustal reworking, suggesting a volcanic source from the volcano-sedimentary Porongos Complex (0.7 to 0.8 Ga) with Paleoproterozoic Nd model ages (Chemale Jr., 2000; Saalmann et al., 2006).
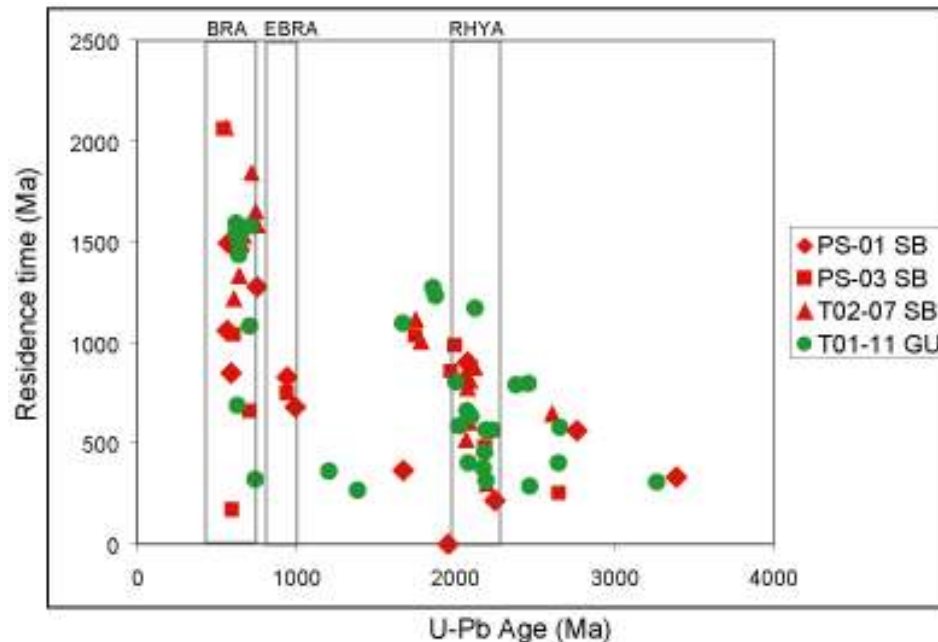
Fig. 18 - Residence time versus U-Pb crystallization age observed in the
Santa Bárbara and Guaritas Group sedimentary rocks.

The sedimentary rocks of the Santa Bárbara and Guaritas groups formed from a mixture of Paleoproterozoic and Neoproterozoic rocks, as shown by the Nd and U-Pb zircon ages. The main source areas for the Santa Bárbara Group are represented primarily by the Paleoproterozoic gneissic rocks and Brasiliano granites of the Taquarembó Terrane. The Guaritas Group samples have a U-Pb detrital zircon signature that indicates similar Paleoproterozoic and Neoproterozoic sources but with some differentiation related to the major contribution of Paleoproterozic material and a greater Early Brasiliano and Mesoproterozoic contribution. The Nd model ages (TDM) of the Guaritas Group are usually somewhat older than those of the Santa Bárbara rocks. These sources are thus identified as those of the Metamorphic Porongos Complex and the related Neoproterozoic granitic intrusion and underlying Paleoproterozoic granitic-gneissic Encantadas Complex, both situated to the east of the Guaritas Group units.

The source areas for the Santa Bárbara and Guaritas basins are the different terranes of the Dom Feliciano Belt and its basement, as confirmed by the diagram "Epsilon Nd x T" (Fig. 14), which shows that the evolution of these basins is similar to that of the Tijucas Terrane and the Pelotas Batholith. The evolution of the other units in the Camaquã Basin is also shown in the diagram, with an identical evolutionary

step for the Paleoproterozoic to Archean terranes and for the Maricá Group, as described by Borba et al. (2006). The Bom Jardim Group has two groups; the evolution of the first group is similar to that of the Tijucas Terrane, and the evolution of the second is similar to that of Pelotas/Tijucas.
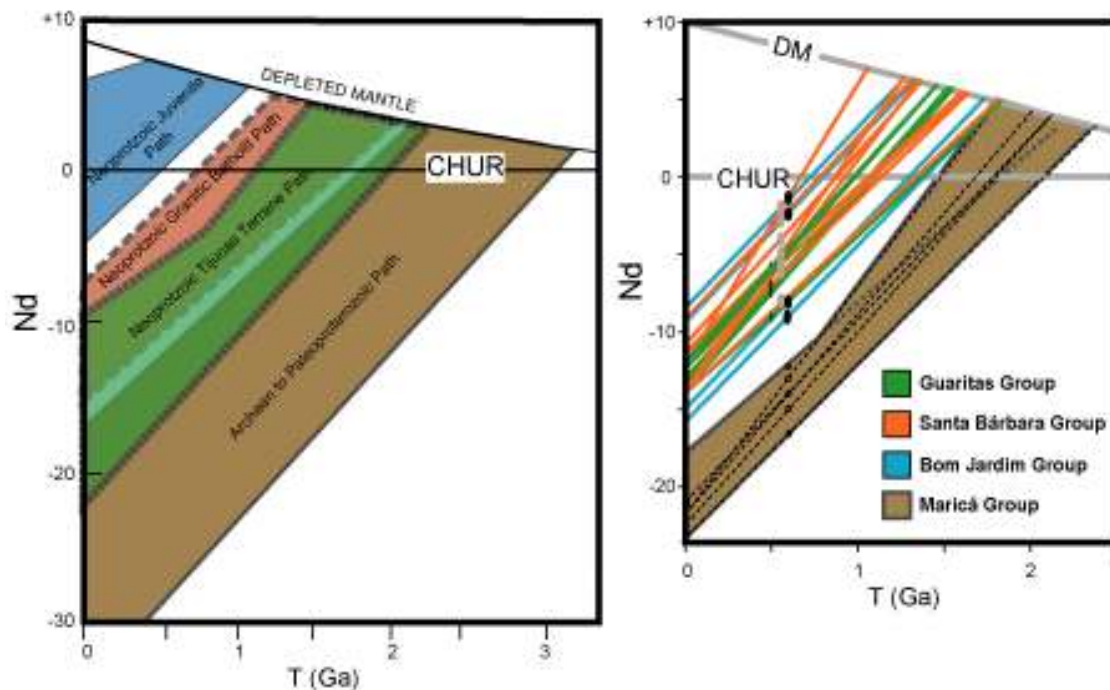
Fig. 19 - Diagram "Epsilon Nd x T" of the different terrains of the Dom Feliciano Belt and its basement and the Camaquã Basin units (data after Leite et al., 1998; Babinski et al., 1997; Phillip et al., 2003; Saalmann et al., 2006; Borba et al., 2003; Borba et al., 2006; Chemale et al., 2012).

Taking into account the Hf Model ages, the Neoproterozoic to Mesoproterozoic zircons range in age from 0.7 to 2.7 Ga, and the dominant Neoproterozoic (Brasiliano) zircons have a Paleoproterozoic signature. The Paleoproterozic zircons generally show Paleoproterozoic to Archean ages, suggesting magmatic sources of juvenile and recycled material for the Encantadas Complex (Chemale Jr., 2000; Hartmann et al., 2003) or Taquarembó Terrane (Hartmann et al., 2008a). The present data can be interpreted to mean that the sedimentary and magmatic rocks of the source areas for the Guaritas and Santa Bárbara groups are the products of a recycled lithosphere, as may be expected for a continental magmatic arc with a great participation of continental crust, such as is presented for the Sierra Nevada Batholith

or even suggested for the Eastern Granitic Belt of the Dom Feliciano Belt (including the Florianópolis, the Pelotas Batholith and the Cutillho Dionisio Terrane) by Chemale et al. (2012). In this study, we demonstrate that the zircon and Nd isotope information provides the magmatic events and/or recycled sedimentary material of the source areas, while the Hf isotope data adds information about the nature of the lithosphere involved in the generation of Brasiliano rocks.

6. Conclusions

An analysis of the data in this study leads to the following conclusions:

(1) The maximum depositional age of the Santa Bárbara basin is 553 ± 16 Ma, as constrained by the intrusion age of the Acampamento Velho Formation, and the minimum depositional age is 540 Ma.

(2) The maximum depositional age of the Guaritas basin is 547 ± 6 Ma (lower section) and 535 Ma (upper section). However, based on the K-Ar data, Maraschin et al. (2010) suggested a maximum depositional age of 473.7 ± 9.4 Ma (top of Pedra Pintada Formation).

(3) The source areas are marked by the ages of detrital zircons, with predominant rocks of the Brasiliano and Trans-Amazonian Cycle. From the base to the top, the contribution of Brasiliano zircon grains decreases the Santa Bárbara basin in favor of the Guaritas basin by increasing the number of Mesoproterozoic and Paleoproterozoic zircons.

(4) The U-Pb zircon data combined with paleocurrent information allow us to define the rocks of the eastern belts (Tijucas Terrane and Pelotas Batholith) and of the southern area of Paleoproterozoic and Brasiliano as the main source areas for these sediments. The contribution of Paleoproterozoic zircons and those of the Mesoproterozoic and Early Neoproterozoic define those terranes of the Tijucas Terrane, the Neoproterozoic Metamorphic Porongos Complex and Paleoproterozoic Santana Gneiss Dome as the main source areas for the Guaritas Group units.

(5) The Lu-Hf model ages (TDM) show that the zircons contain a dominant inheritance of Archean and Paleoproterozoic for the Santa Bárbara and Guaritas basins, with dominantly negative εHf values, indicating a strong crustal origin for the zircons. The Neoproterozoic zircons were most likely generated in older environments (Paleoproterozoic to Archean), but the data set in crustal residence and U-Pb zircon suggest contributions of younger rocks (Mesoproterozoic to Neoproterozoic) because the data of the Santa Bárbara and Guaritas groups include Nd model ages (0.99 to 1.75 Ga) that are younger than the Hf model ages.

Acknowledgments

REFERENCES

Almeida, D.P.M., Conceição, R., Chemale Jr., F., Koester, E., Borba, A.W., Petry, K., 2005. Evolution of Heterogeneous Mantle in the Acampamento Velho and Rodeio Velho Volcanic Events, Camaquã Basin, Southern Brazil. Gondwana Research 8 (4), 479-492.

Almeida, D.P.M., Chemale Jr., F., Machado, A., 2012 Late to Post-Orogenic Brasiliano-Pan-AfricanVolcano-Sedimentary Basins in the Dom Feliciano Belt, Southernmost Brazil. Petrology – New Perspectives and Applications, Tech-Open Acess Publisher, pp. 73-135.

Almeida, R.P., Janikian, L., Fragoso-Cesar, A.R.S., Marconato, A., 2009. Evolution of a rift basin dominated by subaerial deposits: The Guaritas Rift, Early Cambrian, Southern Brazil. Sedimentary Geology 217, 30–51.

Amelin, Y., Lee. D.-C., Halliday, A.N., 2000. Early-middle Archaean crustal evolution deduced from Lu-Hf and U-Pb isotopic studies of single zircon grains. Geochimica et Cosmochimica Acta 64 (24), 4205–4225.

Babinski, M., Chemale Jr., F., Hartmann, L.A., Van Schmus, W.R., Silva, L.C., 1996. Juvenile accretion at 750–700 Ma in southern Brazil. Geology 24, 439-442.

Babinski, M., Chemale Jr., F., Van Schmus, W.R., Hartmann, L.A., Silva, L.C., 1997. U-Pb and Sm-Nd geochronology of the Neoproterozoic granitic-gneissic Dom Feliciano Belt, southernmost Brazil. Journal of South American Earth Sciences 10, 263-274.

Basei, M.A.S., Siga Jr., O., Masquelin, H., Harara, O.M., Reis Neta, J.M., Preciozzi, F., 2000. The Dom Feliciano Belt of Brazil and Uruguay and its Foreland Domain, the Rio de la Plata Craton, framework, tectonic evolution and correlation with similar provinces of Southwestern Africa. In: Cordani, U., Milani, E.J., Campos, D.A. (Org.), Tectonic Evolution of South American Platform. SBG, Rio de Janeiro, v. 1, p. 311-334.

Bicca, M.M., Jelinek, A.R., Oliveira, C.H.E., Chemale Jr., F., Guadagnin, F., 2010. Estudos tectônicos da porção sul da bacia do Camaquã, região de Minas do Camaquã, RS. In: VI Congreso Uruguayo de Geologia e II Simposio Internacional del Neoproterozoico – Cámbrico de la Cuenca del Plata, Minas, pp. 34.

Bodet, F., Schärer, U., 2000. Evolution of the SE-Asian continent from U-Pb and Hf isotopes in single grains of zircon and baddeleyite from large rivers. Geochimica et Cosmochimica Acta 64 (12), 2067–2091.

Borba, A.W., Mizusaki, A.M.P., 2003. Santa Bárbara Formation (Caçapava do Sul, southern Brazil): depositional sequences and evolution of an Early Paleozoic post-collisional basin. Journal of South American Earth Sciences 16(5), 365-380.

Borba, A.W., Mizusaki, A.M.P., Silva, D.R.A., Kawashita, K., 2003. Razões Isotópicas 87Rb/86Sr, 87Sr/86Sr e 143Nd/144Nd como Traçadores de Proveniência de Rochas Sedimentares Siliciclásticas: Exemplos no Grupo Camaquã (Paleozóico inferior, RS, Brasil). Pesquisas em Geociências 30 (2), 39-50.

Borba, A.W., 2006. Evolução geológica da "Bacia do Camaquã" (Neoproterozóico e Paleozóico inferior do Escudo Sul-riograndense, RS, Brasil): uma visão com base na integração de ferramentas de esteatigrafia, petrografia e geologia isotópica. Ph.D. thesis, UFRGS, Porto Alegre, 110p.

Borba, A.W., Mizusaki, A.M.P., Silva, D.R.A., Koester, E., Noronha, F.L., Casagrande, J., 2006, Provenance of the Neoproterozoic Maricá Formation (Sul-rio-grandense Shield, Southern Brazil): Petrographic and Sm-Nd isotopic constraints. Gondwana Research 9, 464–474.

Borba, A.W. Mizusaki, A.M.P., Santos, J.O.S., McNaughton, N.J., Onoe, A.T., Hartmann, L.A., 2008. U–Pb zircon and 40Ar–39Ar K-feldspar dating of syn-sedimentary volcanism of the Neoproterozoic Maricá Formation: constraining the age of foreland basin inception and inversion in the Camaquã Basin of southern Brazil. Basin Research 20, 359–375.

Carvalho, P.F., 1932. Reconhecimento geológico no Estado do Rio Grande do Sul. Boletim do Serviço Geológico e Mineralógico do Brasil 66, 1-72.

Chemale Jr., F., 1993. Bacias molássicas brasilianas. Acta Geológica Leopoldensia 37, 109-118.

Chemale Jr., F., Hartmann, L.A.; Silva, L.C., 1995. Stratigraphy and Tectonism of Precambrian to Early Paleozoic Units. XVIII Acta Geológica Leopoldensia, 42, 5-117.

Chemale Jr., F., 2000. Evolução geológica do Escudo Sul-rio-grandense, in: Holz, M., De Roz, L.F. (Eds), Geologia do Rio Grande do Sul. CIGO/UFRGS, Porto Alegre, pp. 13-52.

Chemale Jr., F., Philipp, R.P., Dussin, I.A., Formoso, M.L.L., Kawashita, K., Berttotti, A.L., 2011. Lu–Hf and U–Pb age determination of Capivarita Anorthosite in the Dom Feliciano Belt, Brazil. Precambrian Research 186, 117–126.

Chemale Jr., F., Mallmann, G., Bitencourt, M.F., Kawashita, K., 2012. Time constraints on magmatism along the Major Gercino Shear Zone, southern Brazil: Implications for West Gondwana reconstruction. Gondwana Research 22 (1),184-189.

Condie, K.C., Beyer, E., Belousova, E., Griffinb, W.L., O'Reilly, S.Y., 2005. U–Pb isotopic ages and Hf isotopic composition of single zircons: The search for juvenile Precambrian continental crust. Precambrian Research 139, 42–100.

Davis, D.W., Amelin, Y., Nowell, G.M., Parrish, R.R., 2005. Hf isotopes in zircon from the western Superior province, Canada: Implications for Archean crustal development and evolution of the depleted mantle reservoir. Precambrian Research 140, 132–156.

De Ros, L.F., Morad, S., Paim, P.S.G., 1994. The role of detrital composition and climate on the diagenetic evolution of continental molasses: evidence from the Cambro-Ordovician Guaritas sequence, southern Brazil. Sedimentary Geology 92, 197–228.

DeCelles, P.G.,Giles, K.A., 1996. Foreland basin systems. Basin Research 15, 379-396.

Dickinson, W.R., 1974. Sedimentation within and besides ancient and modern magmatic arcs. Society of Economic Paleontologists and Mineralogists. Special Publication 19, 230-239.

Fambrini, G.L., Janikian, L. Almeida, R.P., Fragoso-Cesar, A.R.S., 2007. Evolução estratigráfica e paleogeográfica do grupo Santa Bárbara (Ediacarano) na sub-bacia Camaquã Central, RS. Geologia USP Série Científica 7 (2), 1-24.

Fernandes, L.A.D., Tommasi, A., Porcher, C.C., 1992. Deformation patterns in the southern brazilian branch of the Dom Feliciano Belt: a reappraisal. Jounal of South America Earth Sciences 5 (1), 77-96.

Gastal, M.C.P., Lafon, J.M., Hartmann, L.A., Koester, E., 2005. Sm–Nd isotopic compositions as a proxy for magmatic processes during the Neoproterozoic of the southern Brazilian shield. Journal of South American Earth Sciences 18, 255–276.

Gastal, M.C., Lafon, J.M., Chemale Jr., F., 2010. U-Pb and Pb-Pb zircon ages of Neoproterozoic-Eopaleozoic granites from the western portion of the southerm

Brazilian Shield, in: South American Symposium on Isotopic Geology. Short Papers VII SSAGI, Brasília.

Gerdes, A., Zeh, A., 2006. Combined U–Pb and Hf isotope LA-(MC-)ICP-MS analyses of detrital zircons: Comparison with SHRIMP and new constraints for the provenance and age of an Armorican metasediment in Central Germany. Earth and Planetary Science Letters 249, 47–61.

Goñi, J., Goso, H., Issler, R., 1962. Estratigrafía e Geologia Económica do Pré-Cambriano e Eo-Paleozóico uruguaio e sul-Riograndense. Avulso da Escola de Geologia, UFRGS, v. 3, pp.1-105.

Gresse, P.G., Chemale Jr., F., Silva, L., Walraven, F., Hartmann, L., 1996. Late- to post-orogenic basins of the Pan-African-Brasiliano-collision orogen in Southern África and Southern Brazil. Basin Research 8 (2) 157-171.

Gruber, L., Lenz, C., Dussin, I., Chemale Jr, F., 2008. Mesoproterozoic detrital zircons in the Dom Feliciano Belt: zircons age the Porongos Metamorphic Complex, in: VI South American Symposium on Isotope Geology. Book of Abstracts, Bariloche, pp. 109-109.

Hartmann, L.A., Leite, J.A.D., Silva, L.C., Remus, M.V.D., McNaughton, N.J., Groves, D.I., Fletcher, I.R., Santos, J.O.S., Vasconcellos, M.A.Z., 2000. Advances in SHRIMP geochronology and their impact on understanding the tectonic and metallogenic evolution of southern Brazil. Australian Journal of Earth Sciences 47 (5) 829-844.

Hartmann, L.A., Santos, J.O.S, Leite, J.A.D., Porcher, C.C., McNaughton, N.J., 2003. Metamorphic evolution and U-Pb zircon SHRIMP geochronology of the Belizário ultramafic amphibolite, Encantadas Comnplex, southernmost Brazil. Anais da Academia Brasileira de Ciências 75 (3), 393-403.

Hartmann, L.A., Chemale Jr., F., Philipp, R.P., 2007. Evolução geotectônica do Rio Grande do Sul no Pré-Cambriano, in: Ianuzzi, R., Frantz, J.C. (Org.), 50 anos de Geologia. Editora Comunicação e Identidade, Porto Alegre, v. 1, pp. 97-123.

Hartmann, L.A., Liu, D., Wang, Y., Massonne, H.J., Santos, J.O.S., 2008a. Protolith age of Santa Maria Chico granulites dated on zircons from an associated amphibolite-facies granodiorite in southernmost Brazil. Anais da Academia Brasileira de Ciências 80 (3), 543-551.

Hartmann, L.A., Santos, J.O.S., McNaughton, N.J., 2008b. Detrital Zircon U-Pb Age Data, and Precambrian Provenance of the Paleozoic Guaritas Formation, Southern Brazilian Shield. International Geology Review 50, 364-374.

Hartmann, L.A., Philipp, R.P., Santos, J.O.S., McNaughton, N.J., 2011. Time frame of 753–680 Ma juvenile accretion during the São Gabriel orogeny southern Brazilian Shield. Gondwana Research 19, 84-99.

Howard, K.E., Handa, M., Barovicha, K.M., Paynea, J.L., Belousova, E.A., 2011. U–Pb, Lu–Hf and Sm–Nd isotopic constraints on provenance and depositional timing of

metasedimentary rocks in the western Gawler Craton: Implications for Proterozoic reconstruction models. Precambrian Research 184, 43–62.

Ingersoll, R.V., 2008. Subduction-related sedimentary basins of the U.S.A. Cordilera. In Mial, A.D., ed. The sedimentary basins of the United States and Canada. Sedimentary Basins of the World 5, 395-428.

Janikian, L., Almeida, R.P., Fragoso-Cesar, A.R.S., Martins, V.T.S., Dantas, E.L., Tohver, E., McReath, I., D'Agrella-Filho, M.S., 2012. Ages (U-Pb SHRIMP and LA ICPMS) and stratigraphic evolution of the Neoproterozoic volcano-sedimentary successions from the extensional Camaquã Basin, Southern Brazil. Gondwana Research 21, 466-482.

Leinz, V., Almeida, S., 1941. Gênese da jazida de cobre de Camaquã. Boletim da Secretaria de Agricultura, Indústria e Comércio do RS, Porto Alegre, n. 308.

Leite, J.A.D., Hartmann, L.A., McNaughton, N.J., Chemale Jr, F., 1998. SHRIMP U/Pb zircon geochronology of Neoproterozoic juvenile and crustal-reworked terranes in southernmost Brazil. International Geology Reviews 40, 688-705.

Leite, J.A.D., Hartmann, L.A., Fernandes, L.A.D., McNaughton, N.J., Soliani, E., Koester, E., Santos, J.O.S., Vasconcellos, M.A.Z., 2000. Zircon U-Pb SHRIMPdating of gneissic basement of the Dom Feliciano Belt, southernmost Brazil. Journal of South American Earth Sciences 13, 739–750.

Iizuka, T., Hirata, T., Komiya, T., Rino, S., Katayama, I., Motoki, A., Maruyama, S., 2005. U-Pb and Lu-Hf isotope systematics of zircons from the Mississippi River sand: Implications for reworking and growth of continental crust. Geology 33 (6) 485–488.

Marconato, A., Almeida, R.P., Santos, M.G.M., Nóbrega, J.E.S., Souza, R.B., 2009. Alluvial-eolian interaction in a Cambrian rift margin: the Pedra das Torrinhas and Pedra Pintada formations (Guaritas Group, RS). Anais da Academia Brasileira de Ciências 81 (4), 819-836.

Maraschin, A.J., Mizusaki, A.M.P., Zwingmann, H., Borba, A.W., Sbrissa, G.F., 2010. Illite authigenesis in sandstones of the Guaritas Allogroup (Early Paleozoic): Implications for the depositional age, stratigraphy and evolution of the Camaquã Basin (Southern Brazil). Journal of South American Earth Sciences 29, 400-411.

Nardi, L., Lima, E., 1985. A associação shoshonítica de Lavras do Sul, RS. Revista Brasileira de Geociências 15, 139-146.

Oliveira, E.P., Windley, B.F., Araujo, M.N.C., 2010. The Neoproterozoic Sergipano orogenic belt, NE Brazil: A complete plate tectonic cycle in western Gondwana. Precambrian Research 181, 64-84.

Paim, P.S.G., 1994. Depositional Systems and Paleogeographical Evolution of the Camaquã and Santa Bárbara Basins, Brazil. Ph.D. thesis, Oxford, 277 p.

Paim, P.S.G., 1995. Alluvial paleogeography of the Guaritas depositional sequence of southern Brazil. Special Publication International Association of Sedimentologists 22, 3-16.

Paim, P.S.G., Chemale Jr., F., Lopes, R.C., 2000. A Bacia do Camaquã, in: Holz, M., De Roz, L.F. (Eds.), Geologia do Rio Grande do Sul. CIGO-UFRGS, Porto Alegre, pp. 231-274.

Paim, P.S.G., Scherer, C.M.S., 2007. High-resolution stratigraphy and depositional model of wind- and water-laid deposits in the Ordovician Guaritas rift (Southernmost Brazil). Sedimentary Geology 202, 776–795.

Philipp, R.P., Machado, R., Chemale Jr., F., 2003. Reavaliação e novos dados geocronológicos (Ar/Ar, Rb/Sr e Sm–Nd) do Batólito Pelotas no Rio Grande do Sul: Implicações petrogenéticas e idade de reativação das zonas de cisalhamento. Geologia USP Série Cientifica 3, 71–84.

Philipp, R.P., Machado, R., 2005. The Neoproterozoic to Cambrian granitic magmatism of Pelotas Batholith, Southern Brazil. Journal of South American Earth Sciences 19, 61-478.

Philipp, R.P., Machado, R., Chemale Jr., F., 2007. A Geração dos granitóides Neoproterozóicos do Batólito Pelotas: evidências dos isótopos de Sr e Nd e implicações para o crescimento continental da porção sul do Brasil, in: Ianussi, R., Frantz, J.C. (Org.), 50 anos de Geologia. Editora Comunicação e Identidade, Porto Alegre, pp. 59-77.

Philipp, R.P., Lusa, M., Nardi, L.V.S., 2008. Geochemistry and petrology of dioritic, tonalitic and trondhjemitic gneisses from Encantadas Complex, Santana da Boa Vista, southernmost Brazil: a Paleoproterozoic continental-arc magmatism. Anais da Academia Brasileira de Ciências 80, 735-748.

Remus, M.V.D., McNaughton, N.J., Hartmann, L.A., Koppe, J.C., Fletcher, I.R., Groves, D.I., Pinto, V.M., 1999. Gold in the Neoproterozoic juvenile Bossoroca Volcanic Arc of southernmost Brazil: isotopic constraints on timing and sources. Journal of South American Earth Sciences 12, 349-366

Remus, M.V.D., Hartmann, L.A., McNaughton, N.J., Groves, D.I., Reisch, J.L., 2000a. Distal Magmatic-Hydrothermal Origin for the Camaquã Cu (Au-Ag) and Santa Maria Pb, Zn (Cu-Ag) Deposits, Southern Brazil. Gondwana Research 3 (2), 155-174.

Remus, M.V.D., Hartmann, L.A., McNaughton, N.J., Groves, D.I., Fletcher, I.R., 2000b. The link Between Hydrothermal Epigenetic Copper Mineralization and the Caçapava Granite of Brasiliano Cycle in Southern Brazil. Journal of South American Earth Sciences 13, 191-216.

Ribeiro, M., Fantinel, L., 1978. Associações petrotectônicas do Escudo Sul-rio-grandense: I-Tabulação e distribuição das associações petrotectônicas do Rio Grande do Sul. Inheríngia, Série Geológica 5, 19-54.

Robertson, J.F., 1966. Revision of the stratigraphy and nomenclature of rock units in the Caçapava-Lavras region. State of Rio Grande do Sul, Brazil. Notas e Estudos-IG/UFRGS 1 (2), 41–54.

Saalmann, K., Hartmann, L.A., Remus, M.V.D., Koester, E., Conceição, R.V., 2005. Sm–Nd isotope geochemistry of metamorphic volcanosedimentary successions in the São Gabriel Block, southernmost Brazil: evidence for the existence of juvenile Neoproterozoic oceanic crust to the east of the Rio de la Plata craton. Precambrian Research 136, 159-75.

Saalmann, K., Remus, M.V.D., Hartmann, L.A., 2006. Structural evolution and tectonic setting of the Porongos belt, southern Brazil. Geol.Mag. 143 (1), 59-88.

Saalmann, K., Gerdes, A., Lahaye, Y., Hartmann, L.A., Remus, M.V.D., Läufer, A., 2011. Multiple accretion at the eastern margin of the Rio de la Plata craton: the prolonged Brasiliano orogeny in southernmost Brazil. International Journal Earth Sciences 100, 355–378

Sommer, C.A, Lima, E.F., Nardi, L.V.S., Figueiredo, A.M.G., Pierosan, R., 2005. Potassic and low- and high-Ti mildly alkaline volcanism in the Neoproterozoic Ramada Plateau, southernmost Brazil. Journal of South American Earth Sciences 18 (3), 237-254.

Tommasi, A., Vauchez ,A., Fernándes, L.A.D., Porcher, C.C., 1994. Orogen-parallel strike-slip faulting and synkinematic magmatism in the Dom Feliciano Belt, Southern Brazil. Tectonics 13, 421-437.

Wildner, W., Lima, E.F., Nardi, L.V.S, Sommer, C.A., 2002. Volcanic cycles and setting in the Neoproterozoic III to Ordovician Camaquã Basin succession in southern Brazil: characteristics of post-collisional magmatism. Journal of Volcanology and Geothermal Research 118, 261-283.

5 CONCLUSÕES FINAIS E RECOMENDAÇÕES

Compreender o preenchimento de uma bacia sedimentar é um exercício de lógica, onde diversos parâmetros devem ser investigados e a convergência dos fatores conduzirá ao desmembramento de sua história. Desta maneira, entre os principais parâmetros a serem investigados destacam-se o arcabouço estratigráfico e espacial dos sedimentos, a caracterização estrutural dos eventos sedimentares e tectônicos no tempo e no espaço, a avaliação da proveniência sedimentar e a determinação de suas idades deposicionais.

O ambiente tectônico da região onde estão inseridas as bacias Santa Bárbara e Guaritas é caracterizado como um período pós-colisional, posterior ao ápice da colisão continental entre as duas principais unidades cratônicas que viriam a constituir o segmento sul do Gondwana: os Crátons do Rio de La Plata (América do Sul) e Kalahari (África do Sul). O período pós-colisional se caracterizou pela intensa geração e movimentação de zonas de cisalhamento de escala continental, e a idade das diversas etapas de movimentação deste período está registrada principalmente pela geração e posicionamento de diversas suítes e corpos graníticos encontrados na porção leste e oeste do Cinturão Dom Feliciano, bem como pela geração de associações vulcano-sedimentares que caracterizam a Bacia do Camaquã.

Neste contexto, as bacias Santa Bárbara e Guaritas foram geradas em um ambiente de rifte transtracional, com áreas fonte predominantes de rochas do Ciclo Brasiliano e Transamazônico, havendo uma diminuição da contribuição de zircões brasilianos da bacia Santa Bárbara para a bacia Guaritas, e um aumento de zircões Mesoproterozoicos e Paleoproterozoicos. Com base nas idades geocronológicas obtidas e na literatura, foi possível determinar o intervalo de idade de deposição destas bacias. A deposição da bacia Santa Bárbara ocorreu no intervalo de 553 ± 16 Ma a 540 Ma, com a intrusão da Formação Acampamento Velho em 544.2 ± 5.5 Ma, e a da bacia Guaritas ocorreu no intervalo de 547 ± 6 Ma a 473,7 ± 9,4 Ma.

Os dados isotópicos, combinados com as informações de paleocorrentes, permitiram definir que as rochas do Terreno Tijucas e do Batólito de Pelotas, bem como as rochas Paleoproterozoicas e Brasilianas ao sul das bacias, serviram como principais rochas fonte para os sedimentos. O incremento da contribuição de zircões Paleoproterozoicos e alguns Mesoproterozoicos na bacia do Guaritas definem as rochas do Terreno Tijucas, o Complexo Metamórfico Porongos (Meso-Neoproterozoico) e o Domo Gnáissico de Santana (Paleoproterozoico), como as áreas fonte principais para as unidades desta bacia, sugerindo que estas rochas estavam mais expostas durante a sua deposição servindo como um alto estrutural da bacia (Domo de Santana). Os resultados das idades modelo Lu-Hf (TDM) mostram que os zircões contêm uma herança dominantemente Arqueana e Paleoproterozoica para as duas bacias, com valores εHf predominantemente negativos, indicando uma origem crustal a partir de um litosfera subcontinental para as rochas fonte que preencheram as bacias.

Trabalhos futuros podem colaborar para um melhor posicionamento e entendimento tectono-estratigráfico destas bacias, estabelecendo uma melhor correlação com o embasamento adjacente e com desenvolvimento da plataforma Sul-Americana.

REFERÊNCIAS

Almeida, D.P.M., Chemale Jr., F., Machado, A., 2012 Late to Post-Orogenic Brasiliano-Pan-AfricanVolcano-Sedimentary Basins in the Dom Feliciano Belt, Southernmost Brazil. Petrology – New Perspectives and Applications, Tech-Open Acess Publisher, pp. 73-135.

Almeida, R.P., Janikian, L., Fragoso-Cesar, A.R.S., Marconato, A., 2009. Evolution of a rift basin dominated by subaerial deposits: The Guaritas Rift, Early Cambrian, Southern Brazil. Sedimentary Geology 217, 30–51.

Babinski, M., Chemale Jr., F., Hartmann, L.A., Van Schmus, W.R., Silva, L.C., 1996. Juvenile accretion at 750–700 Ma in southern Brazil. Geology 24, 439-442.

Babinski, M., Chemale Jr., F., Van Schmus, W.R., Hartmann, L.A., Silva, L.C., 1997. U-Pb and Sm-Nd geochronology of the Neoproterozoic granitic-gneissic Dom Feliciano Belt, southernmost Brazil. Journal of South American Earth Sciences 10, 263-274.

Basei, M.A.S., Siga Jr., O., Masquelin, H., Harara, O.M., Reis Neta, J.M., Preciozzi, F., 2000. The Dom Feliciano Belt of Brazil and Uruguay and its Foreland Domain, the Rio de la Plata Craton, framework, tectonic evolution and correlation with similar provinces of Southwestern Africa. In: Cordani, U., Milani, E.J., Campos, D.A. (Org.), Tectonic Evolution of South American Platform. SBG, Rio de Janeiro, v. 1, p. 311-334.

Bicca, M.M., Jelinek, A.R., Oliveira, C.H.E., Chemale Jr., F., Guadagnin, F., 2010. Estudos tectônicos da porção sul da bacia do Camaquã, região de Minas do Camaquã, RS. In: VI Congreso Uruguayo de Geologia e II Simposio Internacional del Neoproterozoico – Cámbrico de la Cuenca del Plata, Minas, pp. 34.

Borba, A.W., Mizusaki, A.M.P., 2003. Santa Bárbara Formation (Caçapava do Sul, southern Brazil): depositional sequences and evolution of an Early Paleozoic post-collisional basin. Journal of South American Earth Sciences 16(5), 365-380.

Borba, A.W., 2006. Evolução geológica da "Bacia do Camaquã" (Neoproterozóico e Paleozóico inferior do Escudo Sul-riograndense, RS, Brasil): uma visão com base na integração de ferramentas de esteatigrafia, petrografia e geologia isotópica. Ph.D. thesis, UFRGS, Porto Alegre, 110p.

Borba, A.W., Mizusaki, A.M.P., Silva, D.R.A., Koester, E., Noronha, F.L., Casagrande, J., 2006, Provenance of the Neoproterozoic Maricá Formation (Sul-rio-grandense Shield, Southern Brazil): Petrographic and Sm-Nd isotopic constraints. Gondwana Research 9, 464–474.

Borba, A.W., Maraschin, A.J., Mizusaki, A.M.P., 2007. Evolução Tectono-Estratigráfica e Paleoclimática da Formação Maricá (Escudo Sul-Rio-Grandense, Brasil): um Exercício de Geologia Histórica e Análise Integrada de uma Bacia Sedimentar Neoproterozóica. Revista Pesquisas em Geociências 34 (2), 57-74.

Borba, A.W., Mizusaki, A.M.P., Santos, J.O.S., McNaughton, N.J., Onoe, A.T., Hartmann, L.A., 2008. U–Pb zircon and 40Ar–39Ar K-feldspar dating of syn-sedimentary volcanism of the Neoproterozoic Maricá Formation: constraining the age of foreland basin inception and inversion in the Camaquã Basin of southern Brazil. Basin Research 20, 359–375.

Carvalho, P.F., 1932. Reconhecimento geológico no Estado do Rio Grande do Sul. Boletim do Serviço Geológico e Mineralógico do Brasil 66, 1-72.

Chemale Jr., F., 1993. Bacias molássicas brasilianas. Acta Geológica Leopoldensia 37, 109-118.

Chemale Jr., F., Hartmann, L.A.; Silva, L.C., 1995. Stratigraphy and Tectonism of Precambrian to Early Paleozoic Units. XVIII Acta Geológica Leopoldensia, 42, 5-117.

Chemale Jr., F., 2000. Evolução geológica do Escudo Sul-rio-grandense, in: Holz, M., De Roz, L.F. (Eds), Geologia do Rio Grande do Sul. CIGO/UFRGS, Porto Alegre, pp. 13-52.

Chemale Jr., F., Mallmann, G., Bitencourt, M.F., Kawashita, K., 2012. Time constraints on magmatism along the Major Gercino Shear Zone, southern Brazil: Implications for West Gondwana reconstruction. Gondwana Research 22 (1),184-189.

Chu, N.C., et al., 2002. Hf isotope ratio analysis using multi-collector inductively coupled plasma mass spectrometry: an evaluation of isobaric interference corrections. J Anal Atom Spectrom 17, 1567–1574.

De Ros, L.F., Morad, S., Paim, P.S.G., 1994. The role of detrital composition and climate on the diagenetic evolution of continental molasses: evidence from the Cambro-Ordovician Guaritas sequence, southern Brazil. Sedimentary Geology 92, 197–228.

Dickinson W.R., 1974. Plate tectonics and sedimentation. In: W.R. Dickinson (ed.) Tectonics and Sedimentation, SEPM, Spec. Publ., 22: 1-27.

Fambrini, G.L., 1998. Grupo Camaquã (Transição Proterozóico-Fanerozóico) na região das Minas do Camaquã, RS: Análise estratigráfica de fácies, proveniência e paleocorrentes. Dissertação (Mestrado) – Curso de Pós-Graduação em Geociências, Universidade de São Paulo, São Paulo, SP.

Fambrini, G.L., 2003. O Grupo Santa Bárbara (Neoproterozóico III) da Bacia do Camaquã, Rio Grande do Sul. Tese (Doutorado) – Universidade de São Paulo, São Paulo, SP.

Fambrini, G.L., Janikian, L., Almeida, R.P., Fragoso-Cesar, A.R.S., 2005. O Grupo Santa Bárbara (Ediacarano) na Sub-bacia Camaquã Central, RS: estratigrafia e sistemas deposicionais. Revista Brasileira de Geociências 35, 227-238.

Faure, G., 1986. Principles of isotope geology, 2 ed. New York: John Wiley & Sons.

Faure, G., Mensing, T.M., 2005. Isotopes principles and applications, 3 ed. New Jersey, John Wiley and Sons.

Fernandes, L.A.D., Tommasi, A., Porcher, C.C., 1992. Deformation patterns in the southern brazilian branch of the Dom Feliciano Belt: a reappraisal. Jounal of South America Earth Sciences 5 (1), 77-96.

Fragoso-Cesar, A.R.S., et al., 1985. Revisão na estratigrafia das molassas do Ciclo Brasiliano no Rio Grande do Sul. In: SIMPÓSIO SUL-BRASILEIRO DE GEOLOGIA, 2, 1985. Anais, SBG: p. 477-491.

Fragoso-Cesar, A.R.S. et al., 2000. The Camaquã extensional basin: Neoproterozoic to early Cambrian sequences in southernmost Brazil. Revista Brasileira de Geociências 30 (3), 438-441.

Fragoso-Cesar, A.R.S., 2003. A Bacia Camaquã: um sistema intracontinental anorogênico de rifts do Neoproterozóico III – Eopaleozóico no Rio Grande do Sul. In: I ENCONTRO SOBRE A ESTRATIGRAFIA DO RIO GRANDE DO SUL: ESCUDOS E BACIAS, 2003. Boletim de Resumos: p. 139-144.

Gastal, M.C.P., Lafon, J.M., Hartmann, L.A., Koester, E., 2005. Sm–Nd isotopic compositions as a proxy for magmatic processes during the Neoproterozoic of the southern Brazilian shield. Journal of South American Earth Sciences 18, 255–276.

Gastal, M.C., Lafon, J.M., Chemale Jr., F., 2010. U-Pb and Pb-Pb zircon ages of Neoproterozoic-Eopaleozoic granites from the western portion of the southerm Brazilian Shield, in: South American Symposium on Isotopic Geology. Short Papers VII SSAGI, Brasília.

Goñi, J., Goso, H., Issler, R., 1962. Estratigrafía e Geologia Económica do Pré-Cambriano e Eo-Paleozóico uruguaio e sul-Riograndense. Avulso da Escola de Geologia, UFRGS, v. 3, pp.1-105.

Gresse, P.G., Chemale Jr., F., Silva, L., Walraven, F., Hartmann, L., 1996. Late- to post-orogenic basins of the Pan-African-Brasiliano-collision orogen in Southern África and Southern Brazil. Basin Research 8 (2) 157-171.

Hartmann, L.A., Leite, J.A.D., Silva, L.C., Remus, M.V.D., McNaughton, N.J., Groves, D.I., Fletcher, I.R., Santos, J.O.S., Vasconcellos, M.A.Z., 2000. Advances in SHRIMP geochronology and their impact on understanding the tectonic and metallogenic evolution of southern Brazil. Australian Journal of Earth Sciences 47 (5) 829-844.

Hartmann, L.A., Santos, J.O.S, Leite, J.A.D., Porcher, C.C., McNaughton, N.J., 2003. Metamorphic evolution and U-Pb zircon SHRIMP geochronology of the Belizário ultramafic amphibolite, Encantadas Comnplex, southernmost Brazil. Anais da Academia Brasileira de Ciências 75 (3), 393-403.

Hartmann, L.A., Chemale Jr., F., Philipp, R.P., 2007. Evolução geotectônica do Rio Grande do Sul no Pré-Cambriano, in: Ianuzzi, R., Frantz, J.C. (Org.), 50 anos de Geologia. Editora Comunicação e Identidade, Porto Alegre, v. 1, pp. 97-123.

Hartmann, L.A., Liu, D., Wang, Y., Massonne, H.J., Santos, J.O.S., 2008a. Protolith age of Santa Maria Chico granulites dated on zircons from an associated amphibolite-facies granodiorite in southernmost Brazil. Anais da Academia Brasileira de Ciências 80 (3), 543-551.

Hartmann, L.A., Santos, J.O.S., McNaughton, N.J., 2008b. Detrital Zircon U-Pb Age Data, and Precambrian Provenance of the Paleozoic Guaritas Formation, Southern Brazilian Shield. International Geology Review 50, 364-374.

Hartmann, L.A., Philipp, R.P., Santos, J.O.S., McNaughton, N.J., 2011. Time frame of 753–680 Ma juvenile accretion during the São Gabriel orogeny southern Brazilian Shield. Gondwana Research 19, 84-99.

Janikian, L., 2004. Seqüências deposicionais e evolução paleoambiental do Grupo Bom Jardim e da Formação Acampamento velho, Subgrupo Camaquã, Rio Grande do Sul. Tese (Doutorado) – Instittuto de Geociências, Universidade de São Paulo, São Paulo, SP.

Janikian, L., Almeida, R.P., Fragoso-Cesar, A.R.S., Martins, V.T.S., Dantas, E.L., Tohver, E., McReath, I., D'Agrella-Filho, M.S., 2012. Ages (U-Pb SHRIMP and LA ICPMS) and stratigraphic evolution of the Neoproterozoic volcano-sedimentary successions from the extensional Camaquã Basin, Southern Brazil. Gondwana Research 21, 466-482.

Jost, H., Bitencourt, M.F., 1980. Estratigrafia e tectônica de uma fração da Faixa De Dobramentos de Tijucas no Rio Grande do Sul. Acta Geologica Leopoldensia 4 (7), 27-60.

Leinz, V., Almeida, S., 1941. Gênese da jazida de cobre de Camaquã. Boletim da Secretaria de Agricultura, Indústria e Comércio do RS, Porto Alegre, n. 308.

Leite, J.A.D., Hartmann, L.A., McNaughton, N.J., Chemale Jr, F., 1998. SHRIMP U/Pb zircon geochronology of Neoproterozoic juvenile and crustal-reworked terranes in southernmost Brazil. International Geology Reviews 40, 688-705.

Leite, J.A.D., Hartmann, L.A., Fernandes, L.A.D., McNaughton, N.J., Soliani, E., Koester, E., Santos, J.O.S., Vasconcellos, M.A.Z., 2000. Zircon U-Pb SHRIMPdating of gneissic basement of the Dom Feliciano Belt, southernmost Brazil. Journal of South American Earth Sciences 13, 739–750.

Leites, S.R., et al., 1990. A divisão litofaciológica da Bacia do Camaquã na Folha Passo do Salsinho, Caçapava do Sul, RS, e sua interpretação paleoambiental. In: CONGRESSO BRASILEIRO DE GEOLOGIA, 36, 1990, Natal. Anais... Natal: SBG, 1, p. 300-312.

Marconato, A., Almeida, R.P., Santos, M.G.M., Nóbrega, J.E.S., Souza, R.B., 2009. Alluvial-eolian interaction in a Cambrian rift margin: the Pedra das Torrinhas and Pedra Pintada formations (Guaritas Group, RS). Anais da Academia Brasileira de Ciências 81 (4), 819-836.

Maraschin, A.J., Mizusaki, A.M.P., Zwingmann, H., Borba, A.W., Sbrissa, G.F., 2010. Illite authigenesis in sandstones of the Guaritas Allogroup (Early Paleozoic): Implications for the depositional age, stratigraphy and evolution of the Camaquã Basin (Southern Brazil). Journal of South American Earth Sciences 29, 400-411.

Nardi, L., Lima, E., 1985. A associação shoshonítica de Lavras do Sul, RS. Revista Brasileira de Geociências 15, 139-146.

Oliveira, L.D., Koester, E., Soliani Jr., E., 2001. Geoquímica das rochas graníticas pós-transcorrentes da região de Porto Alegre e Viamão, RS. Geochimica Brasiliensis 15 (2), 65-92.

Paim, P.S.G., et al., 1992. Estratigrafia de seqüências e sistemas deposicionais das bacias do Camaquã e Santa Bárbara, Eopaleozóico do RS (Brasil). Universidad Nacional de Tucumán, Serie Correlación Geologica 9, p.41-45.

Paim, P.S.G., 1994. Depositional Systems and Paleogeographical Evolution of the Camaquã and Santa Bárbara Basins, Brazil. Ph.D. thesis, Oxford, 277 p.

Paim, P.S.G., 1995. Alluvial paleogeography of the Guaritas depositional sequence of southern Brazil. Special Publication International Association of Sedimentologists 22, 3-16.

Paim, P.S.G., Chemale Jr., F., Lopes, R.C., 2000. A Bacia do Camaquã, in: Holz, M., De Roz, L.F. (Eds.), Geologia do Rio Grande do Sul. CIGO-UFRGS, Porto Alegre, pp. 231-274.

Paim, P.S.G., Scherer, C.M.S., 2007. High-resolution stratigraphy and depositional model of wind- and water-laid deposits in the Ordovician Guaritas rift (Southernmost Brazil). Sedimentary Geology 202, 776–795.

Patchett, P.J., Tatsumoto, M., 1980. Lu-Hf total-rock isochron for the eucrite meteorites. Nature 288:571-574

Patchett, P.J., Kouvo, O., Hedge, C.E., Tatsumoto, M., 1981. Evolution of continental crust and mantle heterogeneity: evidence from Hf isotopes. Contrib Mineral Petrol 78, 279-297.

Philipp, R.P., Mesquita, M.J.M., Gomes, M.E.B., Almeida, D.P.M., 1993. Reconhecimento estrutural e geoquímico dos granitóides Brasilianos na região de Pelotas, RS. Revista Pesquisas 20 (1), 3-13.

Pelosi, A.P.M.R., Fragoso-Cesar, A.R.S., 2003. Proposta litoestratigráfica e considerações paleoambientais sobre o Grupo Maricá (Neoproterozóico III), Bacia do Camaquã, Rio Grande do Sul. Revista Brasileira de Geociências 33, 137-148.

Philipp, R.P., Nardi, L.V.S., Bitencourt, M.F., 2000. O Batólito Pelotas no Rio Grande do Sul. In: HOLZ, M.; DE ROS, F.F. (Ed.). Geologia do Rio Grande do Sul. Porto Alegre, RS: CIGO/UFRGS, p.133-160.

Philipp, R.P., Machado, R., Nardi, L.V.S., Lafon, J.M., 2002. O magmatismo granítico Neoproterozóico do Batólito Pelotas no sul do Brasil: novos dados e revisão de geocronologia regional. Revista Brasileira de Geociências 32 (2), 277-290.

Philipp, R.P., Machado, R., Chemale Jr., F., 2003. Reavaliação e novos dados geocronológicos (Ar/Ar, Rb/Sr e Sm–Nd) do Batólito Pelotas no Rio Grande do Sul: Implicações petrogenéticas e idade de reativação das zonas de cisalhamento. Geologia USP Série Cientifica 3, 71–84.

Philipp, R.P., Machado, R., 2005. The Neoproterozoic to Cambrian granitic magmatism of Pelotas Batholith, Southern Brazil. Journal of South American Earth Sciences 19, 61-478.

Philipp, R.P., Machado, R., Chemale Jr., F., 2007. A Geração dos granitóides Neoproterozóicos do Batólito Pelotas: evidências dos isótopos de Sr e Nd e implicações para o crescimento continental da porção sul do Brasil, in: Ianussi, R., Frantz, J.C. (Org.), 50 anos de Geologia. Editora Comunicação e Identidade, Porto Alegre, pp. 59-77.

Philipp, R.P., Lusa, M., Nardi, L.V.S., 2008. Geochemistry and petrology of dioritic, tonalitic and trondhjemitic gneisses from Encantadas Complex, Santana da Boa Vista, southernmost Brazil: a Paleoproterozoic continental-arc magmatism. Anais da Academia Brasileira de Ciências 80, 735-748.

Philipp, R.P., Campos, R.S., 2010. Granitos peraluminosos intrusivos no Complexo Metamórfico Brusque: registro do magmatismo relacionado a colisão neoproterozóica no Terreno Tijucas, Itapema, SC. Revista Brasileira de Geociências, 40, 301-318.

Porcher, C.A., Lopes, R., 2000. da Cachoeira do Sul, folha SH.22-Y-A , estado do Rio Grande do Sul: Programa de Levantamentos Geológicos Básicos do Brasil. Rio de Janeiro: CPRM, 2000. 1 CD ROM.

Remus, M.V.D., McNaughton, N.J., Hartmann, L.A., Koppe, J.C., Fletcher, I.R., Groves, D.I., Pinto, V.M., 1999. Gold in the Neoproterozoic juvenile Bossoroca Volcanic Arc of southernmost Brazil: isotopic constraints on timing and sources. Journal of South American Earth Sciences 12, 349-366

Ribeiro, M., Bocchi, P.R., Figueiredo Fº, P.M., Tessari, R.I., 1996. Geologia da quadrícula de Caçapava do Sul, Rio Grande do Sul, Brasil. Porto Alegre: DNPM/DFPM, 1 v. (Boletim 127).

Ribeiro, M., Fantinel, L., 1978. Associações petrotectônicas do Escudo Sul-rio-grandense: I-Tabulação e distribuição das associações petrotectônicas do Rio Grande do Sul. Inheríngia, Série Geológica 5, 19-54.

Robertson, J.F., 1966. Revision of the stratigraphy and nomenclature of rock units in the Caçapava-Lavras region. State of Rio Grande do Sul, Brazil. Notas e Estudos-IG/UFRGS 1 (2), 41–54.

Saalmann, K., Hartmann, L.A., Remus, M.V.D., Koester, E., Conceição, R.V., 2005. Sm–Nd isotope geochemistry of metamorphic volcanosedimentary successions in the São Gabriel Block, southernmost Brazil: evidence for the existence of juvenile Neoproterozoic oceanic crust to the east of the Rio de la Plata craton. Precambrian Research 136, 159-75.

Santos, E.L., Beckel, J., Macedo, P.M., Gonzales Fº, F., Chaban, N., 1978. Divisão litoestratigráfica do Eo-Cambriano-Pré-Cambriano Superior do Escudo Sul-riograndense. In: CONGRESSO BRASILEIRO DE GEOLOGIA, 30, Recife, 1978. Anais... Recife: SBG, v. 2, p. 670-684.

Silva, L.C., et al., 1999. SHRIMP U/Pb zircon dating of Neoproterozic granitic magmatism and collision in the Pelotas Batholith, Southernmost Brazil. International Geology Review 41, 531-551.

Soliani Jr., E., 1986. Os dados geocronológicos do escudo sul-rio-grandense e suas implicações de ordem geotectônica. Tese (Doutorado em Geologia Geral e de Aplicação) – Instituto de Geociências. Universidade de São Paulo, São Paulo.

Sommer, C.A., Lima, E.F., Nardi, L.V.S., 1999. Evolução Do Vulcanismo Alcalino da Porção Sul do Platô do Taquarembó, Dom Pedrito, RS. Revista Brasileira de Geociências 29 (2), 245-254.

Sommer, C.A, Lima, E.F., Nardi, L.V.S., Figueiredo, A.M.G., Pierosan, R., 2005. Potassic and low- and high-Ti mildly alkaline volcanism in the Neoproterozoic Ramada Plateau, southermost Brazil. Journal of South American Earth Sciences 18 (3), 237-254.

Tatsumoto, M., Unruh, D.M., Patchett, P.J., 1981. U-Pb and Lu-Hf systematics of Antarctic meteorites. Proc 6th Symp. Antarctic Meteor, Natl Inst Polar Res, Tokyo, p 237-249.

Teixeira, G., Gonzales, A.P., Gonzales, M.A., Licht, O.A.B., 1978. Situação das Minas do Camaquã, Rio Grande do Sul. In: CONGRESSO BRASILEIRO DE GEOLOGIA 30, Recife, 1978. Anais... v. 4 , 1893-1905.

Wildner, W., Nardi, L.V.S., Lima, E.F., 1999. Post-collisional Alkaline Magmatism on the Taquarembó Plateau: a well Preserved Neoproterozoic-Cambrian Plutono-volcanic Association in Southern Brazil. International Geology Review 41, 1082-1098.

ANEXO A – CARTA DE SUBMISSÃO DO ARTIGO

Acknowledgement of receipt of your submitted article

Dear Geologist Oliveira,

Your submission entitled "U-Pb AND Lu-Hf ISOTOPES APPLIED TO THE LATE TO POST-OROGENIC TRANSTENSIONAL BASINS OF THE DOM FELICIANO BELT, BRAZIL." has been received by Precambrian Research

Please note that submission of an article is understood to imply that the article is original and is not being considered for publication elsewhere. Submission also implies that all authors have approved the paper for release and are in agreement with its content.

You will be able to check on the progress of your paper by logging on to http://ees.elsevier.com/precam/ as Author.

Your manuscript will be given a reference number in due course.

Thank you for submitting your work to this journal.

Kind regards,

Precambrian Research

ANEXO B – TABLE 1

Table 1a: U-Pb in situ zircon data of sample T01-11, Guaritas Gr.

						Isotope ratios[b]							Ages (Ma)							Best estimated age (Ma)	
Spot num	f 206	Pb ppm	U ppm	Th ppm	Th/U[a]	$^{207}Pb/^{235}U$	1 s [%]	$^{206}Pb/^{238}U$	1 s [%]	Rho[c]	$^{207}Pb/^{206}Pb^{d}$	1 s [%]	$^{206}Pb/^{238}U$	1 s abs	$^{207}Pb/^{235}U$	1 s abs	$^{207}Pb/^{206}Pb$	1 s abs	% Conc[e]		
005-Z2	0.0007	151	31	310	0.10	11.3260	2.38	0.4727	1.56	0.65	0.1738	1.80	2495	39	2550	61	2594	47	96	2594	47
006-Z3	0.0009	10	91	74	1.23	0.8300	14.79	0.0956	11.24	0.76	0.0629	9.62	589	66	614	91	707	68	83		
007-Z4	0.0159	3	19	29	0.65	0.6963	40.14	0.0752	30.61	0.76	0.0672	25.97	467	143	537	215	844	219	55		
008-Z5	0.0091	6	12	12	1.09	7.1806	5.08	0.3882	1.91	0.38	0.1341	4.70	2115	40	2134	108	2153	101	98	2153	101
009-Z6	0.0012	46	68	85	0.80	6.5786	3.24	0.3692	2.40	0.74	0.1292	2.18	2026	49	2056	67	2088	45	97	2088	45
010-Z7	0.0644	120	838	1047	0.81	0.8607	47.68	0.0465	28.36	0.59	0.1342	38.33	293	83	630	301	2154	826	14		
011-Z8	0.0013	48	89	81	1.11	7.8908	6.97	0.4111	2.89	0.41	0.1392	6.35	2220	64	2219	155	2217	141	100	2217	141
012-Z9	0.0008	113	206	196	1.06	7.3324	2.96	0.3893	2.55	0.86	0.1366	1.51	2120	54	2153	64	2184	33	97	2184	33
015-Z10	0.0000	5	32	20	1.65	1.2749	37.20	0.1364	26.33	0.71	0.0678	26.28	824	217	835	310	862	227	96	862	227
016-Z11	0.0015	38	23	50	0.46	13.5314	5.93	0.5289	5.24	0.88	0.1856	2.78	2737	143	2717	161	2703	75	101	2703	75
017-Z12	0.0002	13	67	77	0.87	0.7656	14.62	0.0941	12.88	0.88	0.0590	6.90	579	75	577	84	569	39	102	569	39
018-Z13	0.0029	33	176	239	0.74	0.7845	9.15	0.0955	7.92	0.87	0.0596	4.59	588	47	588	54	589	27	100	589	27
019-Z14	0.0005	95	170	225	0.76	4.4293	3.61	0.2662	3.20	0.89	0.1207	1.68	1522	49	1718	62	1966	33	77		
020-Z15	0.0006	76	113	167	0.68	4.8378	2.96	0.3049	2.18	0.74	0.1151	2.00	1715	37	1791	53	1881	38	91	1881	38
021-Z16	0.0015	92	123	174	0.71	6.0353	3.67	0.3307	2.93	0.80	0.1324	2.22	1842	54	1981	73	2129	47	86		
022-Z17	0.0014	62	50	112	0.45	6.4081	3.08	0.3361	2.23	0.72	0.1383	2.12	1868	42	2033	63	2206	47	85		
023-Z18	0.0013	44	44	77	0.57	6.9241	4.72	0.3914	3.96	0.84	0.1283	2.56	2129	84	2102	99	2075	53	103	2075	53
024-Z19	0.0016	38	57	70	0.82	6.4852	4.38	0.3587	3.69	0.84	0.1311	2.37	1976	73	2044	90	2113	50	94	2113	50
027-Z20	0.0013	27	68	93	0.74	1.3544	11.49	0.0881	10.62	0.92	0.1115	4.40	544	58	869	100	1825	80	30		
028-Z21	0.0028	146	135	180	0.76	12.7589	8.74	0.5131	8.56	0.98	0.1803	1.78	2670	229	2662	233	2656	47	101	2656	47
029-Z22	0.0394	44	213	342	0.63	1.0932	5.65	0.0785	4.80	0.85	0.1011	2.98	487	23	750	42	1644	49	30		
030-Z23	0.0009	39	174	288	0.61	0.7840	6.71	0.0957	4.87	0.73	0.0594	4.61	589	29	588	39	583	27	101	583	27
031-Z24	0.0159	10	42	10	4.37	4.3057	34.30	0.2497	28.84	0.84	0.1251	18.56	1437	414	1694	581	2030	377	71		
032-Z25	0.0026	28	29	49	0.58	5.1499	3.01	0.3284	2.45	0.81	0.1137	1.76	1831	45	1844	56	1860	33	98	1860	33
033-Z26	0.0008	143	156	267	0.59	7.5622	2.21	0.3939	1.49	0.67	0.1392	1.63	2141	32	2180	48	2218	36	97	2218	36
034-Z27	0.0007	37	276	185	1.50	0.9008	4.76	0.1079	3.33	0.70	0.0606	3.41	660	22	652	31	624	21	106	624	21
035-Z28	0.0005	209	175	255	0.69	10.8945	2.15	0.4879	1.47	0.69	0.1620	1.57	2561	38	2514	54	2476	39	103	2476	39
036-Z29	0.0020	33	87	62	1.41	4.4243	2.43	0.3125	1.59	0.65	0.1027	1.84	1753	28	1717	42	1673	31	105	1673	31
040-Z30	0.0012	63	56	101	0.56	6.7133	4.27	0.3804	3.75	0.88	0.1280	2.05	2078	78	2074	89	2070	42	100	2070	42
041-Z31	0.0005	120	11	95	0.11	23.7128	2.95	0.6505	2.27	0.77	0.2644	1.88	3230	73	3257	96	3273	61	99	3273	61
042-Z32	0.0005	278	267	356	0.75	9.2069	2.82	0.4457	2.43	0.86	0.1498	1.42	2376	58	2359	66	2344	33	101	2344	33
043-Z33	0.0009	79	116	114	1.03	7.0361	3.67	0.3940	3.24	0.88	0.1295	1.72	2141	69	2116	78	2091	36	102	2091	36
044-Z34	0.0009	50	49	83	0.59	6.1742	5.31	0.3587	4.66	0.88	0.1248	2.55	1976	92	2001	106	2026	52	98	2026	52
045-Z35	0.0004	152	358	194	1.86	6.3138	3.01	0.3703	2.38	0.79	0.1237	1.84	2031	48	2020	61	2010	37	101	2010	37
046-Z36	0.0003	223	86	279	0.31	9.2680	2.93	0.4385	2.39	0.81	0.1533	1.70	2344	56	2365	69	2383	41	98	2383	41
047-Z37	0.0025	24	29	64	0.45	3.2225	9.36	0.2035	8.30	0.89	0.1148	4.33	1194	99	1463	137	1877	81	64		
048-Z38	0.0762	494	833	1854	0.45	4.0163	6.55	0.1389	6.33	0.97	0.2097	1.70	839	53	1638	107	2903	49	29		
051-Z39	0.0005	224	107	364	0.30	7.0251	3.94	0.3933	2.92	0.74	0.1295	2.64	2138	62	2115	83	2092	55	102	2092	55

ID																					
052-Z40	0.0041	20	30	27	1.13	5.9537	7.15	0.3459	4.50	0.63	0.1248	5.56	1915	86	1969	141	2026	113	95	2026	113
053-Z41	0.0015	20	56	124	0.46	0.8258	8.34	0.0986	7.05	0.85	0.0607	4.46	606	43	611	51	629	28	96	629	28
054-Z42	0.0026	30	36	46	0.80	7.2126	5.32	0.4060	3.51	0.66	0.1288	4.00	2197	77	2138	114	2082	83	105	2082	83
055-Z43	0.0014	31	31	46	0.67	6.7381	4.81	0.3924	3.71	0.77	0.1245	3.06	2134	79	2078	100	2022	62	106	2022	62
056-Z44	0.0009	94	113	130	0.88	7.6000	2.14	0.4120	1.28	0.60	0.1338	1.72	2224	28	2185	47	2148	37	104	2148	37
057-Z45	0.0009	198	118	350	0.34	7.0269	1.70	0.3974	1.07	0.63	0.1282	1.33	2157	23	2115	36	2074	27	104	2074	27
058-Z46	0.0051	25	180	125	1.46	0.8646	9.33	0.1028	7.04	0.76	0.0610	6.11	631	44	633	59	639	39	99	639	39
059-Z47	0.0050	10	38	51	0.75	0.8347	22.25	0.0995	17.94	0.81	0.0608	13.17	612	110	616	137	633	83	97	633	83
060-Z48	0.0008	79	45	108	0.42	8.0099	2.77	0.4226	2.06	0.74	0.1375	1.86	2272	47	2232	62	2196	41	103	2196	41
063-Z49	0.0021	31	160	226	0.71	0.8454	7.78	0.1011	5.95	0.76	0.0606	5.02	621	37	622	48	627	31	99	627	31
064-Z50	0.0006	146	163	323	0.51	6.6087	3.08	0.3727	2.71	0.88	0.1286	1.48	2042	55	2061	64	2079	31	98	2079	31
065-Z51	0.0019	40	98	239	0.41	1.1421	5.69	0.1270	3.93	0.69	0.0652	4.11	771	30	774	44	782	32	99	782	32
066-Z52	0.0014	163	150	343	0.44	7.8287	3.18	0.4233	2.81	0.88	0.1341	1.49	2275	64	2212	70	2153	32	106	2153	32
067-Z53	0.0028	19	60	154	0.39	0.8872	9.31	0.1054	8.33	0.90	0.0610	4.15	646	54	645	60	640	27	101	640	27
068-Z54	0.0050	16	184	99	1.88	0.8220	11.26	0.0982	8.67	0.77	0.0607	7.19	604	52	609	69	628	45	96	628	45
069-Z55	0.0467	2	1	4	0.34	4.8464	46.12	0.3787	37.46	0.81	0.0928	26.90	2070	776	1793	827	1484	399	140		
070-Z56	0.0015	27	250	142	1.77	1.0402	10.78	0.1192	8.10	0.75	0.0633	7.12	726	59	724	78	717	51	101	717	51
071-Z57	0.0015	18	131	129	1.02	0.8500	9.86	0.1057	8.43	0.86	0.0583	5.11	648	55	625	62	541	28	120		
072-Z58	0.0010	71	120	131	0.92	6.0319	4.42	0.3742	3.83	0.87	0.1169	2.21	2049	78	1980	88	1909	42	107	1909	42
076-Z59	0.0091	56	51	91	0.56	7.9188	6.57	0.4074	5.51	0.84	0.1410	3.58	2203	121	2222	146	2239	80	98	2239	80
077-Z60	0.0009	85	89	560	0.16	0.8974	5.87	0.1074	4.56	0.78	0.0606	3.70	657	30	650	38	626	23	105	626	23
078-Z61	0.0008	313	251	418	0.60	9.8619	2.07	0.4451	1.21	0.59	0.1607	1.68	2373	29	2422	50	2463	41	96	2463	41
079-Z62	0.0110	285	560	581	0.97	5.9391	2.42	0.3120	1.66	0.68	0.1381	1.77	1751	29	1967	48	2203	39	79		
080-Z63	0.0005	139	118	167	0.71	6.9562	3.94	0.3707	3.61	0.92	0.1361	1.57	2033	73	2106	83	2178	34	93	2178	34
081-Z64	0.0025	35	57	159	0.36	1.2318	5.80	0.1363	4.94	0.85	0.0656	3.04	823	41	815	47	792	24	104	792	24
082-Z65	0.0032	25	34	35	1.00	6.3461	8.11	0.3646	6.79	0.84	0.1263	4.43	2004	136	2025	164	2046	91	98	2046	91
083-Z66	0.0032	24	30	31	0.97	7.3566	6.13	0.3871	4.80	0.78	0.1378	3.83	2110	101	2156	132	2200	84	96	2200	84
084-Z67	0.0034	25	96	131	0.74	0.8728	9.08	0.1036	7.40	0.82	0.0611	5.25	636	47	637	58	642	34	99	642	34
087-Z68	0.0040	19	122	90	1.36	0.8833	11.69	0.1047	9.33	0.80	0.0612	7.04	642	60	643	75	645	45	99	645	45
088-Z69	0.0011	75	404	402	1.01	0.7835	6.10	0.0945	5.07	0.83	0.0601	3.39	582	30	587	36	608	21	96	608	21
089-Z70	0.0014	53	39	85	0.46	6.2900	4.18	0.3507	3.37	0.81	0.1301	2.47	1938	65	2017	84	2099	52	92	2099	52
090-Z71	0.0017	31	55	29	1.90	10.1859	7.13	0.4364	5.04	0.71	0.1693	5.05	2334	118	2452	175	2551	129	92	2551	129
091-Z72	0.0064	190	159	347	0.46	3.5963	7.51	0.2083	7.04	0.94	0.1252	2.61	1220	86	1549	116	2032	53	60		
092-Z73	0.0013	60	185	388	0.48	0.7576	6.65	0.0908	5.54	0.83	0.0605	3.69	560	31	573	38	621	23	90	621	23
093-Z74	0.0012	68	77	63	1.23	8.8649	11.50	0.4296	10.81	0.94	0.1497	3.93	2304	249	2324	267	2342	92	98	2342	92
094-Z75	0.0025	27	31	31	0.99	8.2128	7.48	0.4329	6.03	0.81	0.1376	4.42	2319	140	2255	169	2197	97	106	2197	97
095-Z76	0.0007	87	60	119	0.51	7.5733	3.71	0.4166	2.99	0.80	0.1318	2.20	2245	67	2182	81	2123	47	106	2123	47
096-Z77	0.0334	64	300	331	0.91	1.2443	5.93	0.0961	5.24	0.88	0.0940	2.78	591	31	821	49	1507	42	39		
099-Z78	0.0003	189	114	186	0.62	13.3274	4.17	0.5351	3.90	0.94	0.1806	1.47	2763	108	2703	113	2659	39	104	2659	39
100-Z79	0.0065	58	110	382	0.29	0.8587	6.43	0.0944	5.56	0.87	0.0660	3.22	581	32	629	40	806	26	72		
101-Z80	0.0018	12	55	59	0.93	1.0304	11.47	0.1215	7.47	0.65	0.0615	8.70	739	55	719	83	657	57	112		
102-Z81	0.0031	24	27	32	0.86	6.9732	7.02	0.3897	5.21	0.74	0.1298	4.71	2122	111	2108	148	2095	99	101	2095	99
103-Z82	0.0133	28	102	147	0.70	1.1268	15.95	0.1107	7.12	0.45	0.0738	14.28	677	48	766	122	1037	148	65		
104-Z83	0.0012	30	85	79	1.08	2.1008	4.53	0.1979	3.20	0.71	0.0770	3.21	1164	37	1149	52	1121	36	104	1121	36

105-Z84	0.0012	41	64	51	1.25	6.5822	4.61	0.3791	3.74	0.81	0.1259	2.69	2072	77	2057	95	2042	55	101	2042	55
106-Z85	0.0003	175	117	183	0.64	13.5684	1.55	0.5356	1.06	0.68	0.1838	1.13	2765	29	2720	42	2687	30	103	2687	30
107-Z86	0.0010	20	27	55	0.49	2.3727	4.47	0.2134	3.72	0.83	0.0806	2.48	1247	46	1234	55	1212	30	103	1212	30
108-Z87	0.0170	50	183	283	0.65	0.9169	7.91	0.0894	6.52	0.82	0.0744	4.49	552	36	661	52	1052	47	52		
112-Z88	0.0125	23	89	155	0.58	0.9515	7.34	0.1025	5.36	0.73	0.0673	5.01	629	34	679	50	848	42	74	848	42
113-Z89	0.0008	125	120	196	0.62	7.2532	7.14	0.3981	6.94	0.97	0.1321	1.68	2160	150	2143	153	2127	36	102	2127	36
114-Z90	0.0006	101	72	163	0.44	7.0508	1.99	0.3983	1.49	0.75	0.1284	1.33	2161	32	2118	42	2076	28	104	2076	28
115-Z91	0.0007	139	303	477	0.64	2.1185	2.88	0.2062	2.04	0.71	0.0745	2.04	1209	25	1155	33	1055	21	115		
116-Z92	0.0010	57	204	331	0.62	0.9155	4.41	0.1097	3.26	0.74	0.0605	2.96	671	22	660	29	623	18	108	623	18
117-Z93	0.0009	37	31	51	0.62	7.2151	6.75	0.3832	5.71	0.85	0.1366	3.60	2091	119	2138	144	2184	79	96	2184	79
118-Z94	0.0069	16	83	117	0.71	0.7282	9.75	0.0900	7.08	0.73	0.0587	6.69	555	39	556	54	556	37	100	556	37
119-Z95	0.0034	76	69	86	0.80	8.5351	5.89	0.3736	5.40	0.92	0.1657	2.34	2046	111	2290	135	2515	59	81		
120-Z96	0.0001	25	86	162	0.53	0.9018	5.19	0.1064	4.42	0.85	0.0615	2.73	652	29	653	34	656	18	99	656	18
123-Z97	0.0046	8	31	40	0.80	0.9951	19.79	0.1141	15.89	0.80	0.0632	11.80	697	111	701	139	716	85	97	716	85
124-Z98	0.0314	42	195	247	0.79	1.2696	8.71	0.0990	6.18	0.71	0.0930	6.13	608	38	832	72	1489	91	41		
125-Z99	0.0913	73	144	246	0.59	2.2705	53.52	0.0963	9.46	0.18	0.1709	52.68	593	56	1203	644	2567	1352	23		
126-Z100	0.0019	55	150	355	0.43	0.7691	6.17	0.0907	5.25	0.85	0.0615	3.24	560	29	579	36	656	21	85		
127-Z101	0.0018	27	96	153	0.63	0.7750	10.18	0.0955	8.44	0.83	0.0588	5.70	588	50	583	59	561	32	105	561	32
128-Z102	0.0012	108	54	86	0.63	12.2101	2.43	0.4833	1.51	0.62	0.1832	1.90	2542	38	2621	64	2682	51	95	2682	51
129-Z103	0.0275	206	221	383	0.58	8.5686	4.21	0.3943	3.60	0.85	0.1576	2.19	2143	77	2293	97	2430	53	88		
130-Z104	0.0024	32	17	182	0.10	1.1010	6.85	0.1243	5.12	0.75	0.0642	4.54	755	39	754	52	749	34	101	749	34
131-Z105	0.0011	92	61	84	0.73	13.6240	3.27	0.5328	2.83	0.87	0.1854	1.63	2753	78	2724	89	2702	44	102	2702	44
132-Z106	0.0023	30	104	160	0.65	0.9427	8.94	0.1106	7.41	0.83	0.0618	5.00	676	50	674	60	669	33	101	669	33
135-Z107	0.0172	94	332	537	0.62	0.9854	12.74	0.0820	10.15	0.80	0.0871	7.70	508	52	696	89	1363	105	37		
136-Z108	0.0034	14	20	109	0.18	0.8809	8.91	0.1046	6.70	0.75	0.0611	5.88	641	43	641	57	642	38	100	642	38
137-Z109	0.0013	43	30	62	0.49	7.0300	4.59	0.3719	3.94	0.86	0.1371	2.35	2038	80	2115	97	2191	52	93	2191	52
138-Z110	0.0005	194	149	326	0.46	6.9946	3.11	0.3686	2.45	0.79	0.1376	1.92	2023	50	2111	66	2198	42	92	2198	42
139-Z111	0.0012	50	67	66	1.02	6.2414	5.03	0.3428	4.09	0.81	0.1320	2.92	1900	78	2010	101	2125	62	89		
140-Z112	0.0007	156	132	217	0.61	6.5920	2.33	0.3709	1.61	0.69	0.1289	1.68	2034	33	2058	48	2083	35	98	2083	35
141-Z113	0.0080	55	154	290	0.53	1.2223	7.12	0.1082	6.58	0.92	0.0820	2.71	662	44	811	58	1244	34	53		
142-Z114	0.0018	66	61	77	0.80	8.3180	3.71	0.4346	2.82	0.76	0.1388	2.41	2326	66	2266	84	2212	53	105	2212	53
143-Z115	0.0023	54	57	366	0.16	0.8750	6.95	0.1040	5.75	0.83	0.0610	3.90	638	37	638	44	639	25	100	639	25
144-Z116	0.0555	80	443	412	1.08	0.9013	12.20	0.0801	11.59	0.95	0.0816	3.82	497	58	652	80	1237	47	40		
148-Z117	0.0126	131	109	161	0.68	8.2992	2.84	0.4268	2.22	0.78	0.1410	1.77	2291	51	2264	64	2240	40	102	2240	40
149-Z118	0.0002	27	80	110	0.74	0.9286	10.42	0.1114	8.61	0.83	0.0605	5.87	681	59	667	69	620	36	110	620	36
150-Z119	0.0238	87	322	381	0.85	1.3261	6.12	0.1108	5.24	0.86	0.0868	3.17	677	35	857	52	1356	43	50		
151-Z120	0.0011	65	178	277	0.65	0.9184	7.01	0.1093	5.98	0.85	0.0609	3.65	669	40	661	46	637	23	105	637	23
152-Z121	0.0005	333	308	313	0.99	10.9607	1.92	0.5014	1.23	0.64	0.1585	1.48	2620	32	2520	48	2440	36	107	2440	36
153-Z122	0.0008	68	265	277	0.96	1.0331	6.64	0.1207	5.43	0.82	0.0621	3.83	734	40	720	48	678	26	108	678	26
154-Z123	0.0015	130	427	580	0.74	0.9751	6.37	0.1141	5.14	0.81	0.0620	3.77	696	36	691	44	674	25	103	674	25
155-Z124	0.0018	77	234	392	0.60	0.9407	6.66	0.1100	5.55	0.83	0.0620	3.67	673	37	673	45	674	25	100	674	25
156-Z125	0.0245	118	197	526	0.38	1.6892	22.99	0.1387	4.37	0.19	0.0883	22.57	837	37	1004	231	1389	314	60		

Table 1b: U-Pb in situ zircon data of sample GU-01, Guaritas Gr.

						Isotope ratios							Ages (Ma)							
Spot num	f 206	Pb ppm	U ppm	Th ppm	Th/U^a	^{207}Pb/^{235}U	1 s [%]	^{206}Pb/^{238}U	1 s [%]	Rho^c	^{207}Pb/^{206}Pb^d	1 s [%]	^{206}Pb/^{238}U	1 s abs	^{207}Pb/^{235}U	1 s abs	^{207}Pb/^{206}Pb	1 s abs	% Conc^e	Best estimated age (Ma)
003-Z1	0.0003	12	14	43	0.32	2.46448	3.79	0.20764	2.33	0.62	0.08608	2.99	1216	28	1262	48	1340	40	91	1340 40
004-Z2	0.0146	20	189	149	1.28	0.84997	13.03	0.10054	2.42	0.19	0.06132	12.80	618	15	625	81	650	83	95	650 83
005-Z3	0.0088	42	348	257	1.36	1.10532	4.93	0.12269	2.61	0.53	0.06534	4.19	746	19	756	37	785	33	95	785 33
006-Z4	0.0024	31	293	235	1.25	0.75616	7.10	0.09189	4.44	0.63	0.05968	5.54	567	25	572	41	592	33	96	592 33
007-Z5	0.0008	13	48	100	0.49	0.79293	9.08	0.09459	5.35	0.59	0.06080	7.33	583	31	593	54	632	46	92	632 46
008-Z6	**0.0000**	**83**	**152**	**173**	**0.89**	**8.74671**	**2.82**	**0.32913**	**2.30**	**0.81**	**0.19274**	**1.63**	**1834**	**42**	**2312**	**65**	**2766**	**45**	**66**	
009-Z7	0.0008	20	122	132	0.93	0.84781	6.00	0.10036	3.06	0.51	0.06127	5.16	617	19	623	37	649	33	95	649 33
010-Z8	0.0000	132	170	299	0.57	6.98085	1.05	0.36472	0.92	0.88	0.13882	0.51	2005	18	2109	22	2213	11	91	2213 11
011-Z9	0.0140	55	778	405	1.93	0.74477	9.52	0.09028	2.90	0.30	0.05983	9.06	557	16	565	54	597	54	93	597 54
012-Z10	**0.0000**	**9**	**58**	**62**	**0.95**	**0.96558**	**4.49**	**0.10770**	**3.74**	**0.83**	**0.06503**	**2.49**	**659**	**25**	**686**	**31**	**775**	**19**	**85**	
015-PAD	0.0000	10	70	74	0.95	0.94252	4.88	0.10886	4.52	0.93	0.06280	1.82	666	30	674	33	701	13	95	701 13
016-Z11	**0.0000**	**19**	**186**	**113**	**1.66**	**1.26203**	**12.52**	**0.08524**	**9.23**	**0.74**	**0.10738**	**8.46**	**527**	**49**	**829**	**104**	**1755**	**149**	**30**	
017-Z12	0.0049	56	469	489	0.97	0.80727	5.85	0.09589	3.56	0.61	0.06106	4.65	590	21	601	35	641	30	92	641 30
018-Z13	0.0000	26	126	153	0.83	1.24096	3.78	0.13205	3.11	0.82	0.06816	2.14	800	25	819	31	873	19	92	873 19
019-Z14	**0.0000**	**60**	**123**	**151**	**0.83**	**4.93764**	**3.03**	**0.28764**	**2.93**	**0.97**	**0.12450**	**0.78**	**1630**	**48**	**1809**	**55**	**2022**	**16**	**81**	
020-Z15	0.0110	24	501	205	2.46	0.88975	15.27	0.10364	3.04	0.20	0.06226	14.96	636	19	646	99	683	102	93	683 102
021-Z16	0.0000	21	492	162	3.06	0.95007	2.31	0.10791	1.81	0.78	0.06386	1.44	661	12	678	16	737	11	90	707 11
022-Z17N	**0.0001**	**44**	**114**	**133**	**0.86**	**4.36322**	**1.98**	**0.26680**	**1.18**	**0.60**	**0.11861**	**1.59**	**1525**	**18**	**1705**	**34**	**1935**	**31**	**79**	
023-Z17B	**0.0065**	**22**	**219**	**174**	**1.27**	**0.91270**	**7.54**	**0.10057**	**2.84**	**0.38**	**0.06582**	**6.98**	**618**	**18**	**658**	**50**	**801**	**56**	**77**	
024-Z18B	**0.0000**	**21**	**500**	**209**	**2.41**	**5.16924**	**3.44**	**0.09266**	**2.83**	**0.82**	**0.40462**	**1.96**	**571**	**16**	**1848**	**64**	**3926**	**77**	**15**	
028-Z19	0.0003	19	29	89	0.33	1.95635	4.20	0.17958	3.00	0.71	0.07901	2.94	1065	32	1101	46	1172	34	91	1172 34
029-Z20	0.0011	59	376	445	0.85	1.09145	3.77	0.12032	2.35	0.62	0.06579	2.95	732	17	749	28	800	24	92	800 24
030-Z21	**0.0000**	**28**	**105**	**178**	**0.59**	**1.52506**	**4.33**	**0.13826**	**3.78**	**0.87**	**0.08000**	**2.11**	**835**	**32**	**941**	**41**	**1197**	**25**	**70**	
031-Z22	0.0050	25	466	245	1.92	0.75657	5.05	0.09141	2.23	0.44	0.06003	4.53	564	13	572	29	605	27	93	605 27
032-Z23	**0.0112**	**30**	**417**	**268**	**1.57**	**0.84438**	**8.03**	**0.09484**	**3.49**	**0.43**	**0.06457**	**7.23**	**584**	**20**	**622**	**50**	**761**	**55**	**77**	
033-Z24B	**0.0331**	**59**	**1277**	**607**	**2.12**	**0.79768**	**18.03**	**0.08837**	**13.95**	**0.77**	**0.06547**	**11.41**	**546**	**76**	**596**	**107**	**789**	**90**	**69**	
034-Z24N	0.0006	51	232	378	0.62	1.10420	4.15	0.12229	2.50	0.60	0.06548	3.31	744	19	755	31	790	26	94	790 26
035-Z25N	**0.0000**	**28**	**117**	**141**	**0.84**	**4.05372**	**2.11**	**0.21562**	**1.43**	**0.68**	**0.13635**	**1.55**	**1259**	**18**	**1645**	**35**	**2181**	**34**	**58**	
036-Z25B	**0.0322**	**85**	**1457**	**929**	**1.58**	**0.66871**	**7.36**	**0.07924**	**3.39**	**0.46**	**0.06120**	**6.54**	**492**	**17**	**520**	**38**	**646**	**42**	**76**	
037-Z26	0.0001	16	82	151	0.55	0.79362	3.78	0.09548	2.23	0.59	0.06029	3.05	588	13	593	22	614	19	96	614 19
040-Z27	**0.0085**	**22**	**388**	**192**	**2.04**	**0.83314**	**6.72**	**0.09542**	**1.61**	**0.24**	**0.06333**	**6.52**	**587**	**9**	**615**	**41**	**719**	**47**	**82**	
041-Z28	0.0000	5	67	44	1.54	0.93057	4.41	0.10857	3.47	0.79	0.06216	2.72	664	23	668	29	680	18	98	680 18
042-Z29	0.0027	19	195	170	1.15	0.75611	14.30	0.09262	12.93	0.90	0.05921	6.11	571	74	572	82	575	35	99	575 35
043-Z30	0.0004	16	41	107	0.38	1.05679	6.31	0.11842	4.06	0.64	0.06472	4.83	721	29	732	46	765	37	94	765 37
044-Z31	0.0178	16	447	143	3.15	0.87059	14.20	0.10306	4.67	0.33	0.06127	13.41	632	30	636	90	649	87	97	649 87
045-Z32	0.0000	33	51	123	0.42	3.19001	2.59	0.24333	2.27	0.88	0.09508	1.23	1404	32	1455	38	1530	19	92	1530 19
046-Z33	**0.0049**	**10**	**63**	**74**	**0.86**	**0.90193**	**10.32**	**0.10066**	**7.22**	**0.70**	**0.06499**	**7.37**	**618**	**45**	**653**	**67**	**774**	**57**	**80**	
046-Z34	**0.0029**	**13**	**29**	**92**	**0.32**	**1.16149**	**9.23**	**0.12115**	**5.14**	**0.56**	**0.06954**	**7.67**	**737**	**38**	**783**	**72**	**915**	**70**	**81**	

ID	f206(%)	Pb	U	Th	Th/U	207Pb/235U	±%	206Pb/238U	±%	Rho	207Pb/206Pb	±%	206/238	±	207/235	±	207/206	±	Conc.	Age	±
047-Z35	0.0000	12	119	103	1.17	0.81864	3.18	0.09819	2.44	0.77	0.06047	2.05	604	15	607	19	620	13	97	620	13
048-Z36	**0.0057**	**49**	**658**	**500**	**1.33**	**0.69124**	**7.40**	**0.08296**	**5.08**	**0.69**	**0.06043**	**5.39**	**514**	**26**	**534**	**40**	**619**	**33**	**83**		
051-Z37	0.0003	42	19	345	0.06	0.91136	3.93	0.10628	2.40	0.61	0.06219	3.12	651	16	658	26	681	21	96	681	21
052-Z38	0.0027	30	479	281	1.72	0.86657	6.01	0.10248	2.98	0.50	0.06133	5.22	629	19	634	38	651	34	97	651	34
053-Z39	0.0083	20	320	170	1.89	0.82369	6.71	0.09843	2.37	0.35	0.06070	6.28	605	14	610	41	628	39	96	628	39
054-Z40	0.0000	29	604	233	2.61	0.97914	4.07	0.11336	3.00	0.74	0.06264	2.76	692	21	693	28	696	19	99	696	19
055-Z41	**0.0055**	**50**	**453**	**451**	**1.01**	**0.99881**	**7.87**	**0.11147**	**7.02**	**0.89**	**0.06499**	**3.57**	**681**	**48**	**703**	**55**	**774**	**28**	**88**		
056-Z42	**0.0001**	**18**	**56**	**107**	**0.53**	**1.60471**	**2.62**	**0.15540**	**1.51**	**0.58**	**0.07490**	**2.13**	**931**	**14**	**972**	**25**	**1066**	**23**	**87**		
057-Z43	0.0001	14	44	130	0.34	0.78504	5.12	0.09473	2.28	0.45	0.06011	4.58	583	13	588	30	607	28	96	607	28
058-Z44	0.0000	1	9	7	1.31	0.79679	10.67	0.09621	8.77	0.82	0.06007	6.09	592	52	595	64	606	37	98	606	37
059-Z45B	0.0000	35	402	333	1.22	0.79517	4.53	0.09456	1.79	0.40	0.06099	4.16	582	10	594	27	639	27	91	639	27
060-Z45N	**0.0158**	**37**	**943**	**385**	**2.47**	**0.71911**	**9.30**	**0.08537**	**5.43**	**0.58**	**0.06109**	**7.55**	**528**	**29**	**550**	**51**	**642**	**48**	**82**		
063-Z46	0.0001	10	128	89	1.45	0.79219	5.92	0.09644	3.97	0.67	0.05958	4.39	594	24	592	35	588	26	101	588	26
064-Z47	**0.0008**	**8**	**17**	**22**	**0.77**	**5.92358**	**3.58**	**0.33005**	**2.71**	**0.76**	**0.13017**	**2.34**	**1839**	**50**	**1965**	**70**	**2100**	**49**	**88**		
065-Z48N	**0.0000**	**2**	**7**	**12**	**0.55**	**1.45541**	**5.32**	**0.14016**	**2.31**	**0.43**	**0.07531**	**4.80**	**846**	**20**	**912**	**49**	**1077**	**52**	**79**		
066-Z48B	**0.0159**	**9**	**112**	**97**	**1.16**	**0.72315**	**19.36**	**0.08441**	**7.75**	**0.40**	**0.06214**	**17.74**	**522**	**40**	**553**	**107**	**679**	**120**	**77**		
067-Z49	0.0015	14	51	102	0.50	1.74831	6.83	0.17063	3.34	0.49	0.07431	5.95	1016	34	1027	70	1050	63	97	1050	63
068-Z50	**0.0001**	**8**	**64**	**72**	**0.90**	**0.88538**	**3.87**	**0.09372**	**3.29**	**0.85**	**0.06852**	**2.04**	**577**	**19**	**644**	**25**	**884**	**18**	**65**		
069-Z51	**0.0290**	**11**	**239**	**109**	**2.20**	**0.68578**	**9.86**	**0.08243**	**4.03**	**0.41**	**0.06034**	**9.00**	**511**	**21**	**530**	**52**	**616**	**55**	**83**		
070-Z52	0.0000	3	21	29	0.73	0.76728	5.43	0.09255	3.96	0.73	0.06013	3.72	571	23	578	31	608	23	94	608	23
071-Z53	0.0001	13	42	114	0.37	0.82086	4.61	0.09817	3.91	0.85	0.06064	2.45	604	24	609	28	627	15	96	627	15
072-Z54	0.0053	24	276	207	1.34	0.86652	4.60	0.10186	3.25	0.71	0.06170	3.27	625	20	634	29	664	22	94	664	22
075-Z55N	**0.0000**	**11**	**22**	**59**	**0.38**	**1.75202**	**3.08**	**0.15640**	**2.06**	**0.67**	**0.08125**	**2.28**	**937**	**19**	**1028**	**32**	**1227**	**28**	**76**		
076-Z55B	**0.0336**	**44**	**375**	**345**	**1.09**	**0.93318**	**7.60**	**0.09698**	**1.94**	**0.25**	**0.06979**	**7.35**	**597**	**12**	**669**	**51**	**922**	**68**	**65**		
077-Z56	0.0001	14	91	118	0.78	0.76859	4.24	0.09175	1.80	0.43	0.06075	3.84	566	10	579	25	631	24	90	631	24
078-Z57	0.0022	20	190	162	1.18	0.85531	4.53	0.10039	1.80	0.40	0.06179	4.16	617	11	628	28	667	28	92	667	28
079-Z58	**0.0123**	**40**	**757**	**343**	**2.22**	**0.74126**	**6.26**	**0.08762**	**1.96**	**0.31**	**0.06136**	**5.94**	**541**	**11**	**563**	**35**	**652**	**39**	**83**		
080-Z59	0.0000	5	40	44	0.93	0.85273	3.04	0.09959	1.62	0.53	0.06210	2.58	612	10	626	19	678	17	90	678	17
081-Z60	0.0001	15	140	130	1.09	0.81291	3.78	0.09688	2.17	0.57	0.06086	3.10	596	13	604	23	634	20	94	634	20
070-Z52	0.0000	3	21	28	0.74	0.78230	3.76	0.09322	2.05	0.54	0.06086	3.16	575	12	587	22	634	20	91	634	20
071-Z53	0.0002	14	42	112	0.38	0.81281	4.33	0.09775	3.08	0.71	0.06031	3.05	601	19	604	26	615	19	98	615	19
072-Z54	0.0025	25	271	198	1.38	0.85712	3.29	0.09994	1.92	0.58	0.06220	2.67	614	12	629	21	681	18	90	681	18

[a] Th/U ratios are calculated relative to GJ-1 reference zircon

[b] Corrected for background and within-run Pb/U fractionation and normalised to reference zircon GJ-1 (ID-TIMS values/measured value); 207Pb/235U calculated using $(^{207}Pb/^{206}Pb)/(^{238}U/^{206}Pb * 1/137.88)$

[c] Rho is the error correlation defined as the quotient of the propagated errors of the $^{206}Pb/^{238}U$ and the $^{207}/^{235}U$ ratio

[d] Corrected for mass-bias by normalising to GJ-1 reference zircon and common Pb using the model Pb composition of Stacey and Kramers (1975)

[e] Degree of concordance = $(^{206}Pb/^{238}U$ age $* 100/^{207}Pb/^{206}U$ age)

Table 1c: U-Pb in situ zircon data of sample GU-02, Guaritas Gr.

						Isotope ratios							Ages (Ma)							
Spot num	f 206	Pb ppm	U ppm	Th ppm	Th/Ua	$^{207}Pb/^{235}U$	1 s [%]	$^{206}Pb/^{238}U$	1 s [%]	Rho	$^{207}Pb/^{206}Pb$	1 s [%]	$^{206}Pb/^{238}U$	1 s abs	$^{207}Pb/^{235}U$	1 s abs	$^{207}Pb/^{206}Pb$	1 s abs	% Conc	Best estimated age (Ma)
-Z1.static.	0.0000	17	115	130	0.90	0.8832	4.21	0.1053	3.70	0.88	0.0609	2.02	645	24	643	27	634	13	102	634	13
-Z2.static.	0.0000	47	59	64	0.93	15.0795	1.96	0.5517	1.69	0.86	0.1982	0.99	2832	48	2820	55	2812	28	101	2812	28
-Z3.static.	0.0000	11	40	57	0.70	1.2139	2.81	0.1339	1.94	0.69	0.0657	2.03	810	16	807	23	798	16	102	798	16
-Z4.static.	0.0050	109	281	718	0.39	1.1128	11.60	0.1257	11.02	0.95	0.0642	3.63	764	84	759	88	748	27	102	748	27
-Z5.static.	0.0018	80	576	542	1.07	0.8854	4.30	0.1040	2.73	0.64	0.0617	3.32	638	17	644	28	664	22	96	664	22
-Z6.static.	0.0016	76	783	577	1.37	0.8664	3.54	0.1033	2.17	0.61	0.0608	2.79	634	14	634	22	634	18	100	634	18
-Z7.static.	0.0006	28	213	188	1.14	0.8894	4.41	0.1067	1.85	0.42	0.0605	4.00	653	12	646	29	621	25	105	621	25
-Z8.static.	0.0000	29	179	186	0.96	0.9408	2.51	0.1125	1.68	0.67	0.0606	1.86	687	12	673	17	626	12	110	626	12
-Z9.static.	0.0000	11	94	74	1.29	0.8467	3.16	0.1029	2.31	0.73	0.0597	2.16	632	15	623	20	591	13	107	591	13
Z11.static	0.0167	61	608	412	1.49	1.10033	237.46	0.13187	17.95	0.08	0.06051	236.78	799	143	754	1789	622	1473	128		
Z12.static	0.0157	79	1295	878	1.48	0.74517	35.80	0.08349	3.86	0.11	0.06473	35.59	517	20	565	202	766	273	68		
Z13.static	0.0051	31	107	199	0.54	0.98227	6.62	0.11578	2.88	0.43	0.06153	5.97	706	20	695	46	658	39	107	658	39
Z14.static	0.0000	89	97	207	0.47	6.20139	1.84	0.34740	1.08	0.59	0.12947	1.49	1922	21	2005	37	2091	31	92	2091	31
Z15.static	0.0000	17	222	120	1.87	0.93549	2.22	0.10637	1.47	0.66	0.06379	1.67	652	10	671	15	735	12	89		
Z16.static	0.0000	102	738	901	0.83	1.45285	5.81	0.09659	1.29	0.22	0.10909	5.66	594	8	911	53	1784	101	33		
Z17.static	0.0093	59	788	459	1.73	0.81508	6.09	0.10031	3.73	0.61	0.05893	4.81	616	23	605	37	565	27	109	565	27
Z18.static	0.0000	93	72	725	0.10	0.89213	2.48	0.09998	1.79	0.72	0.06472	1.72	614	11	648	16	765	13	80		
Z19.static	0.0000	102	94	154	0.61	11.15612	3.76	0.49586	3.49	0.93	0.16317	1.39	2596	91	2536	95	2489	35	104	2489	35
Z20.static	0.0024	85	459	379	1.22	1.97429	3.92	0.17942	2.47	0.63	0.07981	3.05	1064	26	1107	43	1192	36	89		
Z21.static	0.0001	52	69	86	0.82	7.10731	1.95	0.39948	1.82	0.93	0.12904	0.70	2167	39	2125	41	2085	15	104	2085	15
Z22.static	0.0012	45	255	259	0.99	0.93476	5.02	0.11114	4.00	0.80	0.06100	3.03	679	27	670	34	639	19	106	639	19
Z23.static	0.0000	19	100	129	0.78	0.84603	4.52	0.10184	3.09	0.68	0.06025	3.30	625	19	622	28	613	20	102	613	20
~~Z24.static~~	~~0.0200~~	~~92~~	~~1654~~	~~680~~	~~2.45~~	~~0.62314~~	~~9.95~~	~~0.07713~~	~~8.33~~	~~0.84~~	~~0.05859~~	~~5.45~~	~~479~~	~~40~~	~~492~~	~~49~~	~~552~~	~~30~~	87	~~552~~	~~30~~
Z25.static	0.0000	63	107	99	1.09	7.59394	1.19	0.43588	0.92	0.77	0.12636	0.76	2332	21	2184	26	2048	16	114		
Z26.static	0.0273	92	1483	711	2.10	0.76577	12.83	0.08987	2.31	0.18	0.06180	12.62	555	13	577	74	667	84	83		
Z27.static	0.0000	60	189	430	0.44	1.03604	11.45	0.10021	11.31	0.99	0.07498	1.79	616	70	722	83	1068	19	58		
Z28.static	0.0003	93	40	173	0.23	6.87065	1.60	0.39252	1.25	0.78	0.12695	1.00	2135	27	2095	34	2056	21	104	2056	21
Z29.static	0.0001	76	149	473	0.32	1.03751	5.34	0.11784	2.29	0.43	0.06386	4.83	718	16	723	39	737	36	97	737	36
Z30.static	0.0004	112	160	165	0.98	13.08243	5.09	0.50825	2.79	0.55	0.18668	4.25	2649	74	2686	137	2713	115	98	2713	115
Z31.static	0.0002	32	27	68	0.40	6.04490	2.78	0.35935	2.49	0.90	0.12200	1.24	1979	49	1982	55	1986	25	100	1986	25
Z32.static	0.0015	41	112	265	0.42	0.89586	3.92	0.10845	2.38	0.06	2.71925	3.12	664	16	652	24	612	17	107	612	17
Z33.static	0.0008	79	155	477	0.33	0.83712	4.32	0.10025	3.48	0.81	0.06056	2.56	616	21	618	27	624	16	99	624	16
Z34.static	0.0020	52	121	246	0.50	1.31634	6.37	0.14343	4.60	0.72	0.06656	4.41	864	40	853	54	824	36	105	824	36
Z35.static	0.0065	97	223	305	0.74	3.83883	5.81	0.23155	4.23	0.73	0.12024	3.98	1343	57	1601	93	1960	78	69		
Z36.static	0.0020	82	270	165	1.65	6.85449	3.68	0.37912	1.47	0.40	0.13113	3.38	2072	30	2093	77	2113	71	98	2113	71
Z37.static	0.0001	57	129	189	0.69	2.56095	1.85	0.22272	1.38	0.75	0.08339	1.22	1296	18	1290	24	1278	16	101	1278	16
Z38.static	0.0000	200	227	451	0.51	5.51922	12.23	0.27158	9.42	0.77	0.14739	7.80	1549	146	1904	233	2316	181	67		
Z39.static	0.0002	18	202	130	1.57	0.98972	18.81	0.10679	10.19	0.54	0.06722	15.81	654	67	699	131	845	134	77		

Z40.static	0.0017	36	156	183	0.86	1.27458	6.18	0.13862	2.21	0.36	0.06669	5.77	837	18	834	52	828	48	101	828	48
Z41.static	0.0008	68	76	102	0.75	8.44148	1.30	0.44625	1.16	0.89	0.13719	0.58	2379	28	2280	30	2192	13	109	2192	13
Z42.static	0.0046	81	395	555	0.72	1.18603	8.68	0.13014	7.67	0.88	0.06610	4.06	789	60	794	69	809	33	97	809	33
Z43.static	0.0000	53	174	283	0.62	1.33321	2.64	0.14737	1.81	0.69	0.06561	1.92	886	16	860	23	794	15	112		
Z44.static	0.0021	81	143	290	0.50	2.79582	3.33	0.22467	1.28	0.38	0.09025	3.07	1306	17	1354	45	1431	44	91	1431	44
Z45.static	0.0000	14	118	112	1.07	0.83925	3.45	0.10115	2.85	0.83	0.06018	1.95	621	18	619	21	610	12	102	610	12
Z46.static	0.0002	62	75	176	0.43	3.30471	3.55	0.25656	3.23	0.91	0.09342	1.48	1472	47	1482	53	1496	22	98	1496	22
Z47.static	0.0128	49	342	184	1.88	2.26898	5.66	0.21753	2.71	0.48	0.07565	4.96	1269	34	1203	68	1086	54	117		
Z48.static	0.0022	18	142	121	1.17	0.94716	8.55	0.12178	2.59	0.30	0.05641	8.15	741	19	677	58	468	38	158		
Z49.static	0.0001	88	82	176	0.47	7.69265	2.88	0.40642	2.20	0.76	0.13728	1.86	2199	48	2196	63	2193	41	100	2193	41
Z50.static	0.0010	49	120	94	1.28	6.59668	4.23	0.37692	3.98	0.94	0.12693	1.44	2062	82	2059	87	2056	30	100	2056	30
Z51.static	0.0221	89	2319	914	2.56	0.62592	24.01	0.07279	3.00	0.12	0.06236	23.82	453	14	494	119	687	164	66		
Z52.static	0.0077	44	227	257	0.89	0.97990	10.81	0.11486	4.63	0.43	0.06188	9.77	701	32	694	75	670	65	105	670	65
Z53.static	0.0062	84	1244	704	1.78	0.91255	10.04	0.10666	6.13	0.61	0.06205	7.95	653	40	658	66	676	54	97	676	54
Z54.static	0.0002	46	82	163	0.51	1.79957	2.32	0.17811	1.31	0.56	0.07328	1.92	1057	14	1045	24	1022	20	103	1022	20
Z55.static	0.0000	13	54	91	0.59	0.85365	2.59	0.10316	2.12	0.82	0.06002	1.50	633	13	627	16	604	9	105	604	9
Z56.static	0.0106	102	107	228	0.47	7.13413	2.35	0.33972	1.53	0.65	0.15231	1.78	1885	29	2128	50	2372	42	79		
Z57.static	0.0001	50	109	245	0.45	1.23921	5.03	0.13660	4.71	0.94	0.06579	1.77	825	39	819	41	800	14	103	800	14
Z58.static	0.0092	122	975	421	2.33	3.13515	3.63	0.20625	2.26	0.62	0.11025	2.84	1209	27	1441	52	1803	51	67		
Z59.static	0.0059	37	369	370	1.00	0.61369	29.13	0.07653	22.69	0.78	0.05816	18.27	475	108	486	142	536	98	89	536	98
Z60.static	0.0000	72	127	216	0.59	2.43252	1.52	0.22223	1.14	0.75	0.07939	1.01	1294	15	1252	19	1182	12	109	1182	12
Z10.static	0.0006	39	313	233	1.35	0.94878	4.04	0.11054	2.66	0.66	0.06225	3.05	676	18	677	27	683	21	99	683	21

[a] Th/U ratios are calculated relative to GJ-1 reference zircon

[b] Corrected for background and within-run Pb/U fractionation and normalised to reference zircon GJ-1 (ID-TIMS values/measured value); 207Pb/235U calculated
using $(^{207}Pb/^{206}Pb)/(^{238}U/^{206}Pb * 1/137.88)$

[c] Rho is the error correlation defined as the quotient of the propagated errors of the $^{206}Pb/^{238}U$ and the $^{207}Pb/^{235}U$ ratio

[d] Corrected for mass-bias by normalising to GJ-1 reference zircon and common Pb using the model Pb composition of Stacey and Kramers (1975)

[e] Degree of concordance = ($^{206}Pb/^{238}U$ age * 100/$^{207}Pb/^{206}U$ age)

Table 1d : U-Pb in situ zircon data of sample PS-03 SB III, Santa Barbara Gr.

Spot num	f 206	Pb ppm	U ppm	Th ppm	Th/U^a	^{207}Pb/^{235}U	1 s [%]	^{206}Pb/^{238}U	1 s [%]	Rho^c	^{207}Pb/^{206}Pb^d	1 s [%]	^{206}Pb/^{238}U	1 s abs	^{207}Pb/^{235}U	1 s abs	^{207}Pb/^{206}Pb	1 s abs	% Conc^e	Best estimated age (Ma)	
004-Z1	0.0001	4	67	38	1.79	0.79189	3.83	0.09656	2.30	0.60	0.05948	3.06	594	14	592	23	585	18	102	594	14
005-Z2	**0.0000**	**9**	**45**	**46**	**0.99**	**1.23967**	**5.19**	**0.10771**	**4.53**	**0.87**	**0.08347**	**2.54**	**659**	**30**	**819**	**43**	**1280**	**33**	**52**		
006-Z3	**0.0001**	**52**	**448**	**409**	**1.10**	**0.76795**	**6.29**	**0.08874**	**4.17**	**0.66**	**0.06276**	**4.71**	**548**	**23**	**579**	**36**	**700**	**33**	**78**		
007-Z4	0.0002	79	64	113	0.57	13.70688	2.44	0.53261	1.82	0.75	0.18665	1.62	2752	50	2730	67	2713	44	101	2713	44
008-Z5	**0.0000**	**29**	**215**	**218**	**0.99**	**0.88481**	**3.39**	**0.09716**	**2.58**	**0.76**	**0.06605**	**2.19**	**598**	**15**	**644**	**22**	**808**	**18**	**74**		
009-Z6	0.0001	41	79	65	1.22	10.51277	3.01	0.47784	2.97	0.98	0.15956	0.52	2518	75	2481	75	2451	13	103	2451	13
010-Z7	0.0002	26	113	150	0.76	0.80061	4.90	0.09700	4.42	0.90	0.05986	2.12	597	26	597	29	599	13	100	599	13
011-Z8	0.0008	7	114	58	1.99	0.75085	3.92	0.09148	2.89	0.74	0.05953	2.65	564	16	569	22	586	16	96	586	16
012-Z9	**0.0005**	**87**	**200**	**152**	**1.33**	**14.64018**	**2.72**	**0.34988**	**2.33**	**0.86**	**0.30348**	**1.40**	**1934**	**45**	**2792**	**76**	**3488**	**49**	**55**		
016-Z11	0.0001	42	347	327	1.07	0.76624	3.02	0.09358	1.91	0.63	0.05938	2.35	577	11	578	17	581	14	99	577	11
017-Z12	0.0002	34	204	244	0.84	0.81424	4.94	0.09834	3.25	0.66	0.06005	3.73	605	20	605	30	605	23	100	605	23
018-Z13	0.0000	21	81	140	0.58	0.89835	2.42	0.10639	1.51	0.62	0.06124	1.89	652	10	651	16	648	12	101	648	12
019-Z14	0.0005	22	187	169	1.12	0.79791	5.33	0.09451	2.94	0.55	0.06123	4.45	582	17	596	32	647	29	90	647	29
020-Z15	**0.0001**	**26**	**138**	**174**	**0.80**	**0.82184**	**1.97**	**0.09613**	**1.39**	**0.71**	**0.06200**	**1.39**	**592**	**8**	**609**	**12**	**674**	**9**	**88**		
021-Z16	0.0001	73	140	165	0.86	6.21183	3.59	0.34581	2.12	0.59	0.13028	2.89	1915	41	2006	72	2102	61	91	2102	61
022-Z17	0.0107	11	58	27	2.19	4.41277	5.76	0.30246	1.43	0.25	0.10581	5.58	1704	24	1715	99	1728	97	99	1728	97
023-Z18	**0.0011**	**59**	**266**	**540**	**0.49**	**0.62411**	**6.31**	**0.07751**	**3.27**	**0.52**	**0.05840**	**5.40**	**481**	**16**	**492**	**31**	**545**	**29**	**88**		
024-Z19	**0.0018**	**7**	**30**	**33**	**0.94**	**1.74458**	**19.11**	**0.13717**	**3.41**	**0.18**	**0.09224**	**18.80**	**829**	**28**	**1025**	**196**	**1472**	**277**	**56**		
025-Z20	0.0001	17	162	113	1.44	0.90508	3.37	0.10766	2.68	0.80	0.06097	2.04	659	18	654	22	638	13	103	638	13
028-Z21	0.0005	53	570	477	1.20	0.85114	3.31	0.09959	2.48	0.75	0.06198	2.18	612	15	625	21	674	15	91	674	15
029-Z22	**0.0072**	**83**	**25**	**253**	**0.10**	**7.07826**	**9.53**	**0.34943**	**9.20**	**0.97**	**0.14692**	**2.48**	**1932**	**178**	**2121**	**202**	**2310**	**57**	**84**		
030-Z23	0.0008	60	49	94	0.52	7.46079	3.50	0.40160	1.35	0.39	0.13474	3.23	2176	29	2168	76	2161	70	101	2161	70
031-Z24	0.0003	58	53	105	0.51	7.89135	2.99	0.40575	2.71	0.91	0.14105	1.26	2195	60	2219	66	2240	28	98	2240	28
032-Z25	0.0003	28	144	226	0.64	0.76230	3.69	0.09266	2.70	0.73	0.05967	2.51	571	15	575	21	592	15	97	571	15
033-Z26	0.0004	52	74	107	0.70	7.64602	1.87	0.40532	1.27	0.68	0.13682	1.38	2193	28	2190	41	2187	30	100	2187	30
034-Z27	**0.0018**	**65**	**110**	**107**	**1.04**	**17.18648**	**3.79**	**0.48370**	**3.12**	**0.82**	**0.25770**	**2.16**	**2543**	**79**	**2945**	**112**	**3233**	**70**	**79**		
035-Z28	0.0000	15	120	129	0.93	0.72073	3.67	0.08954	2.82	0.77	0.05838	2.35	553	16	551	20	544	13	102	553	16
036-Z29	0.0000	22	175	181	0.98	0.92045	4.23	0.10606	2.86	0.68	0.06294	3.12	650	19	663	28	706	22	92	706	22
037-Z30	0.0002	69	345	508	0.68	0.88829	4.90	0.10533	3.58	0.73	0.06117	3.34	646	23	645	32	645	22	100	645	22
040-Z31	0.0003	16	83	104	0.80	0.93689	3.27	0.10987	2.31	0.71	0.06184	2.32	672	16	671	22	669	15	100	669	15
041-Z32	0.0004	12	34	56	0.61	1.51146	3.53	0.15519	2.01	0.57	0.07064	2.90	930	19	935	33	947	27	98	947	27
042-Z33	0.0000	6	72	44	1.64	0.72920	3.95	0.08962	2.90	0.73	0.05901	2.69	553	16	556	22	568	15	97	553	16
043-Z34	0.0001	50	129	115	1.13	4.45712	2.22	0.30342	1.73	0.78	0.10654	1.40	1708	30	1723	38	1741	24	98	1741	24
044-Z35	0.0008	18	353	142	2.50	0.91491	7.47	0.10555	3.74	0.50	0.06287	6.46	647	24	660	49	704	45	92	704	45
045-Z36	**0.0017**	**86**	**76**	**259**	**0.29**	**9.84343**	**3.90**	**0.41601**	**2.52**	**0.65**	**0.17161**	**2.97**	**2242**	**56**	**2420**	**94**	**2573**	**77**	**87**		
046-Z37	0.0012	66	74	87	0.85	27.90831	4.35	0.71103	3.31	0.76	0.28467	2.83	3462	115	3416	149	3389	96	102	3389	96
047-Z38	0.0014	44	223	370	0.61	0.84043	4.48	0.10158	2.44	0.54	0.06000	3.76	624	15	619	28	604	23	103	604	23
048-Z39	0.0002	55	20	131	0.15	7.10093	3.53	0.38148	3.14	0.89	0.13500	1.62	2083	65	2124	75	2164	35	96	2164	35

049-Z40	0.0006	51	384	392	0.99	0.82160	3.21	0.10038	2.55	0.79	0.05936	1.95	617	16	609	20	580	11	106	580	11
052-Z41	0.0000	11	86	86	1.00	0.78092	4.33	0.09550	2.19	0.50	0.05931	3.74	588	13	586	25	578	22	102	588	13
053-Z42	0.0000	12	102	75	1.36	1.15591	3.18	0.12531	1.38	0.44	0.06690	2.86	761	11	780	25	835	24	91	835	24
054-Z43	0.0000	63	263	432	0.61	8.90046	1.24	0.06059	1.41	0.88	0.06059	1.41	686	9	672	13	625	9	110	625	9
055-Z44	**0.0001**	**72**	**105**	**201**	**0.53**	**6.04409**	**4.16**	**0.27049**	**1.66**	**0.40**	**0.16206**	**3.81**	**1543**	**26**	**1982**	**82**	**2477**	**94**	**62**		
056-Z45	**0.0000**	**8**	**74**	**59**	**1.25**	**0.89975**	**2.63**	**0.10922**	**1.50**	**0.57**	**0.05975**	**2.16**	**668**	**10**	**652**	**17**	**594**	**13**	**112**		
057-Z46	0.0000	13	85	96	0.89	0.80015	3.91	0.09758	3.34	0.85	0.05947	2.04	600	20	597	23	584	12	103	584	12
058-Z47	0.0073	61	69	100	0.70	9.98966	1.25	0.45805	0.59	0.48	0.15817	1.10	2431	14	2434	30	2436	27	100	2436	27
059-Z48	0.0000	17	144	136	1.07	0.75057	3.31	0.09390	2.37	0.72	0.05797	2.31	579	14	569	19	529	12	109	579	14
060-Z49	0.0001	73	184	165	1.12	5.38267	2.23	0.35000	2.06	0.92	0.11154	0.86	1935	40	1882	42	1825	16	106	1825	16
061-Z50	0.0000	10	66	81	0.82	0.75666	3.10	0.09367	1.60	0.52	0.05859	2.66	577	9	572	18	552	15	105	577	9
064-Z51	0.0004	80	177	138	1.29	10.62582	2.67	0.48425	2.31	0.87	0.15914	1.34	2546	59	2491	66	2447	33	104	2447	33
065-Z52	0.0001	60	268	447	0.60	0.88158	2.43	0.10656	1.69	0.69	0.06000	1.75	653	11	642	16	604	11	108	604	11
066-Z53	0.0005	56	171	121	1.43	5.99764	2.46	0.35444	2.20	0.90	0.12273	1.10	1956	43	1976	49	1996	22	98	1996	22
067-Z54	0.0007	17	12	35	0.35	6.08085	3.05	0.36358	2.46	0.81	0.12130	1.80	1999	49	1988	61	1975	36	101	1975	36
068-Z55	0.0011	70	569	800	0.72	5.94925	6.09	0.33808	2.28	0.37	0.12763	5.65	1877	43	1968	120	2066	117	91	2066	117
069-Z56	0.0001	55	111	122	0.92	5.12660	1.57	0.34665	1.23	0.79	0.10726	0.97	1919	24	1841	29	1753	17	109	1753	17
070-Z57	0.0005	54	40	89	0.46	9.50491	2.11	0.45608	1.80	0.85	0.15115	1.11	2422	44	2388	50	2359	26	103	2359	26
071-Z58	0.0001	78	70	130	0.54	11.53972	2.91	0.49691	2.35	0.81	0.16843	1.72	2601	61	2568	75	2542	44	102	2542	44
072-Z59	0.0000	26	101	205	0.50	0.97173	1.79	0.11166	0.82	0.46	0.06311	1.59	682	6	689	12	712	11	96	712	11
073-Z60	0.0004	91	66	146	0.45	12.88437	3.11	0.52003	2.68	0.86	0.17969	1.58	2699	72	2671	83	2650	42	102	2650	42
076-Z10	0.0031	33	185	233	0.80	0.74368	22.16	0.09120	18.82	0.85	0.05914	11.69	563	106	565	125	572	67	98	563	106

[a] Th/U ratios are calculated relative to GJ-1 reference zircon

[b] Corrected for background and within-run Pb/U fractionation and normalised to reference zircon GJ-1 (ID-TIMS values/measured value); 207Pb/235U calculated using $(^{207}Pb/^{206}Pb)/(^{238}U/^{206}Pb * 1/137.88)$

[c] Rho is the error correlation defined as the quotient of the propagated errors of the $^{206}Pb/^{238}U$ and the $^{207}/^{235}U$ ratio

[d] Corrected for mass-bias by normalising to GJ-1 reference zircon and common Pb using the model Pb composition of Stacey and Kramers (1975)

[e] Degree of concordance = $(^{206}Pb/^{238}U$ age $* 100/^{207}Pb/^{206}U$ age)

Table 1e : U-Pb in situ zircon data of sample T02-07 SB II, Santa Barbara Gr.

						Isotope ratios							Ages (Ma)								
Spot num	f 206	Pb ppm	U ppm	Th ppm	Th/Ua	$^{207}Pb/^{235}U$	1 s [%]	$^{206}Pb/^{238}U$	1 s [%]	Rho[c]	$^{207}Pb/^{206}Pb^d$	1 s [%]	$^{206}Pb/^{238}U$	1 s abs	$^{207}Pb/^{235}U$	1 s abs	$^{207}Pb/^{206}Pb$	1 s abs	% Conc[e]	Best estimated age (Ma)	
004-Z1	0.0037	5	20	40	0.51	0.79722	5.36	0.09446	3.04	0.57	0.06121	4.42	582	18	595	32	647	29	90	647	29
005-Z2	0.0016	9	43	80	0.54	0.72749	4.63	0.08486	4.00	0.86	0.06217	2.32	525	21	555	26	680	16	77		
006-Z3	0.0036	7	46	56	0.82	0.76543	11.34	0.09023	8.82	0.78	0.06153	7.13	557	49	577	65	658	47	85		
007-Z4	0.0017	14	21	30	0.70	6.15833	3.07	0.34285	1.43	0.47	0.13027	2.71	1900	27	1999	61	2102	57	90	2102	57
008-Z5	0.0005	6	30	47	0.65	0.82460	10.28	0.10031	8.11	0.79	0.05962	6.31	616	50	611	63	590	37	104	590	37
009-Z6	0.0008	68	79	124	0.64	7.14171	1.92	0.39872	1.44	0.75	0.12991	1.27	2163	31	2129	41	2097	27	103	2097	27
010-Z7	0.0004	56	65	109	0.60	6.81554	2.42	0.37557	1.53	0.63	0.13162	1.87	2056	31	2088	50	2120	40	97	2120	40
011-Z8	0.0016	15	133	115	1.16	0.75801	5.89	0.09259	4.70	0.80	0.05938	3.55	571	27	573	34	581	21	98	581	21
012-Z9	0.0025	7	52	53	1.00	0.70471	9.83	0.08713	8.53	0.87	0.05866	4.89	539	46	542	53	555	27	97	555	27
015-Z10	0.0089	5	16	35	0.45	0.70499	8.99	0.08681	8.20	0.91	0.05890	3.69	537	44	542	49	563	21	95	563	21
016-Z11	0.0000	9	12	39	0.31	2.29015	4.87	0.15114	4.76	0.98	0.10990	1.03	907	43	1209	59	1798	18	50		
017-Z12	0.0037	27	83	59	1.41	4.41995	3.85	0.28814	2.78	0.72	0.11125	2.67	1632	45	1716	66	1820	49	90	1820	49
018-Z13	0.0100	5	18	41	0.45	0.77489	11.92	0.09247	9.46	0.79	0.06078	7.24	570	54	583	69	631	46	90	631	46
019-Z14	0.0000	2	10	5	2.21	4.55959	4.03	0.26048	1.48	0.37	0.12695	3.74	1492	22	1742	70	2056	77	73		
020-Z15	0.0011	25	31	48	0.66	6.40310	4.54	0.35535	4.05	0.89	0.13069	2.05	1960	79	2033	92	2107	43	93	2107	43
021-Z16	0.0112	5	24	39	0.62	0.75416	10.36	0.09095	8.80	0.85	0.06014	5.48	561	49	571	59	609	33	92	609	33
022-Z17	0.0026	20	13	43	0.29	4.74464	3.90	0.29579	2.42	0.62	0.11634	3.06	1670	40	1775	69	1901	58	88		
023-Z18	0.0000	10	30	79	0.38	0.70422	8.78	0.08688	7.32	0.83	0.05879	4.85	537	39	541	48	559	27	96	559	27
024-Z19	0.0066	8	46	62	0.75	0.77951	10.26	0.09191	8.11	0.79	0.06151	6.28	567	46	585	60	657	41	86		
027-Z20	0.0172	3	21	24	0.91	0.68729	31.75	0.07216	28.29	0.89	0.06908	14.40	449	127	531	169	901	130	50		
028-Z21	0.0063	9	35	19	1.84	3.89396	13.61	0.25499	9.90	0.73	0.11076	9.34	1464	145	1612	219	1812	169	81		
029-Z22	0.0056	7	9	24	0.38	2.69949	8.98	0.18996	6.66	0.74	0.10306	6.03	1121	75	1328	119	1680	101	67		
030-Z23	0.0077	10	63	69	0.93	0.85486	9.70	0.09197	8.37	0.86	0.06741	4.89	567	47	627	61	851	42	67		
031-Z24	0.0003	5	2	45	0.05	0.79666	15.05	0.08976	10.90	0.72	0.06437	10.38	554	60	595	90	754	78	73		
032-Z25	0.0039	16	88	138	0.64	0.72783	6.03	0.08477	5.32	0.88	0.06227	2.84	525	28	555	33	683	19	77		
033-Z26	0.0035	17	46	34	1.38	4.65414	10.38	0.26907	8.97	0.86	0.12545	5.22	1536	138	1759	183	2035	106	75		
034-Z27	0.0030	22	10	34	0.30	11.45561	10.25	0.42092	8.66	0.84	0.19739	5.49	2265	196	2561	263	2805	154	81		
035-Z28	0.0191	4	15	33	0.47	0.64613	32.47	0.07574	25.91	0.80	0.06187	19.57	471	122	506	164	670	131	70		
036-Z29	0.0012	6	26	45	0.59	0.72248	14.59	0.08399	11.92	0.82	0.06239	8.42	520	62	552	81	687	58	76		
040-Z30	0.0052	17	138	116	1.19	0.83216	10.46	0.09306	8.06	0.77	0.06486	6.67	574	46	615	64	770	51	75		
041-Z31	0.0014	36	39	66	0.60	6.38826	2.88	0.35822	2.10	0.73	0.12934	1.97	1974	41	2031	58	2089	41	94	2089	41
042-Z32	0.0020	23	30	44	0.68	5.98637	4.46	0.33782	3.10	0.69	0.12852	3.21	1876	58	1974	88	2078	67	90	2078	67
043-Z33	0.0000	2	9	13	0.67	0.91929	44.37	0.10873	32.46	0.73	0.06132	30.24	665	216	662	294	651	197	102	651	197
044-Z34	0.0034	11	20	22	0.95	6.32174	12.33	0.35663	10.34	0.84	0.12856	6.71	1966	203	2021	249	2078	140	95	2078	140
045-Z35	0.0000	2	19	13	1.53	0.89213	48.09	0.10211	37.33	0.78	0.06337	30.31	627	234	648	311	721	218	87		
046-Z36	0.0008	55	25	63	0.40	23.00266	1.50	0.55225	1.09	0.73	0.30209	1.03	2835	31	3227	48	3481	36	81		
047-Z37	0.0001	6	27	44	0.62	0.72502	11.04	0.08755	7.37	0.67	0.06006	8.21	541	40	554	61	606	50	89		
048-Z38	0.0077	4	18	36	0.50	0.77192	23.32	0.09270	17.19	0.74	0.06039	15.76	571	98	581	135	618	97	93	618	97
051-Z39	0.0137	2	5	20	0.26	0.73153	26.06	0.09415	23.18	0.89	0.05635	11.92	580	134	557	145	466	56	124		

052-Z40	0.0020	17	23	38	0.62	6.20944	2.95	0.34639	2.50	0.85	0.13001	1.58	1917	48	2006	59	2098	33	91	2098	33
053-Z41	0.0013	33	45	44	1.02	12.75134	4.31	0.50335	3.82	0.89	0.18373	1.98	2628	101	2661	115	2687	53	98	2687	53
054-Z42	0.0224	26	392	204	1.94	1.11144	5.78	0.09541	4.21	0.73	0.08449	3.95	587	25	759	44	1304	52	45		
055-Z43	0.0023	23	40	32	1.26	11.69789	2.98	0.49160	2.90	0.98	0.17258	0.65	2578	75	2581	77	2583	17	100	2583	17
056-Z44	0.0019	21	20	56	0.36	5.01332	3.49	0.31980	2.77	0.79	0.11370	2.13	1789	50	1822	64	1859	40	96	1859	40
057-Z45	0.0015	19	18	43	0.41	6.01576	3.18	0.33409	0.83	0.26	0.13059	3.07	1858	16	1978	63	2106	65	88		
058-Z46	0.0051	5	50	47	1.07	0.72912	4.20	0.08965	3.63	0.86	0.05899	2.12	553	20	556	23	567	12	98	567	12
059-Z47	0.0073	8	86	73	1.18	0.65928	6.43	0.08052	4.37	0.68	0.05938	4.72	499	22	514	33	581	27	86		
060-Z48	0.0060	6	34	57	0.61	0.76134	14.11	0.09330	9.10	0.65	0.05918	10.78	575	52	575	81	574	62	100	574	62
063-Z49	0.0056	6	67	46	1.47	0.74561	12.39	0.08527	10.44	0.84	0.06342	6.68	527	55	566	70	722	48	73		
064-Z50	0.0047	8	42	62	0.68	0.80390	12.45	0.09543	10.10	0.81	0.06110	7.28	588	59	599	75	643	47	91	643	47
065-Z51	0.0025	13	17	103	0.16	0.79302	5.69	0.09592	4.40	0.77	0.05996	3.61	590	26	593	34	602	22	98	602	22
066-Z52	0.0047	9	88	73	1.22	0.83576	8.21	0.09648	6.70	0.82	0.06283	4.73	594	40	617	51	702	33	85		
067-Z53	0.0010	40	37	73	0.51	6.62399	2.87	0.37199	2.41	0.84	0.12915	1.56	2039	49	2063	59	2086	33	98	2086	33
068-Z54	0.0037	9	34	59	0.59	0.79153	11.04	0.09540	9.01	0.82	0.06018	6.38	587	53	592	65	610	39	96	610	39
069-Z55	0.0008	47	39	83	0.47	6.76159	2.11	0.38151	0.95	0.45	0.12854	1.88	2083	20	2081	44	2078	39	100	2078	39
070-Z56	0.0011	53	46	69	0.66	11.32257	6.19	0.46078	5.69	0.92	0.17822	2.45	2443	139	2550	158	2636	65	93	2636	65
071-Z57	0.0127	3	9	25	0.38	0.78258	32.66	0.08727	23.95	0.73	0.06504	22.21	539	129	587	192	776	172	70		
072-Z58	0.0016	17	18	29	0.62	6.56868	3.71	0.37350	0.95	0.26	0.12755	3.58	2046	19	2055	76	2065	74	99	2065	74
076-Z59	0.0040	10	54	91	0.60	0.83479	11.59	0.09858	9.82	0.85	0.06141	6.17	606	59	616	71	654	40	93	654	40
077-Z60	0.0011	46	64	79	0.82	7.19413	2.91	0.40363	2.22	0.76	0.12927	1.89	2186	48	2136	62	2088	39	105	2088	39
078-Z61	0.0020	28	28	50	0.57	5.59312	6.66	0.30104	6.09	0.91	0.13475	2.70	1696	103	1915	128	2161	58	79		
079-Z62	0.0014	32	168	291	0.58	0.78445	5.12	0.09273	4.22	0.82	0.06136	2.91	572	24	588	30	652	19	88		
080-Z63	0.0018	9	33	80	0.42	0.84669	11.16	0.10039	8.53	0.76	0.06117	7.20	617	53	623	70	645	46	96	645	46
081-Z64	0.0041	8	69	63	1.11	0.80630	16.41	0.09225	12.81	0.78	0.06339	10.25	569	73	600	99	721	74	79		
082-Z65	0.0034	8	30	68	0.44	0.88084	13.14	0.10489	9.12	0.69	0.06091	9.46	643	59	641	84	636	60	101	636	60
083-Z66	0.0021	8	63	64	0.99	0.85787	9.29	0.10030	6.44	0.69	0.06203	6.70	616	40	629	58	675	45	91	675	45
084-Z67	0.0029	9	12	85	0.14	0.90713	12.30	0.10569	9.26	0.75	0.06225	8.09	648	60	656	81	683	55	95	683	55
087-Z68	0.0021	25	32	56	0.57	6.58511	4.92	0.36854	4.00	0.81	0.12959	2.86	2023	81	2057	101	2092	60	97	2092	60
088-Z69	0.0168	4	15	11	1.34	3.11569	28.74	0.24482	24.15	0.84	0.09230	15.58	1412	341	1437	413	1474	230	96	1474	230
089-Z70	0.0031	11	4	104	0.04	0.82286	9.38	0.09404	7.44	0.79	0.06346	5.71	579	43	610	57	724	41	80		
090-Z71	0.0019	27	31	40	0.78	11.21244	6.52	0.46311	5.28	0.81	0.17559	3.82	2453	130	2541	166	2612	100	94	2612	100
091-Z72	0.0031	12	47	104	0.45	0.80412	6.54	0.09570	5.32	0.81	0.06094	3.81	589	31	599	39	637	24	92	637	24
092-Z73	0.0049	8	7	72	0.10	0.91872	8.56	0.10600	6.47	0.76	0.06286	5.62	649	42	662	57	703	40	92	703	40
093-Z74	0.0022	13	125	94	1.33	0.80576	7.31	0.09601	6.16	0.84	0.06087	3.92	591	36	600	44	635	25	93	635	25
094-Z75	0.0044	15	138	116	1.20	0.80250	6.62	0.09652	5.50	0.83	0.06030	3.67	594	33	598	40	614	23	97	614	23
095-Z76	0.0003	7	49	56	0.88	0.77940	7.49	0.09369	5.30	0.71	0.06034	5.29	577	31	585	44	616	33	94	617	33
096-Z77	0.0015	6	22	54	0.41	0.82876	8.92	0.09960	7.56	0.85	0.06035	4.73	612	46	613	55	616	29	99	618	29
099-Z78	0.0004	122	121	164	0.74	8.09600	5.18	0.42306	4.17	0.80	0.13879	3.08	2274	95	2242	116	2212	68	103	2212	68
100-Z79	0.0024	21	50	31	1.63	4.55303	4.88	0.30877	3.60	0.74	0.10695	3.29	1735	63	1741	85	1748	58	99	1748	58
101-Z80	0.0032	22	90	132	0.69	0.95714	5.78	0.10908	4.35	0.75	0.06364	3.81	667	29	682	39	730	28	91	730	28
102-Z81	0.0004	170	169	213	0.80	7.95162	1.60	0.42639	1.14	0.71	0.13525	1.12	2289	26	2226	36	2167	24	106	2167	24
103-Z82	0.0007	78	69	110	0.63	7.07636	4.83	0.39937	4.61	0.96	0.12851	1.42	2166	100	2121	102	2078	30	104	2078	30
104-Z83	0.0062	8	18	48	0.38	0.97972	12.55	0.11330	8.94	0.71	0.06272	8.81	692	62	693	87	699	62	99	699	62

105-Z84	0.0043	12	32	43	0.76	1.72789	5.01	0.14064	3.41	0.68	0.08911	3.67	848	29	1019	51	1406	52	60		
106-Z85	0.0019	17	112	123	0.92	0.67966	7.12	0.07684	6.42	0.90	0.06415	3.08	477	31	527	37	747	23	64		
107-Z86	0.0012	37	31	56	0.56	7.17135	2.33	0.38279	1.69	0.72	0.13588	1.62	2089	35	2133	50	2175	35	96	2175	35
108-Z87	0.0012	38	30	56	0.53	6.73484	1.93	0.37679	1.64	0.85	0.12964	1.02	2061	34	2077	40	2093	21	98	2093	21
112-Z88	0.0023	12	112	79	1.43	0.7959	7.33	0.0952	6.03	0.82	0.0606	4.17	586	35	595	44	625	26	94	625	26
113-Z89	0.0009	9	44	58	0.75	0.7616	11.37	0.0928	9.34	0.82	0.0595	6.47	572	53	575	65	586	38	98	586	38
114-Z90	0.0018	17	75	119	0.63	0.8564	7.46	0.1022	6.10	0.82	0.0608	4.28	627	38	628	47	631	27	99	631	27
115-Z91	0.0015	26	156	166	0.94	0.8223	4.04	0.0993	3.70	0.92	0.0601	1.63	610	23	609	25	606	10	101	606	10
116-Z92	0.0003	495	336	789	0.43	6.6727	2.17	0.3765	1.94	0.90	0.1285	0.97	2060	40	2069	45	2078	20	99	2078	20
117-Z93	0.0018	21	7	113	0.06	0.8646	3.76	0.1029	2.83	0.75	0.0609	2.48	631	18	633	24	637	16	99	637	16
118-Z94	0.0074	17	74	110	0.68	0.7852	7.64	0.0948	6.08	0.80	0.0601	4.63	584	36	588	45	606	28	96	606	28
119-Z95	0.0018	18	74	109	0.69	0.9115	4.93	0.1092	3.77	0.77	0.0606	3.17	668	25	658	32	623	20	107	623	20
120-Z96	0.0006	108	130	221	0.59	6.4260	1.82	0.3717	1.32	0.72	0.1254	1.26	2038	27	2036	37	2034	26	100	2034	26
123-Z97	0.0009	18	246	158	1.57	0.70215	8.27	0.07870	7.54	0.91	0.06470	3.39	488	37	540	45	765	26	64		
124-Z98	0.0035	12	55	74	0.75	0.82035	12.88	0.09816	11.33	0.88	0.06062	6.12	604	68	608	78	626	38	96	626	38
125-Z99	0.0020	31	211	193	1.10	0.83700	4.75	0.10123	3.68	0.77	0.05997	3.01	622	23	617	29	603	18	103	603	18
126-Z100	0.0006	50	40	102	0.39	4.87087	3.28	0.31332	2.11	0.64	0.11275	2.51	1757	37	1797	59	1844	46	95	1844	46
127-Z101	0.0010	45	39	63	0.63	7.95539	2.42	0.42027	2.05	0.85	0.13729	1.28	2262	46	2226	54	2193	28	103	2193	28
128-Z102	0.0012	42	45	69	0.67	6.77669	2.47	0.38389	2.05	0.83	0.12803	1.37	2094	43	2083	51	2071	28	101	2071	28
129-Z103	0.0016	10	51	63	0.81	0.73746	10.55	0.08881	9.38	0.89	0.06022	4.83	549	51	561	59	612	30	90	612	30
130-Z104	0.0014	20	66	145	0.46	0.83471	5.57	0.09913	4.50	0.81	0.06107	3.27	609	27	616	34	642	21	95	642	21
131-Z105	0.0012	30	188	180	1.05	0.82409	5.19	0.09865	4.49	0.87	0.06059	2.60	606	27	610	32	625	16	97	625	16
132-Z106	0.0050	10	29	66	0.43	0.84953	9.17	0.10108	7.62	0.83	0.06095	5.11	621	47	624	57	638	33	97	638	33
135-Z107	0.0028	14	63	83	0.76	0.91759	10.36	0.10766	7.88	0.76	0.06181	6.72	659	52	661	68	668	45	99	668	45
136-Z108	0.0017	32	145	209	0.70	1.06015	7.07	0.12005	4.08	0.58	0.06405	5.77	731	30	734	52	743	43	98	743	43
137-Z109	0.0011	42	189	288	0.66	0.80031	4.91	0.09845	4.43	0.90	0.05896	2.14	605	27	597	29	566	12	107	566	12
138-Z110	0.0010	23	139	135	1.04	0.92046	5.56	0.10935	4.65	0.84	0.06105	3.06	669	31	663	37	641	20	104	641	20
139-Z111	0.0312	6	23	9	2.67	4.49110	17.19	0.25383	11.78	0.69	0.12832	12.53	1458	172	1729	297	2075	260	70		
140-Z112	0.0022	21	79	120	0.66	0.95379	5.68	0.11206	4.44	0.78	0.06173	3.55	685	30	680	39	665	24	103	665	24
141-Z113	0.0019	27	155	189	0.83	0.78447	5.47	0.09565	4.86	0.89	0.05948	2.52	589	29	588	32	585	15	101	585	15
142-Z114	0.0015	5	22	26	0.86	1.18425	15.25	0.12825	4.69	0.31	0.06697	14.51	778	36	793	121	837	121	93	837	121
143-Z115	0.0025	23	52	36	1.44	4.84085	5.62	0.32103	4.74	0.84	0.10937	3.03	1795	85	1792	101	1789	54	100	1789	54
144-Z116	0.0026	27	191	170	1.13	0.83718	5.85	0.09943	5.21	0.89	0.06107	2.66	611	32	618	36	642	17	95	642	17
148-Z117	0.0012	51	61	57	1.09	7.36723	13.61	0.39176	12.08	0.89	0.13639	6.28	2131	257	2157	294	2182	137	98	2182	137
149-Z118	0.0024	24	53	49	1.08	3.62544	6.30	0.28043	5.76	0.91	0.09376	2.55	1594	92	1555	98	1503	38	106	1503	38
150-Z119	0.0019	21	17	33	0.52	7.19096	3.74	0.39274	2.74	0.73	0.13280	2.55	2136	59	2135	80	2135	55	100	2135	55
151-Z120	0.0019	24	88	145	0.61	0.86825	6.54	0.10261	5.19	0.79	0.06137	3.97	630	33	635	42	652	26	97	652	26
140-Z112	0.0020	22	80	119	0.68	0.97062	6.36	0.11369	4.82	0.76	0.06192	4.15	694	33	689	44	671	28	103	671	28
141-Z113	0.0006	28	161	187	0.87	0.78110	5.73	0.09467	4.89	0.85	0.05984	2.99	583	28	586	34	598	18	98	598	18
142-Z114	0.0048	6	25	27	0.93	1.15762	17.18	0.12160	12.60	0.73	0.06905	11.68	740	93	781	134	900	105	82		
143-Z115	0.0019	23	52	35	1.50	4.71209	5.68	0.31709	4.92	0.87	0.10778	2.85	1776	87	1769	101	1762	50	101	1762	50
144-Z116	0.0022	28	226	179	1.27	0.81784	5.23	0.09685	4.70	0.90	0.06124	2.29	596	28	607	32	648	15	92	648	15

Table 1f : U-Pb in situ zircon data of sample T02-202 SB I, Santa Barbara Gr.

Spot num	f 206	Pb ppm	U ppm	Th ppm	Th/U[a]	207Pb/ 235U	1 s [%]	206Pb/ 238U	1 s [%]	Rho[c]	207Pb/ 206Pb[d]	1 s [%]	206Pb/ 238U	1 s abs	207Pb/ 235U	1 s abs	207Pb/ 206Pb	1 s abs	% Conc[e]	Best estimated age (Ma)	
004-Z1	0.0024	6	21	13	1.64	3.45659	19.19	0.24499	18.14	0.95	0.10233	6.28	1413	256	1517	291	1667	105	85		
005-Z2	0.0303	3	29	21	1.37	0.62418	47.61	0.06970	39.03	0.82	0.06495	27.26	434	170	492	234	773	211	56		
006-Z3	0.0031	18	37	56	0.66	4.18086	8.50	0.24357	7.13	0.84	0.12449	4.63	1405	100	1670	142	2022	94	70		
007-Z4	0.0042	12	125	102	1.24	0.73937	5.60	0.08067	3.86	0.69	0.06648	4.05	500	19	562	31	821	33	61		
008-Z5	0.0022	66	361	734	0.49	0.54248	6.31	0.06557	5.61	0.89	0.06001	2.87	409	23	440	28	604	17	68		
009-Z6	0.0044	13	94	126	0.75	0.65317	6.58	0.07783	5.19	0.79	0.06086	4.05	550	19	561	24	604	15	91	604	15
010-Z7	0.0012	22	96	160	0.60	0.87920	5.26	0.10342	3.75	0.71	0.06166	3.69	634	24	641	34	662	24	96	662	24
011-Z8	0.0017	12	124	89	1.40	0.71558	6.54	0.07978	5.37	0.82	0.06505	3.73	495	27	548	36	776	29	64		
012-Z9	0.0522	12	356	153	2.34	0.59319	15.39	0.04263	11.63	0.76	0.10091	10.07	269	31	473	73	1641	165	16		
015-Z10	0.0078	50	1168	819	1.44	0.47567	8.17	0.05025	7.79	0.95	0.06865	2.47	316	25	395	32	888	22	36		
016-Z11	0.0033	24	467	322	1.46	0.44278	10.00	0.04785	9.03	0.90	0.06711	4.28	301	27	372	37	841	36	36		
017-Z12	0.0025	10	39	68	0.58	1.00938	8.26	0.11059	5.30	0.64	0.06620	6.33	676	36	709	59	813	51	83		
018-Z13	0.0004	14	89	76	1.18	1.12259	10.98	0.11935	8.76	0.80	0.06822	6.63	727	64	764	84	875	58	83		
019-Z14	0.0030	48	167	94	1.79	9.25292	2.74	0.42363	1.77	0.65	0.15841	2.09	2277	40	2363	65	2439	51	93	2439	51
020-Z15	0.3893	28	2	46	0.04	16.33359	17.63	0.15402	11.97	0.68	0.76912	12.94	923	111	2897	511	4866	630	19		
021-Z16	0.0059	13	157	93	1.71	0.79978	9.21	0.09100	6.66	0.72	0.06374	6.37	561	37	597	55	733	47	77		
022-Z17	0.0321	19	1273	317	4.05	0.45326	20.42	0.03357	16.53	0.81	0.09793	12.00	213	35	380	78	1585	190	13		
023-Z18	0.0026	22	100	90	1.12	2.13925	5.54	0.18524	4.55	0.82	0.08376	3.17	1096	50	1162	64	1287	41	85		
024-Z19	0.0203	106	2949	1245	2.39	0.72423	10.07	0.04608	9.91	0.98	0.11398	1.84	290	29	553	56	1864	34	16		
027-Z20	0.0039	36	651	324	2.02	0.60816	10.15	0.06784	9.52	0.94	0.06502	3.53	423	40	482	49	775	27	55		
028-Z21	0.0049	17	261	85	3.09	0.76380	5.46	0.09061	4.09	0.75	0.06114	3.61	559	23	576	31	644	23	87		
029-Z22	0.0008	116	194	199	0.98	9.32853	1.85	0.43370	1.47	0.80	0.15600	1.12	2322	34	2371	44	2413	27	96	2413	27
030-Z23	0.0021	44	380	348	1.10	0.80759	6.27	0.09524	5.67	0.90	0.06150	2.69	586	33	601	38	657	18	89	657	18
031-Z24	0.1632	93	251	167	1.51	4.00897	84.50	0.09419	10.36	0.12	0.30871	83.86	580	60	1636	1382	3514	2947	17		
032-Z25	0.0093	15	219	119	1.85	0.78118	13.02	0.08909	10.89	0.84	0.06359	7.14	550	60	586	76	728	52	76		
033-Z26	0.0035	14	90	97	0.93	0.80499	7.13	0.09461	5.42	0.76	0.06171	4.63	583	32	600	43	664	31	88	664	31
034-Z27	0.0000	7	95	41	2.35	0.77849	14.59	0.08857	12.99	0.89	0.06375	6.64	547	71	585	85	733	49	75		
035-Z28	0.0018	42	126	318	0.40	0.93291	4.51	0.10270	3.79	0.84	0.06588	2.44	630	24	669	30	803	20	79		
036-Z29	0.0067	6	30	46	0.66	0.818974	11.25	0.10004	10.32	0.92	0.059375	4.50	615	63	607	68	581	26	106	580	26
040-Z30	0.0098	22	278	165	1.69	0.66747	6.27	0.07817	5.05	0.81	0.06193	3.72	485	25	519	33	672	25	72		
041-Z31	0.0021	11	109	70	1.57	0.72587	16.62	0.08592	12.09	0.73	0.06127	11.40	531	64	554	92	649	74	82		
042-Z32	0.0019	17	191	113	1.70	0.78336	13.80	0.09430	11.26	0.82	0.06025	7.98	581	65	587	81	613	49	95	613	49
043-Z33	0.0023	24	554	177	3.14	0.62218	6.99	0.07370	5.96	0.85	0.06122	3.66	458	27	491	34	647	24	71		
044-Z34	0.0249	30	962	428	2.27	0.44532	20.75	0.03657	16.43	0.79	0.08831	12.67	232	38	374	78	1389	176	17		

ID																					
045-Z35	0.0025	49	436	371	1.18	0.73665	5.99	0.08331	4.73	0.79	0.06413	3.67	516	24	560	34	746	27	69		
046-Z36	0.0014	42	315	252	1.26	0.74849	6.50	0.08870	4.45	0.68	0.06120	4.73	548	24	567	37	646	31	85		
047-Z37	0.0013	34	149	203	0.74	0.87190	5.35	0.10387	4.25	0.80	0.06088	3.24	637	27	637	34	635	21	100	635	21
048-Z38	0.0034	16	82	111	0.74	0.70930	11.32	0.08818	9.15	0.81	0.05834	6.66	545	50	544	62	542	36	100	542	36
051-Z39	0.0026	14	159	87	1.84	0.88090	9.32	0.10369	6.45	0.69	0.06162	6.72	636	41	641	60	661	44	96	661	44
052-Z40	0.0006	19	177	119	1.50	0.74163	6.69	0.09041	5.32	0.80	0.05949	4.05	558	30	563	38	585	24	95	585	24
053-Z41	0.0019	30	326	208	1.58	0.80080	9.51	0.09462	8.18	0.86	0.06139	4.84	583	48	597	57	653	32	89		
054-Z42	0.0002	13	91	96	0.95	0.85802	7.91	0.10051	6.19	0.78	0.06192	4.93	617	38	629	50	671	33	92	671	33
055-Z43	0.0008	11	60	67	0.91	1.26297	5.94	0.13256	2.69	0.45	0.06910	5.29	802	22	829	49	902	48	89	902	48
056-Z44	0.0604	26	473	288	1.66	2.12838	31.30	0.11631	8.23	0.26	0.13272	30.20	709	58	1158	362	2134	645	33		
057-Z45	0.0012	31	247	190	1.31	0.86852	5.20	0.10376	3.85	0.74	0.06071	3.51	636	24	635	33	629	22	101	629	22
058-Z46	0.0088	27	539	307	1.77	0.49672	11.57	0.05233	10.65	0.92	0.06884	4.50	329	35	409	47	894	40	37		
059-Z47	0.0007	22	239	210	1.15	0.78437	16.65	0.09102	16.41	0.99	0.06250	2.81	562	92	588	98	691	19	81		
060-Z48	0.0094	23	210	160	1.32	1.05140	13.76	0.11846	11.97	0.87	0.06437	6.79	722	86	730	100	754	51	96	754	51
063-Z49	0.0000	4	23	34	0.68	0.75145	24.11	0.05169	23.62	0.98	0.10544	4.83	325	77	569	137	1722	83	19		
064-Z50	0.0004	24	277	251	1.11	0.64269	14.24	0.07545	13.09	0.92	0.06178	5.61	469	61	504	72	667	37	70		
065-Z51	0.0019	10	70	77	0.91	0.93729	5.93	0.10823	5.35	0.90	0.06281	2.55	662	35	671	40	702	18	94	702	18
066-Z52	0.0034	24	192	238	0.81	0.82769	5.47	0.09133	4.35	0.79	0.06573	3.33	563	24	612	34	798	27	71		
067-Z53	0.0029	29	326	191	1.72	0.95794	5.93	0.11018	4.27	0.72	0.06305	4.12	674	29	682	40	710	29	95	710	29
068-Z54	0.0024	19	162	129	1.26	0.93290	8.54	0.10876	6.37	0.75	0.06221	5.68	666	42	669	57	681	39	98	681	39
069-Z55	0.0030	43	470	314	1.51	0.79013	7.40	0.09526	6.35	0.86	0.06016	3.79	587	37	591	44	609	23	96	609	23
070-Z56	0.0077	25	760	391	1.96	0.54108	9.04	0.05527	7.80	0.86	0.07101	4.57	347	27	439	40	958	44	36		
071-Z57	0.0096	10	133	105	1.28	0.60422	8.34	0.06770	6.81	0.82	0.06473	4.82	422	29	480	40	766	37	55		
072-Z58	0.0030	24	227	168	1.36	0.83362	6.95	0.09838	3.28	0.47	0.06146	6.13	605	20	616	43	655	40	92	655	40
076-Z59	0.0015	26	220	164	1.35	0.82858	7.24	0.09470	6.28	0.87	0.06346	3.61	583	37	613	44	724	26	81		
077-Z60	0.0008	13	104	102	1.02	1.03054	14.89	0.11252	14.08	0.95	0.06642	4.84	687	97	719	107	820	40	84		
078-Z61	0.0044	42	861	523	1.66	0.69882	5.38	0.08396	4.55	0.85	0.06036	2.87	520	24	538	29	617	18	84		
079-Z62	0.0013	23	135	237	0.57	0.69082	5.22	0.08258	4.44	0.85	0.06067	2.76	512	23	533	28	628	17	81		
080-Z63	0.0031	37	508	389	1.32	0.64939	5.84	0.07245	5.15	0.88	0.06501	2.76	451	23	508	30	775	21	58		
081-Z64	0.0027	29	250	252	1.00	0.77630	7.14	0.09423	5.49	0.77	0.05975	4.57	580	32	583	42	595	27	98	595	27
082-Z65	0.0008	15	110	96	1.15	0.83933	6.51	0.10126	5.21	0.80	0.06012	3.90	622	32	619	40	608	24	102	608	24
083-Z66	0.0018	21	70	81	0.87	2.21477	5.37	0.19917	3.87	0.72	0.08065	3.72	1171	45	1186	64	1213	45	97	1213	45
084-Z67	0.0022	40	751	407	1.86	0.69948	9.50	0.07890	8.72	0.92	0.06430	3.79	490	43	538	51	751	28	65		
087-Z68	0.0032	33	508	334	1.53	0.76978	5.17	0.08643	4.57	0.89	0.06460	2.41	534	24	580	30	761	18	70		
088-Z69	0.0028	25	190	203	0.94	0.83139	4.97	0.10123	4.11	0.83	0.05956	2.80	622	26	614	31	588	16	106	588	16
089-Z70	0.0008	28	323	251	1.29	0.81534	21.27	0.09101	19.08	0.90	0.06498	9.39	561	107	605	129	774	73	73		
090-Z71	0.0026	20	195	172	1.14	0.74707	8.80	0.09128	7.10	0.81	0.05936	5.20	563	40	567	50	580	30	97	580	30
091-Z72	0.0015	33	56	245	0.23	0.90640	6.33	0.10648	3.92	0.62	0.06174	4.97	652	26	655	41	665	33	98	665	33

092-Z73	0.0000	8	97	75	1.30	0.76631	6.29	0.09195	5.75	0.91	0.06044	2.56	567	33	578	36	619	16	92	619	16
093-Z74	0.0017	19	231	116	2.02	0.89974	6.15	0.10428	4.40	0.71	0.06258	4.30	639	28	652	40	694	30	92	694	30
094-Z75	0.0007	19	55	155	0.36	0.86564	5.63	0.10274	4.53	0.81	0.06111	3.34	630	29	633	36	643	21	98	643	21
095-Z76	0.0003	17	75	109	0.69	0.97402	5.04	0.11247	3.85	0.76	0.06281	3.26	687	26	691	35	702	23	98	702	23
096-Z77	0.0013	16	170	129	1.32	0.74147	9.28	0.09152	7.74	0.83	0.05876	5.11	565	44	563	52	558	29	101	558	29
099-Z78	0.0017	21	52	108	0.48	1.29072	8.97	0.14058	6.49	0.72	0.06659	6.19	848	55	842	75	825	51	103	825	51
100-Z79	0.0031	17	124	143	0.87	0.76331	9.63	0.09188	8.30	0.86	0.06026	4.87	567	47	576	55	613	30	92	613	30
101-Z80	0.0043	15	140	131	1.08	0.61566	13.57	0.07197	10.78	0.79	0.06204	8.23	448	48	487	66	676	56	66		
102-Z81	0.0021	22	136	158	0.87	0.69783	9.34	0.08467	8.01	0.86	0.05977	4.80	524	42	537	50	595	29	88	595	29
103-Z82	0.0011	30	148	215	0.70	0.73684	7.79	0.09073	6.82	0.88	0.05890	3.77	560	38	561	44	563	21	99	563	21
104-Z83	0.0026	38	618	348	1.79	0.69548	8.10	0.07814	7.00	0.86	0.06455	4.08	485	34	536	43	760	31	64		
105-Z84	0.0000	8	81	49	1.66	0.76281	25.74	0.08304	19.55	0.76	0.06662	16.75	514	101	576	148	826	138	62		
106-Z85	0.0015	31	268	202	1.34	0.78633	7.31	0.09510	6.33	0.87	0.05997	3.66	586	37	589	43	602	22	97	602	22
107-Z86	0.0041	40	278	282	1.00	0.82606	7.84	0.09431	6.59	0.84	0.06353	4.25	581	38	611	48	726	31	80		
108-Z87	0.0021	29	275	169	1.64	0.79969	7.27	0.09651	5.96	0.82	0.06010	4.17	594	35	597	43	607	25	98	607	25
112-Z88	0.0007	13	156	86	1.82	0.82051	7.87	0.09847	7.07	0.90	0.06043	3.47	605	43	608	48	619	21	98	619	21
113-Z89	0.0020	9	51	66	0.77	0.93117	8.74	0.10967	4.63	0.53	0.06158	7.42	671	31	668	58	660	49	102	660	49
114-Z90	0.0073	14	135	93	1.46	0.81631	17.06	0.09479	11.84	0.69	0.06246	12.28	584	69	606	103	690	85	85		
115-Z91	0.3323	24	0	97	0.00	-0.37602	34.10	0.12503	9.94	0.29	-0.02181	-32.62	759	75	-479	-163	#NÚM!	#NÚM!	#NÚM!		
116-Z92	0.0025	12	89	86	1.04	0.86359	13.85	0.10295	10.64	0.77	0.06084	8.87	632	67	632	88	633	56	100	633	56
117-Z93	0.0042	12	96	110	0.88	0.76376	9.29	0.08997	7.81	0.84	0.06157	5.02	555	43	576	53	659	33	84		
118-Z94	0.0046	26	241	251	0.97	0.75841	9.90	0.08289	6.22	0.63	0.06636	7.71	513	32	573	57	818	63	63		
119-Z95	0.0000	10	97	73	1.34	1.02086	13.29	0.11632	11.82	0.89	0.06365	6.07	709	84	714	95	730	44	97	730	44
120-Z96	0.0016	41	371	236	1.58	0.98777	6.81	0.11401	5.95	0.87	0.06283	3.31	696	41	698	47	703	23	99	703	23
123-Z97	0.1087	36	87	146	0.60	2.85291	37.22	0.09810	8.07	0.22	0.21091	36.34	603	49	1370	510	2913	1058	21		
124-Z98	0.0006	30	208	180	1.16	0.82839	8.97	0.09809	7.76	0.86	0.06125	4.51	603	47	613	55	648	29	93	648	29
125-Z99	0.0047	60	1365	672	2.05	0.48714	10.02	0.05248	9.62	0.96	0.06733	2.79	330	32	403	40	848	24	39		
126-Z100	0.0058	59	702	545	1.30	0.73619	6.58	0.08214	5.96	0.91	0.06500	2.78	509	30	560	37	774	22	66		
127-Z101	0.0094	25	540	181	3.00	0.67455	11.29	0.07449	9.16	0.81	0.06567	6.60	463	42	523	59	796	53	58		
128-Z102	0.0029	16	166	89	1.89	0.80570	12.17	0.09123	9.95	0.82	0.06405	7.00	563	56	600	73	743	52	76		
129-Z103	0.0362	42	1123	473	2.39	0.85319	8.87	0.06033	8.01	0.90	0.10257	3.80	378	30	626	56	1671	64	23		
130-Z104	0.0051	30	266	221	1.21	0.73311	7.92	0.08530	6.81	0.86	0.06233	4.05	528	36	558	44	685	28	77		
131-Z105	0.0018	16	161	85	1.91	0.85066	7.38	0.10350	6.17	0.84	0.05961	4.05	635	39	625	46	589	24	108	589	24
132-Z106	0.0018	24	90	159	0.57	0.81819	9.23	0.09731	8.63	0.94	0.06098	3.27	599	52	607	56	638	21	94	638	21
135-Z107	0.0036	53	677	424	1.61	0.66127	7.55	0.07440	6.85	0.91	0.06446	3.17	463	32	515	39	757	24	61		
136-Z108	0.0031	51	651	434	1.51	0.65101	6.85	0.07420	5.92	0.86	0.06363	3.45	461	27	509	35	729	25	63		
137-Z109	0.0006	53	306	332	0.93	0.81307	5.12	0.09887	4.18	0.82	0.05964	2.95	608	25	604	31	591	17	103	591	17
138-Z110	0.0000	6	118	57	2.08	1.09438	9.02	0.08855	5.90	0.65	0.08963	6.83	547	32	751	68	1418	97	39		

139-Z111	0.0079		18	378	146	2.60	0.52299	13.68	0.05867	12.11	0.88	0.06466	6.37	368	44	427	58	763	49	48		
140-Z112	0.0054		18	59	152	0.39	1.08854	6.40	0.12335	3.50	0.55	0.06401	5.36	750	26	748	48	742	40	101	742	40
141-Z113	0.0011		33	227	213	1.07	0.84512	5.76	0.10034	4.72	0.82	0.06109	3.30	616	29	622	36	642	21	96	642	21

[a] Th/U ratios are calculated relative to GJ-1 reference zircon

[b] Corrected for background and within-run Pb/U fractionation and normalised to reference zircon GJ-1 (ID-TIMS values/measured value); 207Pb/235U calculated using $(^{207}Pb/^{206}Pb)/(^{238}U/^{206}Pb * 1/137.88)$

[c] Rho is the error correlation defined as the quotient of the propagated errors of the $^{206}Pb/^{238}U$ and the $^{207}/^{235}U$ ratio

[d] Corrected for mass-bias by normalising to GJ-1 reference zircon and common Pb using the model Pb composition of Stacey and Kramers (1975)

[e] Degree of concordance = $(^{206}Pb/^{238}U$ age $* 100/^{207}Pb/^{206}U$ age)

Table 1g : U-Pb in situ zircon data of sample PS-01 SB I, Santa Barbara Gr.

						Isotope ratios[b]							Ages (Ma)							
Spot number	f 206	Pb ppm	U ppm	Th ppm	Th/U[a]	$^{207}Pb/^{235}U$	1 s [%]	$^{206}Pb/^{238}U$	1 s [%]	Rho[c]	$^{207}Pb/^{206}Pb$[d]	1 s [%]	$^{206}Pb/^{238}U$	1 s abs	$^{207}Pb/^{235}U$	1 s abs	$^{207}Pb/^{206}Pb$	1 s abs	% Conc[e]	Best estimated age (Ma)
004-Z1	0.0000	70	8	69	1.00	0.73578	3.86	0.09008	2.19	0.57	0.05924	3.17	556	12	560	22	576	18	97	576	18
005-Z2	0.0002	241	63	108	0.45	3.35630	1.77	0.24758	1.19	0.68	0.09832	1.30	1426	17	1494	26	1593	21	90	1593	21
006-Z3	0.0001	175	26	89	0.52	1.12326	2.79	0.12557	1.84	0.66	0.06488	2.10	763	14	765	21	770	16	99	770	16
007-Z4	0.0001	57	6	49	0.87	0.74919	3.89	0.09160	2.53	0.65	0.05932	2.95	565	14	568	22	579	17	98	579	17
008-Z5	0.0003	19	9	14	0.75	8.23081	3.71	0.42189	3.27	0.88	0.14150	1.76	2269	74	2257	84	2246	40	101	2246	40
009-Z6	0.0004	61	26	51	0.84	7.10983	1.91	0.37832	1.39	0.73	0.13630	1.31	2068	29	2125	41	2181	29	95	2181	29
010-Z7	0.0003	153	39	103	0.68	3.36646	3.36	0.23672	2.31	0.69	0.10314	2.44	1370	32	1497	50	1681	41	81		
011-Z8	0.0000	123	13	97	0.79	0.83004	4.09	0.10057	3.13	0.77	0.05986	2.64	618	19	614	25	598	16	103	598	16
012-Z9	0.0000	128	20	67	0.52	1.16938	4.27	0.13145	3.68	0.86	0.06452	2.16	796	29	786	34	759	16	105	759	16
016-Z11	0.0001	110	56	43	0.40	6.91239	2.24	0.39874	1.94	0.87	0.12573	1.12	2163	42	2100	47	2039	23	106	2039	23
017-Z12	0.0000	72	9	120	1.68	0.83873	3.59	0.10278	2.62	0.73	0.05918	2.46	631	17	618	22	574	14	110	574	14
018-Z13	0.0001	56	7	77	1.39	0.78676	3.76	0.09624	2.90	0.77	0.05929	2.39	592	17	589	22	578	14	103	578	14
019-Z14	0.0000	25	6	16	0.65	1.66547	3.33	0.17098	2.66	0.80	0.07065	2.01	1017	27	995	33	947	19	107	947	19
020-Z15	0.0059	245	77	125	0.51	3.24402	3.27	0.24810	1.54	0.47	0.09483	2.88	1429	22	1468	48	1525	44	94	1525	44
021-Z16	0.0000	186	87	164	0.89	19.68803	28.78	0.22642	24.95	0.87	0.63066	14.35	1316	328	3076	885	4580	657	29		
022-Z17	0.0000	66	25	40	0.60	1.51760	29.20	0.11295	24.27	0.83	0.09745	16.23	690	167	938	274	1576	256	44		
023-Z18	0.0034	534	57	454	0.86	0.75338	4.83	0.09048	2.97	0.62	0.06039	3.81	558	17	570	28	617	24	90	617	24
024-Z19	0.0000	73	29	55	0.77	5.70078	2.06	0.31888	1.53	0.74	0.12966	1.39	1784	27	1931	40	2093	29	85		
025-Z20	0.0000	38	5	42	1.12	0.93890	5.56	0.10144	4.71	0.85	0.06713	2.95	623	29	672	37	842	25	74		
028-Z21	0.0001	77	28	80	1.05	4.13033	2.66	0.29196	2.36	0.89	0.10260	1.23	1651	39	1660	44	1672	21	99	1672	21
029-Z22	0.0005	93	45	106	1.15	6.69311	5.17	0.37819	4.90	0.95	0.12836	1.68	2068	101	2072	107	2076	35	100	2076	35
030-Z23	0.0005	279	66	91	0.33	3.85678	3.04	0.27371	1.42	0.47	0.10220	2.68	1560	22	1605	49	1664	45	94	1664	45
031-Z24	0.0003	95	49	58	0.61	6.66813	4.58	0.37881	4.24	0.93	0.12767	1.72	2071	88	2068	95	2066	35	100	2066	35
032-Z25	0.0007	58	33	25	0.44	9.80151	2.55	0.44948	1.59	0.62	0.15815	2.00	2393	38	2416	62	2436	49	98	2436	49
033-Z26	0.0003	9	1	5	0.57	1.02466	5.82	0.11533	2.59	0.44	0.06444	5.22	704	18	716	42	756	39	93	756	39
034-Z27	0.0003	115	44	87	0.76	5.40404	2.18	0.32043	1.88	0.87	0.12232	1.09	1792	34	1885	41	1990	22	90	1990	22
035-Z28	0.0006	57	27	84	1.47	5.99318	2.74	0.35860	2.07	0.75	0.12121	1.80	1976	41	1975	54	1974	36	100	1974	36
036-Z29	0.0011	89	42	55	0.63	5.77934	2.79	0.34453	2.04	0.73	0.12166	1.90	1908	39	1943	54	1981	38	96	1981	38
037-Z30	0.0000	109	15	95	0.88	0.85946	3.84	0.10403	2.73	0.71	0.05992	2.71	638	17	630	24	601	16	106	601	16
040-Z31	0.0000	66	9	100	1.52	0.80855	4.35	0.09830	3.64	0.84	0.05966	2.38	604	22	602	26	591	14	102	591	14
041-Z32	0.0000	182	30	146	0.81	0.95753	2.97	0.11055	2.62	0.88	0.06282	1.41	676	18	682	20	702	10	96	702	10
042-Z33	0.0000	222	42	40	0.18	1.54038	4.16	0.14612	3.36	0.81	0.07646	2.45	879	30	947	39	1107	27	79		
043-Z34	0.0001	34	5	37	1.09	0.89780	4.34	0.10808	3.22	0.74	0.06025	2.91	662	21	651	28	612	18	108	612	18
044-Z35	0.0001	55	7	50	0.91	0.78749	4.51	0.09680	3.72	0.82	0.05900	2.56	596	22	590	27	567	15	105	567	15
045-Z36	0.0000	121	22	72	0.60	1.21311	2.95	0.13441	2.63	0.89	0.06546	1.34	813	21	807	24	789	11	103	789	11
046-Z37	0.0002	84	40	46	0.55	5.64318	2.00	0.34053	1.42	0.71	0.12019	1.42	1889	27	1923	39	1959	28	96	1959	28
047-Z38	0.0028	99	30	161	1.64	4.06907	4.92	0.23360	3.53	0.72	0.12633	3.42	1353	48	1648	81	2048	70	66		
048-Z39	0.0005	15	8	8	0.55	6.27324	3.40	0.35921	2.70	0.79	0.12666	2.08	1978	53	2015	69	2052	43	96	2052	43

049-Z40	0.0005	89	43	42	0.47	5.85175	3.06	0.35389	2.77	0.90	0.11993	1.32	1953	54	1954	60	1955	26	100	1955	26
052-Z41	0.0000	166	28	85	0.51	1.15738	2.65	0.12771	1.84	0.70	0.06573	1.90	775	14	781	21	798	15	97	798	15
053-Z42	0.0003	106	52	44	0.42	7.59460	2.00	0.40109	1.44	0.72	0.13733	1.39	2174	31	2184	44	2194	30	99	2194	30
054-Z43	0.0009	261	34	167	0.64	0.92083	3.26	0.10004	2.60	0.80	0.06676	1.97	615	16	663	22	830	16	74		
055-Z44	0.0002	60	31	40	0.68	7.87943	1.49	0.41300	1.01	0.68	0.13837	1.10	2229	22	2217	33	2207	24	101	2207	24
056-Z45	0.0001	124	14	132	1.07	0.79101	4.38	0.09459	2.90	0.66	0.06065	3.28	583	17	592	26	627	21	93	627	21
057-Z46	0.0006	223	38	82	0.37	1.38527	2.77	0.13916	1.53	0.55	0.07220	2.31	840	13	883	24	992	23	85		
058-Z47	0.0002	192	123	110	0.58	13.39205	3.22	0.50569	1.31	0.41	0.19207	2.94	2638	35	2708	87	2760	81	96	2760	81
059-Z48	0.0079	295	37	324	1.11	0.87754	8.75	0.10528	4.34	0.50	0.06045	7.60	645	28	640	56	620	47	104	620	47
060-Z49	0.0010	42	12	31	0.76	2.81104	6.31	0.24095	3.69	0.59	0.08461	5.11	1392	51	1358	86	1307	67	106	1307	67
061-Z50	0.0110	226	84	219	0.98	2.98556	7.17	0.21953	5.49	0.77	0.09864	4.61	1279	70	1404	101	1598	74	80		
064-Z51	0.0004	369	42	359	0.98	0.86678	3.13	0.10278	2.03	0.65	0.06116	2.38	631	13	634	20	645	15	98	645	15
065-Z52	0.0002	204	82	242	1.19	6.44751	3.25	0.36633	3.11	0.96	0.12765	0.96	2012	63	2039	66	2066	20	97	2066	20
066-Z53	0.0002	376	88	306	0.82	2.26670	2.92	0.20242	2.61	0.89	0.08121	1.32	1188	31	1202	35	1227	16	97	1227	16
067-Z54	0.0002	191	24	41	0.22	0.78914	4.70	0.09639	2.65	0.56	0.05938	3.87	593	16	591	28	581	23	102	581	23
068-Z55	0.0001	110	49	127	1.16	7.23481	2.00	0.40190	1.81	0.90	0.13056	0.85	2178	39	2141	43	2105	18	103	2105	18
069-Z56	0.0000	390	45	303	0.78	0.82089	3.50	0.09871	3.02	0.86	0.06031	1.77	607	18	609	21	615	11	99	615	11
070-Z57	0.0000	270	32	7	0.03	0.90507	2.87	0.10701	1.88	0.66	0.06134	2.16	655	12	654	19	651	14	101	651	14
071-Z58	0.0001	39	4	39	1.01	0.88536	4.39	0.09363	2.85	0.65	0.06858	3.34	577	16	644	28	886	30	65		
072-Z59	0.0001	136	67	75	0.56	6.68268	3.13	0.37370	2.81	0.90	0.12970	1.38	2047	58	2070	65	2094	29	98	2094	29
073-Z60	0.0003	200	83	128	0.64	8.16702	1.75	0.43008	1.37	0.78	0.13772	1.10	2306	32	2250	39	2199	24	105	2199	24

[a] Th/U ratios are calculated relative to GJ-1 reference zircon

[b] Corrected for background and within-run Pb/U fractionation and normalised to reference zircon GJ-1 (ID-TIMS values/measured value); 207Pb/235U calculated using $(^{207}Pb/^{206}Pb)/(^{238}U/^{206}Pb * 1/137.88)$

[c] Rho is the error correlation defined as the quotient of the propagated errors of the $^{206}Pb/^{238}U$ and the $^{207}/^{235}U$ ratio

[d] Corrected for mass-bias by normalising to GJ-1 reference zircon and common Pb using the model Pb composition of Stacey and Kramers (1975)

[e] Degree of concordance = $(^{206}Pb/^{238}U$ age * 100/$^{207}Pb/^{206}U$ age)

Table 1h : U-Pb in situ zircon data of sample T01-144 SB II, Santa Barbara Gr.

						Isotope ratios[b]							Ages (Ma)								
Spot numb	f 206	Pb ppm	U ppm	Th ppm	Th/U[a]	207Pb/235U	1 s [%]	206Pb/238U	1 s [%]	Rho[c]	207Pb/206Pb[d]	1 s [%]	206Pb/238U	1 s abs	207Pb/235U	1 s abs	207Pb/206Pb	1 s abs	% Conc[e]	Best estima age (Ma)	
004-Z1	0.0042	30	18	45	0.41	7.88019	5.12	0.41266	3.77	0.74	0.13850	3.47	2227	84	2217	114	2208	77	101	2208	77
005-Z2	0.0063	16	100	86	1.17	0.87748	7.40	0.10417	4.22	0.57	0.06109	6.08	639	27	640	47	643	39	99	643	39
006-Z3	0.0127	9	61	50	1.23	1.14109	10.92	0.12897	8.71	0.80	0.06417	6.59	782	68	773	84	747	49	105	747	49
007-Z4	0.0048	31	102	215	0.48	0.86179	6.10	0.10347	4.79	0.78	0.06041	3.78	635	30	631	38	618	23	103	618	23
008-Z5	0.0064	19	129	109	1.19	0.88405	7.60	0.10388	5.93	0.78	0.06172	4.76	637	38	643	49	664	32	96	664	32
009-Z6	0.0034	38	145	232	0.63	0.83024	6.49	0.10084	5.31	0.82	0.05971	3.73	619	33	614	40	593	22	104	593	22
010-Z7	0.0025	103	301	492	0.62	1.31978	4.14	0.14419	2.15	0.52	0.06638	3.54	868	19	854	35	819	29	106	819	29
011-Z8	0.0067	17	113	92	1.24	0.81670	15.44	0.09798	12.64	0.82	0.06045	8.87	603	76	606	94	620	55	97	620	55
012-Z9	0.0018	34	281	219	1.29	0.81721	7.82	0.09898	6.48	0.83	0.05988	4.37	608	39	606	47	599	26	102	599	26
015-Z10	0.0022	87	350	413	0.85	0.89942	6.60	0.10689	5.70	0.86	0.06103	3.32	655	37	651	43	640	21	102	640	21
016-Z11	0.0004	267	245	403	0.61	5.12261	3.66	0.33090	2.90	0.79	0.11228	2.24	1843	53	1840	67	1837	41	100	1837	41
017-Z12	0.0052	39	91	128	0.72	1.21335	7.47	0.13134	4.56	0.61	0.06700	5.91	795	36	807	60	838	50	95	838	50
018-Z13	0.0003	96	373	424	0.88	0.81817	7.28	0.09835	6.56	0.90	0.06034	3.17	605	40	607	44	616	20	98	616	20
019-Z14	0.0164	201	1144	737	1.57	1.23329	5.21	0.11953	4.44	0.85	0.07483	2.73	728	32	816	42	1064	29	68		
020-Z15	0.0028	203	159	410	0.39	4.60058	2.82	0.29118	2.05	0.73	0.11459	1.93	1647	34	1749	49	1873	36	88		
021-Z16	0.0008	281	277	580	0.48	4.90233	2.60	0.28696	1.90	0.73	0.12390	1.78	1626	31	1803	47	2013	36	81		
022-Z17	0.0005	339	28	537	0.05	6.49980	2.60	0.35795	2.15	0.83	0.13170	1.46	1972	42	2046	53	2121	31	93	2121	31
023-Z18	0.0010	92	256	424	0.61	1.09216	5.38	0.12600	4.39	0.82	0.06286	3.12	765	34	750	40	704	22	109	704	22
024-Z19	0.0030	52	108	304	0.36	0.79928	9.30	0.09659	7.15	0.77	0.06002	5.94	594	43	596	55	604	36	98	604	36
027-Z20	0.0034	21	52	100	0.53	1.00535	10.54	0.11645	8.64	0.82	0.06262	6.04	710	61	707	74	695	42	102	695	42
028-Z21	0.0014	38	152	157	0.98	0.93246	9.09	0.11031	7.20	0.79	0.06131	5.56	675	49	669	61	650	36	104	650	36
029-Z22	0.0026	58	129	217	0.60	0.72104	14.24	0.08993	11.93	0.84	0.05815	7.78	555	66	551	79	535	42	104	555	42
030-Z23	0.0025	42	131	212	0.62	0.83442	8.89	0.10111	7.18	0.81	0.05986	5.23	621	45	616	55	598	31	104	598	31
031-Z24	0.0012	659	1006	774	1.31	6.71817	3.53	0.38910	2.67	0.76	0.12522	2.31	2119	57	2075	73	2032	47	104	2032	47
032-Z25	0.0027	66	283	253	1.13	0.97525	7.41	0.11683	5.41	0.73	0.06054	5.06	712	39	691	51	623	32	114		
033-Z26	0.0016	44	169	240	0.71	0.84509	10.57	0.09440	9.50	0.90	0.06493	4.62	582	55	622	66	772	36	75		
034-Z27	0.0014	79	77	196	0.40	2.07392	5.64	0.19329	3.65	0.65	0.07782	4.31	1139	42	1140	64	1142	49	100	1142	49
035-Z28	0.0036	36	123	178	0.69	0.92580	10.04	0.10986	8.07	0.80	0.06112	5.97	672	54	665	67	643	38	104	643	38
036-Z29	0.0012	13	33	71	0.47	0.77960	10.80	0.09468	9.25	0.86	0.05972	5.57	583	54	585	63	593	33	98	593	33
040-Z30	0.0000	8	34	50	0.68	0.80781	11.11	0.09737	9.65	0.87	0.06017	5.51	599	58	601	67	610	34	98	610	34
041-Z31	0.0008	195	124	281	0.44	4.61153	3.89	0.30508	2.74	0.71	0.10963	2.76	1716	47	1751	68	1793	49	96	1793	49
042-Z32	0.0006	347	212	445	0.48	6.67653	2.66	0.38914	1.72	0.65	0.12444	2.03	2119	36	2070	55	2021	41	105	2021	41
043-Z33	0.0021	67	327	344	0.96	0.83129	6.35	0.10019	4.20	0.66	0.06017	4.77	616	26	614	39	610	29	101	610	29
044-Z34	0.0027	142	189	410	0.46	2.46793	5.42	0.19123	4.48	0.83	0.09360	3.05	1128	51	1263	68	1500	46	75		
045-Z35	0.0024	292	203	358	0.57	8.24485	2.45	0.44301	1.05	0.43	0.13498	2.21	2364	25	2258	55	2164	48	109	2164	48
046-Z36	0.0009	144	92	159	0.58	8.59583	3.15	0.44361	2.05	0.65	0.14054	2.39	2367	49	2296	72	2234	53	106	2234	53
047-Z37	0.0000	18	107	82	1.31	0.88996	20.98	0.09957	18.95	0.90	0.06483	9.00	612	116	646	136	769	69	80		
048-Z38	0.0035	158	146	256	0.57	7.14558	3.01	0.37957	1.46	0.48	0.13653	2.63	2074	30	2130	64	2184	57	95	2184	57

051-Z39	0.0041	23	49	163	0.31	1.12899	9.84	0.12761	8.71	0.89	0.06417	4.57	774	67	767	75	747	34	104	747	34
052-Z40	0.0019	47	22	259	0.08	1.92527	5.52	0.15195	5.07	0.92	0.09190	2.17	912	46	1090	60	1465	32	62		
053-Z41	0.0214	7	37	39	0.94	0.88489	53.02	0.10248	44.27	0.84	0.06263	29.17	629	278	644	341	696	203	90	696	203
054-Z42	0.0039	166	137	903	0.15	1.52761	6.79	0.14658	5.67	0.83	0.07559	3.73	882	50	942	64	1084	40	81		
055-Z43	0.0035	97	104	518	0.20	1.46444	6.37	0.15312	4.93	0.77	0.06937	4.03	918	45	916	58	910	37	101	910	37
056-Z44	0.0095	97	228	514	0.45	2.04823	9.07	0.14710	8.26	0.91	0.10099	3.77	885	73	1132	103	1642	62	54		
057-Z45	0.0019	24	67	215	0.32	0.90767	13.33	0.10823	12.52	0.94	0.06082	4.57	662	83	656	87	633	29	105	633	29
058-Z46	0.0212	9	83	46	1.80	0.90124	38.74	0.10279	33.39	0.86	0.06359	19.66	631	211	652	253	728	143	87		
059-Z47	0.0055	52	564	225	2.52	0.86257	12.32	0.10160	10.25	0.83	0.06157	6.84	624	64	632	78	659	45	95	659	45
060-Z48	0.0018	68	212	351	0.61	1.36415	6.16	0.15098	4.80	0.78	0.06553	3.86	906	43	874	54	791	31	115		
063-Z49	0.0016	68	575	341	1.70	0.93630	4.40	0.11200	3.13	0.71	0.06063	3.09	684	21	671	30	626	19	109	626	19
064-Z50	0.0010	25	137	146	0.95	1.00947	8.49	0.11680	6.50	0.77	0.06268	5.46	712	46	709	60	697	38	102	697	38
065-Z51	0.0089	79	158	135	1.18	9.07714	3.45	0.43350	2.35	0.68	0.15186	2.52	2321	55	2346	81	2367	60	98	2367	60
066-Z52	0.0074	30	211	127	1.67	1.07176	10.71	0.12255	7.46	0.70	0.06343	7.70	745	56	740	79	723	56	103	723	56
067-Z53	0.0027	110	525	434	1.22	1.27381	6.34	0.13873	5.29	0.83	0.06660	3.50	837	44	834	53	825	29	101	825	29
068-Z54	0.0013	92	46	126	0.37	8.34394	2.44	0.44101	1.99	0.81	0.13722	1.42	2355	47	2269	55	2192	31	107	2192	31
069-Z55	0.0022	38	84	200	0.42	1.32946	5.28	0.14288	4.02	0.76	0.06748	3.42	861	35	859	45	853	29	101	853	29
070-Z56	0.0026	40	90	183	0.50	1.25647	4.13	0.14443	2.68	0.65	0.06309	3.14	870	23	826	34	711	22	122		
071-Z57	0.0151	410	203	756	0.27	6.41766	1.58	0.31007	0.73	0.46	0.15011	1.40	1741	13	2035	32	2347	33	74		
072-Z58	0.0016	66	257	357	0.72	0.91331	5.30	0.10945	3.72	0.70	0.06052	3.78	670	25	659	35	622	24	108	622	24
076-Z59	0.0014	246	199	259	0.77	7.78282	2.64	0.42610	1.73	0.66	0.13247	2.00	2288	40	2206	58	2131	43	107	2131	43
077-Z60	0.0014	30	115	106	1.10	1.08620	9.08	0.12407	6.74	0.74	0.06349	6.10	754	51	747	68	725	44	104	725	44
078-Z61	0.0054	27	122	97	1.27	1.23961	8.30	0.13457	7.55	0.91	0.06681	3.44	814	61	819	68	832	29	98	832	29
079-Z62	0.0003	998	1060	1240	0.86	5.23248	2.67	0.36013	1.37	0.51	0.10538	2.29	1983	27	1858	50	1721	39	115		
080-Z63	0.0016	85	139	272	0.51	1.33808	5.49	0.15020	3.78	0.69	0.06461	3.99	902	34	862	47	762	30	118		
081-Z64	0.0005	200	264	391	0.68	3.21529	4.76	0.21490	3.83	0.80	0.10851	2.83	1255	48	1461	69	1775	50	71		
082-Z65	0.0012	158	420	699	0.61	0.94689	6.16	0.11154	4.72	0.77	0.06157	3.96	682	32	676	42	659	26	103	659	26
083-Z66	0.0008	177	51	193	0.27	6.30307	2.46	0.36461	1.38	0.56	0.12538	2.03	2004	28	2019	50	2034	41	99	2034	41
084-Z67	0.0040	36	67	122	0.55	1.24035	7.26	0.13576	5.52	0.76	0.06626	4.72	821	45	819	59	815	38	101	815	38
087-Z68	0.0003	23	111	141	0.79	0.95446	10.10	0.10950	7.61	0.75	0.06322	6.64	670	51	680	69	716	48	94	716	48
088-Z69	0.0023	30	153	217	0.71	0.86804	7.47	0.10269	6.38	0.85	0.06130	3.89	630	40	635	47	650	25	97	650	25
089-Z70	0.0023	49	148	335	0.45	0.95936	7.25	0.11316	5.05	0.70	0.06149	5.20	691	35	683	50	656	34	105	656	34
090-Z71	0.0048	48	162	264	0.62	1.06114	8.29	0.12951	6.52	0.79	0.05942	5.11	785	51	734	61	583	30	135		
091-Z72	0.0018	47	210	227	0.93	0.86945	8.14	0.10463	6.86	0.84	0.06027	4.39	641	44	635	52	613	27	105	613	27
092-Z73	0.0479	357	1738	1675	1.04	0.75665	39.23	0.11335	4.90	0.12	0.04842	38.93	692	34	572	224	120	47	579		
093-Z74	0.0013	65	500	289	1.74	1.07148	8.29	0.12347	7.06	0.85	0.06294	4.35	751	53	739	61	706	31	106	706	31
094-Z75	0.0032	318	1483	1871	0.80	1.03376	6.18	0.11839	4.76	0.77	0.06333	3.94	721	34	721	45	719	28	100	719	28
095-Z76	0.0014	58	517	305	1.71	0.85904	8.35	0.10360	7.18	0.86	0.06014	4.28	635	46	630	53	609	26	104	609	26
096-Z77	0.0016	113	117	251	0.47	3.76085	3.80	0.29129	2.19	0.58	0.09364	3.11	1648	36	1584	60	1501	47	110	1501	47
099-Z78	0.0003	247	310	481	0.65	5.22302	3.56	0.34264	2.40	0.67	0.11056	2.63	1899	46	1856	66	1809	48	105	1809	48
100-Z79	0.0012	67	360	428	0.85	0.89473	7.32	0.10692	5.37	0.73	0.06069	4.98	655	35	649	48	628	31	104	628	31
101-Z80	0.0013	91	153	252	0.61	3.22548	5.41	0.22987	3.66	0.68	0.10177	3.98	1334	49	1463	79	1657	66	81	1657	66
102-Z81	0.0010	153	117	291	0.40	7.04780	3.17	0.39877	1.79	0.56	0.12818	2.62	2163	39	2117	67	2073	54	104	2073	54
103-Z82	0.0030	95	711	493	1.45	0.90178	8.02	0.10667	6.07	0.76	0.06131	5.23	653	40	653	52	650	34	100	650	34

104-Z83	0.0015	67	245	391	0.63	1.08836	7.11	0.13022	4.88	0.69	0.06062	5.18	789	38	748	53	626	32	126		
105-Z84	0.0014	218	264	319	0.83	9.81360	3.04	0.52020	1.48	0.49	0.13682	2.66	2700	40	2417	73	2187	58	123		
106-Z85	0.0017	79	530	460	1.16	0.92766	9.86	0.11273	8.17	0.83	0.05968	5.51	689	56	666	66	592	33	116	592	33
107-Z86	0.0015	59	416	374	1.12	0.92049	7.82	0.11051	5.98	0.77	0.06041	5.04	676	40	663	52	618	31	109	618	31
108-Z87	0.0015	81	469	441	1.07	0.90138	8.29	0.10773	6.58	0.79	0.06069	5.05	660	43	652	54	628	32	105	628	32
112-Z88	0.0011	85	375	526	0.72	0.97745	7.76	0.11878	6.18	0.80	0.05968	4.69	724	45	692	54	592	28	122		
113-Z89	0.0015	49	331	264	1.26	0.95462	6.66	0.11531	3.86	0.58	0.06004	5.43	704	27	681	45	605	33	116		
114-Z90	0.0035	108	562	706	0.80	1.01736	9.15	0.12076	7.48	0.82	0.06110	5.27	735	55	713	65	643	34	114		
115-Z91	0.0005	175	131	325	0.41	6.18968	8.15	0.37835	6.50	0.80	0.11865	4.92	2069	134	2003	163	1936	95	107	1936	95
116-Z92	0.0046	47	300	283	1.07	0.96571	9.52	0.11195	6.40	0.67	0.06256	7.05	684	44	686	65	693	49	99	693	49
117-Z93	0.0034	76	414	407	1.03	0.97922	6.50	0.11299	4.43	0.68	0.06285	4.76	690	31	693	45	703	33	98	703	33
118-Z94	0.0049	43	181	250	0.73	1.01054	8.12	0.11665	5.85	0.72	0.06283	5.63	711	42	709	58	703	40	101	703	40
119-Z95	0.0009	140	494	807	0.62	0.95142	6.16	0.11631	4.27	0.69	0.05933	4.44	709	30	679	42	579	26	122		
120-Z96	0.0015	1344	840	2856	0.30	5.41654	2.70	0.34704	1.35	0.50	0.11320	2.35	1920	26	1887	51	1851	43	104	1851	43
123-Z97	0.0076	39	96	176	0.55	1.59644	9.52	0.15736	7.73	0.81	0.07358	5.55	942	73	969	92	1030	57	91	1030	57
124-Z98	0.0064	132	391	200	1.97	8.02198	2.96	0.42135	1.76	0.60	0.13808	2.38	2267	40	2234	66	2203	52	103	2203	52
125-Z99	0.0033	40	48	56	0.86	7.71116	3.52	0.40060	1.30	0.37	0.13961	3.27	2172	28	2198	77	2222	73	98	2222	73
126-Z100	0.0044	22	57	138	0.42	0.81610	8.24	0.09850	5.67	0.69	0.06009	5.98	606	34	606	50	607	36	100	607	36
127-Z101	0.0023	122	141	667	0.21	0.99219	6.13	0.11472	4.66	0.76	0.06273	3.98	700	33	700	43	699	28	100	699	28
128-Z102	0.0017	58	153	363	0.43	0.88758	7.42	0.10576	5.99	0.81	0.06087	4.37	648	39	645	48	635	28	102	635	28
129-Z103	0.0007	296	232	431	0.54	7.32823	4.05	0.39036	2.87	0.71	0.13616	2.86	2124	61	2152	87	2179	62	98	2179	62
130-Z104	0.0005	244	164	488	0.34	5.04795	8.05	0.32359	7.57	0.94	0.11314	2.74	1807	137	1827	147	1850	51	98	1850	51
131-Z105	0.0019	57	177	314	0.57	0.92890	7.16	0.11084	5.77	0.81	0.06078	4.23	678	39	667	48	632	27	107	632	27
132-Z106	0.0036	91	380	448	0.86	0.91725	7.05	0.10834	5.43	0.77	0.06140	4.49	663	36	661	47	653	29	101	653	29
135-Z107	0.0014	418	210	719	0.29	4.77734	5.51	0.31690	4.96	0.90	0.10934	2.38	1775	88	1781	98	1788	43	99	1788	43
136-Z108	0.0000	6	10	22	0.47	1.88183	23.56	0.21924	14.48	0.61	0.06225	18.58	1278	185	1075	253	683	127	187		
137-Z109	0.0004	130	1182	643	1.85	0.84586	7.72	0.10582	6.11	0.79	0.05798	4.73	648	40	622	48	529	25	123		
138-Z110	0.0023	33	99	204	0.49	0.97230	8.91	0.11887	5.14	0.58	0.05932	7.27	724	37	690	61	579	42	125		
139-Z111	0.0076	33	96	188	0.52	1.11758	6.68	0.11687	5.61	0.84	0.06936	3.63	713	40	762	51	909	33	78		
140-Z112	0.0003	400	81	318	0.26	15.14987	5.09	0.54682	4.09	0.80	0.20094	3.03	2812	115	2825	144	2834	86	99	2834	86
141-Z113	0.0030	29	25	130	0.19	0.67995	15.42	0.08447	13.22	0.86	0.05838	7.94	523	69	527	81	544	43	96	544	43
142-Z114	0.0003	349	105	400	0.26	14.52373	1.70	0.57644	1.16	0.68	0.18273	1.24	2934	34	2785	47	2678	33	110	2678	33
143-Z115	0.0156	16	84	79	1.07	1.02538	19.90	0.10511	16.18	0.81	0.07075	11.58	644	104	717	143	950	110	68		

[a] Th/U ratios are calculated relative to GJ-1 reference zircon

[b] Corrected for background and within-run Pb/U fractionation and normalised to reference zircon GJ-1 (ID-TIMS values/measured value); 207Pb/235U calculated using $(^{207}Pb/^{206}Pb)/(^{238}U/^{206}Pb * 1/137.88)$

[c] Rho is the error correlation defined as the quotient of the propagated errors of the $^{206}Pb/^{238}U$ and the $^{207}/^{235}U$ ratio

[d] Corrected for mass-bias by normalising to GJ-1 reference zircon and common Pb using the model Pb composition of Stacey and Kramers (1975)

[e] Degree of concordance = $(^{206}Pb/^{238}U$ age $* 100/^{207}Pb/^{206}U$ age)

Table 1i: U-Pb in situ zircon data of sample T01-176 SB II, Santa Barbara Gr.

Spot number	f 206	Pb ppm	U ppm	Th ppm	Th/U[a]	Isotope ratios[b] 207Pb/235U	1 s [%]	206Pb/238U	1 s [%]	Rho[c]	207Pb/206Pb[d]	1 s [%]	Ages (Ma) 206Pb/238U	1 s abs	207Pb/235U	1 s abs	207Pb/206Pb	1 s abs	% Conc[e]	Best estim age (Ma)	
004-Z1	0.0015	70	148	431	0.35	1.22258	4.45	0.13574	2.98	0.67	0.06532	3.30	821	24	811	36	785	26	105	785	26
005-Z2	0.1456	346	617	1775	0.35	3.25881	4.80	0.07334	4.49	0.93	0.32228	1.71	456	20	1471	71	3581	61	13		
006-Z3	0.0036	14	90	104	0.87	0.73446	11.46	0.08772	10.45	0.91	0.06072	4.69	542	57	559	64	629	30	86		
007-Z4	0.0055	31	241	207	1.17	0.85494	8.94	0.10093	5.85	0.65	0.06144	6.76	620	36	627	56	655	44	95	655	44
008-Z5	0.0054	24	47	49	0.98	4.44851	7.00	0.30596	5.42	0.77	0.10545	4.43	1721	93	1721	121	1722	76	100	1722	76
009-Z6	0.0008	157	128	292	0.44	9.04851	2.76	0.43738	1.14	0.41	0.15004	2.51	2339	27	2343	65	2346	59	100	2346	59
010-Z7	0.0319	97	117	435	0.27	2.93926	4.29	0.17312	3.40	0.79	0.12314	2.61	1029	35	1392	60	2002	52	51		
011-Z8	0.0014	71	317	473	0.68	0.90252	4.66	0.10877	3.00	0.64	0.06018	3.57	666	20	653	30	610	22	109	610	22
012-Z9	0.0020	269	354	326	1.09	16.60285	1.72	0.61523	1.02	0.59	0.19572	1.39	3091	31	2912	50	2791	39	111		
015-Z10	0.0024	65	125	308	0.41	1.36426	4.04	0.14770	3.29	0.81	0.06699	2.35	888	29	874	35	837	20	106	837	20
016-Z11	0.0021	96	481	512	0.95	1.17592	4.73	0.13560	3.94	0.83	0.06289	2.62	820	32	789	37	705	18	116		
017-Z12	0.0041	54	348	301	1.17	1.00060	7.61	0.11642	6.06	0.80	0.06234	4.60	710	43	704	54	686	32	104	686	32
018-Z13	0.0025	57	172	350	0.49	0.92345	6.48	0.10927	5.40	0.83	0.06129	3.58	669	36	664	43	649	23	103	649	23
019-Z14	0.0043	39	66	60	1.10	4.11121	9.98	0.25598	7.79	0.78	0.11648	6.23	1469	114	1657	165	1903	119	77		
020-Z15	0.0010	104	61	150	0.41	7.53655	2.44	0.42646	1.16	0.48	0.12817	2.14	2290	27	2177	53	2073	44	110	2073	44
021-Z16	0.0015	6	41	47	0.89	0.88312	9.96	0.11012	6.24	0.63	0.05817	7.76	673	42	643	64	536	42	126		
022-Z17	0.0135	8	47	50	0.95	0.76877	16.38	0.10664	15.15	0.92	0.05229	6.23	653	99	579	95	298	19	219		
023-Z18	0.0028	226	33	518	0.06	5.83292	2.01	0.32686	1.53	0.76	0.12943	1.30	1823	28	1951	39	2090	27	87		
024-Z19	0.0054	54	154	348	0.45	1.12637	8.24	0.12540	6.71	0.81	0.06515	4.78	762	51	766	63	779	37	98	779	37
027-Z20	0.0024	35	283	295	0.97	0.87566	7.62	0.10399	6.17	0.81	0.06107	4.47	638	39	639	49	642	29	99	642	29
028-Z21	0.0053	27	261	223	1.18	0.87064	9.73	0.10398	8.87	0.91	0.06073	4.01	638	57	636	62	630	25	101	630	25
029-Z22	0.0047	14	149	109	1.37	0.91239	6.57	0.10941	4.64	0.71	0.06048	4.65	669	31	658	43	621	29	108	621	29
030-Z23	0.0062	24	214	205	1.05	0.83562	11.50	0.10020	7.66	0.67	0.06049	8.57	616	47	617	71	621	53	99	621	53
031-Z24	0.0168	13	139	119	1.18	0.76320	11.77	0.09327	9.14	0.78	0.05935	7.41	575	53	576	68	580	43	99	580	43
033-Z26	0.0513	15	34	153	0.22	1.25981	15.37	0.07990	12.47	0.81	0.11435	8.97	496	62	828	127	1870	168	27		
034-Z27	0.0030	27	19	85	0.22	4.98376	6.75	0.27595	5.78	0.86	0.13099	3.48	1571	91	1817	123	2111	73	74		
035-Z28	0.0163	102	83	422	0.20	5.27579	4.16	0.28767	3.10	0.75	0.13301	2.77	1630	51	1865	77	2138	59	76		
036-Z29	0.0010	18	120	172	0.70	0.77719	8.40	0.09397	5.09	0.61	0.05998	6.69	579	29	584	49	603	40	96	603	40
040-Z30	0.0008	21	128	113	1.14	0.78473	5.51	0.10203	4.27	0.78	0.05578	3.48	626	27	588	32	444	15	141		
041-Z31	0.0016	38	194	233	0.84	0.79780	7.25	0.09684	5.76	0.79	0.05975	4.41	596	34	596	43	594	26	100	594	26
042-Z32	0.0069	15	147	81	1.82	0.90104	16.54	0.10963	11.50	0.70	0.05961	11.88	671	77	652	108	589	70	114		
043-Z33	0.0017	40	29	194	0.15	3.05519	3.25	0.21172	1.54	0.48	0.10466	2.86	1238	19	1422	46	1708	49	72		
044-Z34	0.0012	97	156	187	0.84	2.95886	2.83	0.21237	1.56	0.55	0.10105	2.36	1241	19	1397	40	1643	39	76		
045-Z35	0.0026	39	137	246	0.56	0.86172	8.35	0.10221	6.55	0.78	0.06115	5.17	627	41	631	53	644	33	97	644	33
046-Z36	0.0028	42	221	235	0.95	0.92911	5.94	0.10928	3.83	0.64	0.06166	4.54	669	26	667	40	662	30	101	662	30
047-Z37	0.0018	36	175	196	0.90	0.88844	7.76	0.10635	6.25	0.81	0.06059	4.60	651	41	646	50	625	29	104	625	29
048-Z38	0.0030	10	28	69	0.40	0.82412	13.51	0.09865	11.08	0.82	0.06059	7.73	606	67	610	82	625	48	97	625	48
051-Z39	0.0000	9	53	43	1.23	0.85691	25.54	0.10183	19.15	0.75	0.06103	16.89	625	120	628	160	640	108	98	640	108

052-Z40	0.0038	9	41	38	1.08	1.01486	6.62	0.11782	4.96	0.75	0.06247	4.39	718	36	711	47	690	30	104	690	30
053-Z41	0.0007	179	160	239	0.67	6.79820	2.97	0.39226	1.84	0.62	0.12569	2.33	2133	39	2085	62	2039	47	105	2039	47
054-Z42	0.0015	57	227	273	0.84	0.87117	7.49	0.10584	5.51	0.74	0.05970	5.06	649	36	636	48	593	30	109	593	30
055-Z43	0.0014	73	56	247	0.23	1.89969	5.14	0.16332	4.00	0.78	0.08436	3.22	975	39	1081	56	1301	42	75		
056-Z44	0.0028	41	221	191	1.16	0.90781	8.25	0.10849	5.54	0.67	0.06069	6.11	664	37	656	54	628	38	106	628	38
057-Z45	0.0000	104	526	447	1.18	0.95517	6.13	0.11524	4.34	0.71	0.06011	4.33	703	31	681	42	608	26	116		
058-Z46	0.0235	211	425	993	0.43	1.26740	5.57	0.10944	4.61	0.83	0.08399	3.13	669	31	831	46	1292	40	52		
059-Z47	0.0003	425	98	347	0.28	17.14840	2.00	0.60632	1.43	0.71	0.20513	1.40	3055	44	2943	59	2867	40	107	2867	40
060-Z48	0.0021	108	226	508	0.45	1.00975	6.19	0.11669	4.42	0.71	0.06276	4.33	711	31	709	44	700	30	102	700	30
063-Z49	0.0015	33	240	220	1.10	1.00427	4.88	0.12091	2.38	0.49	0.06024	4.26	736	18	706	34	612	26	120		
064-Z50	0.0015	139	195	197	1.00	7.98963	2.00	0.41468	0.75	0.38	0.13974	1.85	2236	17	2230	44	2224	41	101	2224	41
065-Z51	0.0041	81	166	497	0.34	1.41081	5.37	0.14838	4.03	0.75	0.06896	3.55	892	36	893	48	898	32	99	898	32
066-Z52	0.0014	183	250	399	0.63	7.38902	1.81	0.39991	1.18	0.65	0.13401	1.38	2169	26	2160	39	2151	30	101	2151	30
067-Z53	0.0837	124	474	778	0.61	1.13494	9.73	0.10429	2.39	0.25	0.07893	9.43	640	15	770	75	1170	110	55		
068-Z54	0.0034	40	241	257	0.95	1.01774	4.28	0.12306	1.57	0.37	0.05998	3.98	748	12	713	31	603	24	124		
069-Z55	0.0014	57	269	361	0.75	1.01682	4.80	0.12450	3.40	0.71	0.05923	3.38	756	26	712	34	576	19	131		
070-Z56	0.0027	22	71	139	0.51	1.27425	7.55	0.14361	4.92	0.65	0.06435	5.74	865	43	834	63	753	43	115		
071-Z57	0.0010	95	132	449	0.30	2.03108	3.40	0.19179	1.93	0.57	0.07681	2.80	1131	22	1126	38	1116	31	101	1116	31
072-Z58	0.0104	10	70	63	1.11	0.91756	20.25	0.10634	16.55	0.82	0.06258	11.66	651	108	661	134	694	81	94	694	81
076-Z59	0.0006	201	130	481	0.27	3.71946	2.26	0.30175	1.16	0.51	0.08940	1.94	1700	20	1576	36	1413	27	120		
077-Z60	0.0034	31	146	184	0.80	0.88004	7.70	0.10580	5.75	0.75	0.06033	5.13	648	37	641	49	615	32	105	615	32
078-Z61	0.0025	58	169	322	0.53	1.06748	5.57	0.12298	4.79	0.86	0.06295	2.83	748	36	738	41	707	20	106	707	20
079-Z62	0.0082	60	111	270	0.41	1.34979	9.72	0.12700	7.11	0.73	0.07708	6.62	771	55	867	84	1123	74	69		
080-Z63	0.0044	101	658	538	1.23	1.07310	7.76	0.12109	5.05	0.65	0.06428	5.89	737	37	740	57	751	44	98	751	44
081-Z64	0.0028	55	342	274	1.26	1.00336	4.30	0.11785	2.73	0.64	0.06175	3.32	718	20	706	30	665	22	108	665	22
082-Z65	0.0015	49	166	306	0.55	0.93303	3.99	0.11132	2.94	0.74	0.06079	2.70	680	20	669	27	632	17	108	632	17
083-Z66	0.0020	129	130	405	0.32	4.35847	5.71	0.24185	4.81	0.84	0.13070	3.07	1396	67	1705	97	2107	65	66		
084-Z67	0.1434	1145	394	3249	0.12	6.34254	4.16	0.16488	3.57	0.86	0.27900	2.13	984	35	2024	84	3357	71	29		
087-Z68	0.0048	32	159	258	0.62	0.94183	5.60	0.11145	3.44	0.61	0.06129	4.42	681	23	674	38	650	29	105	650	29
088-Z69	0.0027	36	187	272	0.69	0.86594	8.21	0.10346	6.65	0.81	0.06071	4.81	635	42	633	52	629	30	101	629	30
089-Z70	0.0053	44	266	311	0.86	0.90021	7.06	0.10557	5.21	0.74	0.06184	4.77	647	34	652	46	669	32	97	669	32
090-Z71	0.0037	24	138	161	0.86	0.90046	7.29	0.10745	5.73	0.79	0.06078	4.51	658	38	652	48	631	28	104	631	28
091-Z72	0.0016	64	461	360	1.29	0.89535	6.24	0.10724	4.95	0.79	0.06055	3.80	657	32	649	41	623	24	105	623	24
092-Z73	0.0011	69	543	454	1.21	0.92546	4.95	0.11044	3.47	0.70	0.06078	3.52	675	23	665	33	631	22	107	631	22
093-Z74	0.0013	180	217	297	0.73	8.17985	2.51	0.43292	2.00	0.79	0.13704	1.53	2319	46	2251	57	2190	33	106	2190	33
094-Z75	0.0036	27	89	180	0.50	1.04511	6.62	0.11852	3.71	0.56	0.06395	5.48	722	27	726	48	740	41	98	740	41
095-Z76	0.0038	117	258	942	0.28	1.03163	4.75	0.11493	3.45	0.73	0.06510	3.27	701	24	720	34	778	25	90	778	25
096-Z77	0.0005	45	150	347	0.44	0.98609	6.42	0.11456	5.25	0.82	0.06243	3.70	699	37	697	45	689	25	102	689	25
100-Z78	0.0047	269	917	1163	0.79	1.13278	5.54	0.12648	4.40	0.79	0.06496	3.36	768	34	769	43	773	26	99	773	26
101-Z79	0.0063	24	87	109	0.81	0.87702	13.53	0.10500	11.66	0.86	0.06058	6.86	644	75	639	86	624	43	103	624	43
102-Z80	0.0040	61	180	340	0.53	1.09087	6.63	0.13147	4.54	0.68	0.06018	4.83	796	36	749	50	610	29	131		
103-Z81	0.1162	16	79	65	1.22	2.07663	11.34	0.07404	9.55	0.84	0.20341	6.12	460	44	1141	129	2854	175	16		
104-Z82	0.0032	43	326	165	1.99	0.88703	8.44	0.10613	6.83	0.81	0.06062	4.95	650	44	645	54	626	31	104	626	31
105-Z83	0.0028	55	205	271	0.76	1.02492	6.94	0.12226	5.60	0.81	0.06080	4.11	744	42	716	50	632	26	118		

106-Z84	0.0047	34	155	179	0.87	1.00114	10.28	0.11490	7.85	0.76	0.06319	6.63	701	55	704	72	715	47	98	715	47
107-Z85	0.0044	213	268	1101	0.25	1.22839	5.27	0.13380	4.16	0.79	0.06658	3.23	810	34	814	43	825	27	98	825	27
108-Z86	0.0019	85	659	387	1.72	0.85694	8.28	0.10188	7.13	0.86	0.06100	4.21	625	45	628	52	639	27	98	639	27
112-Z88	0.0062	14	56	64	0.88	0.94332	7.62	0.11145	5.51	0.72	0.06139	5.27	681	38	675	51	653	34	104	653	34
113-Z89	0.0034	34	153	169	0.91	0.88921	8.01	0.10573	6.43	0.80	0.06100	4.77	648	42	646	52	639	30	101	639	30
114-Z90	0.0029	51	284	244	1.17	0.89349	7.62	0.10586	6.15	0.81	0.06121	4.50	649	40	648	49	647	29	100	647	29
115-Z91	0.0046	44	166	252	0.66	0.86614	8.33	0.10256	7.11	0.85	0.06125	4.34	629	45	633	53	648	28	97	648	28
116-Z92	0.0016	43	104	221	0.47	1.03514	7.29	0.11706	6.22	0.85	0.06413	3.80	714	44	721	53	746	28	96	746	28
117-Z93	0.0071	8	22	49	0.45	0.93619	14.51	0.09763	11.05	0.76	0.06955	9.41	601	66	671	97	915	86	66		
118-Z94	0.0056	14	61	84	0.74	0.81599	14.36	0.09530	10.39	0.72	0.06210	9.91	587	61	606	87	678	67	87		
119-Z95	0.0571	2	9	13	0.69	0.18358	1666.76	0.02194	292.72	0.18	0.06069	1640.85	140	409	171	2852	628	10310	22		
120-Z96	0.0037	27	12	44	0.27	6.30774	6.77	0.34828	5.65	0.83	0.13136	3.73	1926	109	2020	137	2116	79	91	2116	79
108-Z86	0.0022	77	519	327	1.60	0.89159	7.51	0.10599	6.47	0.86	0.06101	3.82	649	42	647	49	640	24	102	640	24
123-Z97	0.0046	40	214	285	0.76	0.78083	9.90	0.09468	8.41	0.85	0.05981	5.22	583	49	586	58	597	31	98	597	31
124-Z98	0.0010	118	87	235	0.37	6.73581	2.78	0.38448	1.75	0.63	0.12706	2.16	2097	37	2077	58	2058	45	102	2058	45
125-Z99	0.0018	28	138	180	0.77	0.89071	12.22	0.10553	10.57	0.87	0.06121	6.12	647	68	647	79	647	40	100	647	40
126-Z100	0.0024	38	161	220	0.73	1.02295	7.15	0.11954	5.47	0.77	0.06206	4.61	728	40	715	51	676	31	108	676	31
127-Z101	0.0015	50	402	264	1.54	0.99328	9.14	0.11462	7.61	0.83	0.06285	5.07	700	53	700	64	703	36	99	703	36
128-Z102	0.0009	199	194	327	0.60	8.06883	2.30	0.42945	1.46	0.63	0.13627	1.78	2303	34	2239	52	2180	39	106	2180	39
129-Z103	0.0035	32	20	129	0.15	1.65729	4.91	0.16887	3.69	0.75	0.07118	3.23	1006	37	992	49	963	31	104	963	31
130-Z104	0.0015	39	141	284	0.50	0.81474	7.55	0.10028	6.38	0.85	0.05892	4.04	616	39	605	46	564	23	109	564	23

[a] Th/U ratios are calculated relative to GJ-1 reference zircon

[b] Corrected for background and within-run Pb/U fractionation and normalised to reference zircon GJ-1 (ID-TIMS values/measured value); 207Pb/235U calculated
using $(^{207}Pb/^{206}Pb)/(^{238}U/^{206}Pb * 1/137.88)$

[c] Rho is the error correlation defined as the quotient of the propagated errors of the $^{206}Pb/^{238}U$ and the $^{207}/^{235}U$ ratio

[d] Corrected for mass-bias by normalising to GJ-1 reference zircon and common Pb using the model Pb composition of Stacey and Kramers (1975)

[e] Degree of concordance = ($^{206}Pb/^{238}U$ age * 100/$^{207}Pb/^{206}U$ age)

ANEXO C – TABLE 2

Table 2: Lu-Hf data from the samples of the Santa Bárbara and Guaritas Group

Zircon	U-Pb Age (Ma)	error	eHf(t)	Sample (Present day ratios) ^{176}Hf/^{177}Hf	±2SE	^{176}Lu/^{177}Hf	±2SE	Chur ^{176}Hf/^{177}Hf (t)	DM ^{176}Hf/^{177}Hf (t)	Sample Initial Ratios ^{176}Hf/^{177}Hf (t)	eHf(0)	eHf(t)	±2SE	DM Model Age (Ma) TDM	error	DM Crust	Mafic	Felsic
Sample PS-01 - Santa Bárbara Seq. I																		
122-Z05	2246	40	2.88	0.281441	0.000084	0.000327	2.70E-05	0.281346	0.281589	0.281427	-47.52	2.88	0.29	2461	43	2.61	2.76	2.54
123-Z09	759	16	-19.16	0.281774	0.000058	0.000673	7.50E-05	0.282306	0.282696	0.281765	-35.74	-19.16	2.55	2034	44	2.82	3.65	2.46
124-Z14	947	19	-8.28	0.281962	0.000057	0.000536	4.62E-05	0.282185	0.282558	0.281952	-29.12	-8.28	0.88	1774	36	2.29	2.84	2.06
125-Z31	591	14	-7.48	0.282206	0.000047	0.000465	1.39E-05	0.282412	0.282819	0.282201	-20.48	-7.48	0.40	1439	34	1.97	2.53	1.73
126-Z35	567	15	-12.72	0.282077	0.000046	0.000819	1.07E-05	0.282427	0.282837	0.282068	-25.04	-12.72	0.49	1629	42	2.27	2.96	1.98
127-Z37	1959	28	9.56	0.281822	0.000062	0.000524	5.38E-05	0.281533	0.281805	0.281803	-34.05	9.56	1.12	1962	28	1.96	1.97	1.96
128-Z22	2076	35	-14.93	0.281046	0.000031	0.000218	1.44E-05	0.281457	0.281717	0.281037	-61.51	-14.93	1.24	2976	50	3.58	4.20	3.33
133-Z21	1672	21	1.45	0.281822	0.000053	0.001949	8.20E-05	0.281720	0.282020	0.281761	-34.04	1.45	0.08	2036	25	2.25	2.49	2.15
134-Z47	2760	81	-8.25	0.280815	0.000051	0.000737	3.87E-05	0.281008	0.281198	0.280776	-69.65	-8.25	0.68	3321	98	3.70	4.09	3.54
135-Z48	992	23	-4.36	0.282057	0.000060	0.001210	8.37E-05	0.282157	0.282525	0.282034	-25.75	-4.36	0.40	1674	39	2.09	2.53	1.90
Sample PS-03 - Santa Bárbara Seq. III																		
107-Z14	647	29	-23.66	0.281716	0.000053	0.000642	3.77E-05	0.282376	0.282778	0.281708	-37.80	-23.66	2.45	2111	94	3.00	3.95	2.60
108-Z41	578	22	-22.94	0.281794	0.000138	0.001935	6.26E-05	0.282420	0.282829	0.281772	-35.06	-22.94	1.61	2075	78	2.90	3.84	2.51
109-Z37	3389	96	-4.61	0.280475	0.000072	0.000213	6.26E-06	0.280591	0.280716	0.280461	-81.69	-4.61	0.27	3720	105	3.96	4.19	3.86
110-Z38	604	23	10.13	0.282701	0.000181	0.000993	2.12E-05	0.282404	0.282810	0.282690	-2.96	10.13	0.61	772	29	0.87	0.98	0.83
112-Z32	947	27	-6.21	0.282017	0.000103	0.000366	8.01E-06	0.282186	0.282558	0.282011	-27.16	-6.21	0.32	1691	49	2.16	2.66	1.96
113-Z26	2187	30	-3.94	0.281296	0.000093	0.000543	3.61E-05	0.281384	0.281633	0.281273	-52.65	-3.94	0.32	2668	37	2.99	3.32	2.85
114-Z60	2650	42	0.40	0.281124	0.000057	0.000629	3.42E-05	0.281081	0.281282	0.281092	-58.74	0.40	0.03	2903	46	3.08	3.25	3.00
115-Z59	712	11	-2.98	0.282257	0.000063	0.000431	1.49E-05	0.282335	0.282731	0.282251	-18.67	-2.98	0.15	1368	22	1.78	2.22	1.60
116-Z51	552	15	-39.17	0.281335	0.000043	0.000442	6.96E-05	0.282437	0.282848	0.281331	-51.27	-39.17	7.22	2609	69	3.86	5.18	3.30
119-Z53	1996	22	-16.85	0.281047	0.000054	0.000330	2.35E-05	0.281509	0.281777	0.281035	-61.45	-16.85	1.39	2982	33	3.64	4.31	3.36
120-ZA	1975	36	-13.26	0.281166	0.000050	0.000444	1.65E-05	0.281523	0.281792	0.281149	-57.25	-13.26	0.74	2834	51	3.40	3.99	3.16
121-Z56	1753	17	-16.96	0.2812035	5.135E-05	0.000429498	8.09307E-07	0.281667	0.281959	0.281189	-55.92	-16.96	0.199	2783	27	3.46	4.15	3.17
Sample T02-07 Santa Bárbara Seq. II																		
003-Z07	2120	40	-14.55	0.281028	0.000051	0.000207	4.43E-06	0.281429	0.281684	0.281019	-62.15	-14.55	0.59	2999	56	3.59	4.20	3.34
004-Z14	2056	77	-13.27	0.281113	0.000073	0.000407	1.76E-05	0.281470	0.281732	0.281097	-59.14	-13.27	1.07	2902	109	3.47	4.04	3.22
005-Z15	2107	43	-14.95	0.281026	0.000072	0.000241	1.23E-05	0.281437	0.281693	0.281016	-62.21	-14.95	1.07	3004	61	3.61	4.22	3.35
006-Z18	559	27	-39.43	0.281323	0.000111	0.000401	4.55E-05	0.282432	0.282843	0.281319	-51.70	-39.43	6.40	2623	127	3.88	5.21	3.32
007-Z24	754	78	-27.38	0.281544	0.000086	0.000589	4.53E-05	0.282309	0.282700	0.281536	-43.88	-27.38	4.96	2339	243	3.31	4.34	2.88
008-Z31	2089	41	-12.66	0.281099	0.000078	0.000180	2.48E-06	0.281449	0.281707	0.281092	-59.61	-12.66	0.43	2903	57	3.45	4.01	3.22
009-Z51	602	22	-25.51	0.281689	0.000062	0.000380	3.03E-05	0.282405	0.282811	0.281685	-38.76	-25.51	2.96	2133	77	3.08	4.08	2.66
010-Z53	2086	33	-7.00	0.281268	0.000058	0.000354	1.58E-05	0.281450	0.281709	0.281253	-53.66	-7.00	0.42	2693	42	3.10	3.52	2.93
011-Z55	2078	39	-11.47	0.281143	0.000076	0.000255	6.24E-06	0.281456	0.281715	0.281133	-58.07	-11.47	0.50	2851	54	3.37	3.90	3.15
012-Z60	2088	39	-15.12	0.281036	0.000084	0.000314	2.27E-05	0.281449	0.281708	0.281024	-61.84	-15.12	1.38	2996	57	3.61	4.23	3.35
013-Z70	725	42	-34.16	0.281370	0.000084	0.000531	1.89E-05	0.282327	0.282721	0.281362	-50.05	-34.16	3.18	2569	147	3.70	4.89	3.19
014-Z71	2613	100	-10.20	0.280829	0.000057	0.000219	3.85E-06	0.281105	0.281310	0.280818	-69.15	-10.20	0.57	3259	125	3.71	4.16	3.52
017-Z79	1748	58	-19.19	0.281146	0.000064	0.000486	2.64E-05	0.281670	0.281963	0.281130	-57.96	-19.19	1.68	2863	94	3.59	4.34	3.28
018-Z82	2078	30	-12.94	0.281118	0.000089	0.000662	9.20E-06	0.281456	0.281715	0.281092	-58.95	-12.94	0.37	2913	41	3.46	4.03	3.22

019-Z87	2093	21	-12.41	0.281111	0.000066	0.000350	2.35E-05	0.281446	0.281704	0.281097	-59.20	-12.41	0.96	2900	30	3.44	3.99	3.21
020-Z94	606	28	-16.74	0.281941	0.000062	0.000941	2.35E-05	0.282403	0.282809	0.281930	-29.86	-16.74	1.20	1821	84	2.55	3.34	2.22
021-Z106	638	33	-26.06	0.281650	0.000048	0.000299	2.27E-05	0.282383	0.282785	0.281647	-40.12	-26.06	3.31	2180	111	3.14	4.15	2.71
022-Z104	642	21	-20.08	0.281822	0.000110	0.000758	3.41E-05	0.282380	0.282782	0.281813	-34.05	-20.08	1.57	1974	65	2.78	3.65	2.41
023-Z102	2071	28	-4.48	0.281354	0.000069	0.000505	7.20E-06	0.281460	0.281720	0.281334	-50.60	-4.48	0.13	2588	36	2.93	3.29	2.78
024-Z107	668	45	-25.49	0.281650	0.000051	0.000537	2.07E-05	0.282364	0.282763	0.281644	-40.12	-25.49	2.70	2194	147	3.13	4.12	2.71
025-Z108	743	43	-28.55	0.281524	0.000061	0.001046	8.15E-05	0.282315	0.282708	0.281510	-44.59	-28.55	3.88	2394	138	3.37	4.43	2.93
026-Z115	1789	54	-15.99	0.281227	0.000043	0.000992	2.38E-05	0.281644	0.281932	0.281194	-55.09	-15.99	0.87	2792	84	3.43	4.09	3.15
027-Z101	2193	28	0.94	0.281428	0.000049	0.000506	2.68E-05	0.281381	0.281628	0.281407	-47.98	0.94	0.06	2489	32	2.69	2.89	2.60
028-Z091	606	10	-26.39	0.281662	0.000047	0.000408	1.66E-05	0.282403	0.282808	0.281657	-39.71	-26.39	1.51	2171	35	3.14	4.16	2.71
Sample T01-11 Guaritas Gr.																		
033-Z104	749	34	5.58	0.282476	0.000031	0.000476	4.14E-06	0.282312	0.282703	0.282469	-10.93	5.58	0.30	1071	49	1.27	1.49	1.18
034-Z109	2191	52	-3.31	0.281299	0.000046	0.000240	4.06E-06	0.281382	0.281630	0.281289	-52.55	-3.31	0.13	2644	62	2.95	3.27	2.82
035-Z111	2125	62	-22.48	0.280803	0.000042	0.000249	9.40E-06	0.281425	0.281680	0.280792	-70.11	-22.48	1.51	3297	96	4.09	4.88	3.75
036-Z112	2083	35	-1.39	0.281442	0.000069	0.000725	7.45E-05	0.281453	0.281711	0.281413	-47.49	-1.39	0.17	2485	42	2.75	3.02	2.63
037-Z97	716	85	-13.39	0.281972	0.000073	0.001320	2.38E-05	0.282333	0.282728	0.281955	-28.74	-13.39	1.82	1795	212	2.43	3.13	2.14
038-Z93	2184	79	-1.00	0.281381	0.000061	0.000538	2.12E-05	0.281387	0.281635	0.281358	-49.66	-1.00	0.08	2555	92	2.80	3.06	2.70
039-Z92	623	18	-25.88	0.281666	0.000038	0.000437	1.23E-05	0.282392	0.282796	0.281661	-39.56	-25.88	1.50	2167	64	3.12	4.12	2.69
040-Z86	1212	30	2.93	0.282109	0.000061	0.000457	8.24E-06	0.282016	0.282362	0.282098	-23.91	2.93	0.13	1571	39	1.80	2.05	1.70
041-Z78	2659	39	-8.38	0.280860	0.000049	0.000410	7.64E-06	0.281075	0.281276	0.280840	-68.06	-8.38	0.28	3234	48	3.63	4.03	3.46
042-Z75	2197	97	-6.09	0.281236	0.000079	0.000699	1.77E-05	0.281378	0.281625	0.281207	-54.77	-6.09	0.42	2759	122	3.13	3.52	2.97
043-Z70	2099	52	-7.72	0.281241	0.000051	0.000400	9.53E-06	0.281442	0.281699	0.281225	-54.60	-7.72	0.38	2732	68	3.16	3.59	2.97
044-Z67	642	34	-22.71	0.281747	0.000074	0.000730	3.31E-05	0.282380	0.282782	0.281738	-36.71	-22.71	2.23	2074	109	2.94	3.87	2.55
047-Z66	2200	84	0.43	0.281407	0.000051	0.000437	4.45E-06	0.281376	0.281623	0.281388	-48.74	0.43	0.02	2514	96	2.73	2.94	2.63
048-Z61	2463	41	-13.57	0.280840	0.000067	0.000379	7.58E-06	0.281204	0.281424	0.280822	-68.78	-13.57	0.50	3258	55	3.80	4.35	3.57
049-Z59	2239	80	-6.32	0.281205	0.000036	0.000764	5.14E-05	0.281350	0.281593	0.281173	-55.86	-6.32	0.65	2805	100	3.18	3.56	3.02
050-Z55	717	51	-27.37	0.281561	0.000064	0.000153	1.09E-05	0.282332	0.282727	0.281559	-43.28	-27.37	3.91	2291	163	3.28	4.32	2.85
051-Z53	640	27	-24.75	0.281689	0.000047	0.000616	6.37E-05	0.282381	0.282783	0.281682	-38.75	-24.75	3.59	2146	89	3.06	4.04	2.65
052-Z47	633	83	-3.55	0.282288	0.000082	0.000215	1.17E-05	0.282385	0.282789	0.282285	-17.58	-3.55	0.66	1319	174	1.75	2.21	1.56
053-Z45	2074	27	-8.20	0.281251	0.000046	0.000598	2.60E-05	0.281459	0.281718	0.281228	-54.24	-8.20	0.47	2731	36	3.17	3.62	2.98
054-Z40	2026	113	-6.18	0.281323	0.000060	0.000196	1.41E-05	0.281489	0.281754	0.281315	-51.70	-6.18	0.79	2609	145	3.00	3.41	2.84
055-Z36	2383	41	-13.14	0.280903	0.000057	0.000350	2.95E-05	0.281257	0.281485	0.280887	-66.56	-13.14	1.34	3174	54	3.71	4.26	3.48
056-Z35	2010	37	-11.93	0.281182	0.000039	0.000452	3.99E-06	0.281500	0.281766	0.281164	-56.70	-11.93	0.33	2814	52	3.35	3.90	3.12
057-Z31	3273	61	-3.40	0.280581	0.000061	0.000146	9.98E-06	0.280668	0.280805	0.280572	-77.92	-3.40	0.30	3576	67	3.79	4.01	3.70
058-Z29	1673	31	-18.36	0.281216	0.000060	0.000451	1.45E-05	0.281719	0.282019	0.281202	-55.48	-18.36	0.93	2768	51	3.48	4.22	3.17
061-Z28	2476	39	0.12	0.281207	0.000048	0.000172	1.04E-05	0.281195	0.281414	0.281199	-55.82	0.12	0.01	2761	43	2.96	3.16	2.88
062-Z27	624	21	-26.80	0.281643	0.000075	0.000681	1.59E-04	0.282391	0.282795	0.281635	-40.40	-26.80	7.19	2212	75	3.17	4.20	2.74
063-Z25	1860	33	-24.22	0.280916	0.000058	0.000018	6.27E-07	0.281598	0.281879	0.280916	-66.08	-24.22	1.28	3130	55	3.99	4.85	3.62
064-Z21	2656	47	-3.69	0.281000	0.000131	0.000524	7.39E-05	0.281077	0.281277	0.280973	-63.13	-3.69	0.59	3060	55	3.34	3.62	3.22
065-Z15	1881	38	-23.11	0.280939	0.000073	0.000173	5.17E-05	0.281584	0.281863	0.280933	-65.27	-23.11	7.39	3112	62	3.93	4.77	3.58
066-Z125	1389	314	4.60	0.282039	0.000050	0.000267	5.68E-05	0.281902	0.282230	0.282032	-26.39	4.60	2.02	1658	374	1.83	2.02	1.76